Design, Synthesis, and Evaluation of Aza-Peptide Michael Acceptors as Selective and Potent Inhibitors of Caspases-2, -3, -6, -7, -8, -9, and -10

Özlem Doğan Ekici,[†] Zhao Zhao Li,[†] Amy J. Campbell,[†] Karen Ellis James,[†] Juliana L. Asgian,[†] Jowita Mikolajczyk,[‡] Guy S. Salvesen,[‡] Rajkumar Ganesan,[§] Stjepan Jelakovic,[§] Markus G. Grütter,[§] and James C. Powers*[,†]

School of Chemistry and Biochemistry and the Parker H. Petit Institute for Bioengineering and Bioscience, Georgia Institute of Technology, Atlanta, Georgia 30332-0400, Program in Apoptosis and Cell Death Research, The Burnham Institute, 10901 North Torrey Pines Road, La Jolla, California 92037, and Department of Biochemistry, University of Zurich, 8057-Zurich, Switzerland

Received February 8, 2006

Aza-peptide Michael acceptors are a novel class of inhibitors that are potent and specific for caspases-2, -3, -6, -7, -8, -9, and -10. The second-order rate constants are in the order of 10^6 M^{-1} s^{-1}. The aza-peptide Michael acceptor inhibitor **18t** (Cbz-Asp-Glu-Val-AAsp-*trans*-CH═CH−CON(CH_2-1-Naphth)$_2$ is the most potent compound and it inhibits caspase-3 with a k_2 value of 5620000 M^{-1} s^{-1}. The inhibitor **18t** is 13700, 190, 6.4, 594, 37500, and 173-fold more selective for caspase-3 over caspases-2, -6, -7, -8, -9, and −10, respectively. Aza-peptide Michael acceptors designed with caspase specific sequences are selective and do not show any cross reactivity with clan CA cysteine proteases such as papain, cathepsin B, and calpains. High-resolution crystal structures of caspase-3 and caspase-8 in complex with aza-peptide Michael acceptor inhibitors demonstrate the nucleophilic attack on C2 and provide insight into the selectivity and potency of the inhibitors with respect to the P1′ moiety.

Introduction

Cysteine proteases, also known as thiol proteases have been identified in the biological systems of bacteria, protozoa, fungi, plant viruses, and mammals. Cysteine proteases acylate the peptide bond via a nucleophilic thiol and are involved in numerous physiologically important processes. Cysteine proteases have been grouped into evolutionary families and clans by Rawlings and Barrett.[1,2] The majority of structurally relevant cysteine proteases belong to the well-known clan CA, which includes papain, cathepsins, and calpains. Several important cysteine proteases such as caspases, legumain, gingipain, clostripain, and separase belong to a new but smaller clan of cysteine proteases, which is termed clan CD. The tertiary structure of clan CD proteases shows a unique α/β fold unlike any other protein, with the catalytic residues in the order His, Cys in the sequence. Clan CD cysteine proteases differ from the clan CA proteases also in their substrate specificity requirements. The substrate specificity of clan CD proteases is determined by the S1 pocket, whereas the S2 pocket is the major determinant of substrate specificity with the clan CA cysteine proteases.

Caspases, also known as *c*ysteinyl *asp*artate-specific pro*teases*, are found in worms to flies to humans. Currently, >15 members are identified, with 11 members in humans.[3] One distinctive feature of this family of enzymes is their near absolute specificity for Asp residue at P1. The only other known mammalian protease with the same specificity requirement is the lymphocyte serine protease granzyme B, which acts as a caspase activator. Caspases have been the focus of both industrial and academic research since their discovery. Over the past decade, the exact roles and functions of individual caspases in cellular systems have been intensely investigated. Some caspases are important mediators of inflammation, whereas others are involved in apoptosis (programmed cell death). Excessive neuronal apoptosis leads to a variety of diseases such as stroke, Alzheimer's disease, Huntington's disease, Parkinson's disease, amyotropic lateral sclerosis (ALS), multiple sclerosis (MS), and spinal muscular atrophy.[4] Caspases are recognized as novel therapeutic targets for central nervous diseases in which cell death occurs mainly by an apoptosis mechanism.[5−8] Hence, potent and specific inhibitors of caspases could lead to the development of potential drugs, which can modulate the apoptotic process.

A number of different classes of inhibitors have been developed for cysteine proteases including reversible transition state inhibitors and a variety of irreversible inhibitors.[9] Relatively few classes have been applied to clan CD cysteine proteases, particulary caspases. Several substrate based caspase inhibitors have been extensively used to address the roles of caspases in cellular systems over the past few years.[10] These include reversible inhibitors such as peptide aldehydes (Ac-YVAD-CHO, Ac-DEVD-CHO, Ac-WEHD-CHO) and irreversible inhibitors such as fluoro- or chloromethyl ketones (Z-VAD-FMK, Z-YVAD-FMK/CMK, Z-DEVD-FMK/CMK). A few of these inhibitors have even entered preclinical studies with animal models of human diseases. However, the major disadvantage of these inhibitors is their lack of selectivity. Several of these caspase inhibitors have been recently shown to efficiently inactivate other cysteine proteases, such as cathepsins B, L, and S.[11] Cathepsin B inhibition by Ac-YVAD-CMK rescued neuronal cells against glucose/oxygen deprivation-induced apop-

* Corresponding author. Tel: (404) 894−4038, Fax: (404) 894−2295. E-mail: james.powers@chemistry.gatech.edu.
[†] Georgia Institute of Technology.
[‡] The Burnham Institute.
[§] University of Zurich.

[a] Abbreviations: AA, amino acid residue; AAsn, aza-asparagine; AAsp, aza-aspartic acid; Ac, acetyl; AcOH, acetic acid; AFC, 7-amino-4-trifluoromethylcoumarin; AMC, 7-amino-4-methylcoumarin; Boc, *tert*-butoxycarbonyl; Bzl, benzyl, CH_2Ph; Cbz, benzyloxycarbonyl; $CDCl_3$, deuterated chloroform; CHAPS, 3-[(3-cholamidopropyl)dimethylammonio]-1-propanesulfonate; CMK, chloromethyl ketone; DMF, *N*,*N*-dimethylformamide; DMSO, dimethyl sulfoxide; DMSO-d_6, dimethyl sulfoxide-d_6 deuterated; DTT, dithiothreitol; E-64c, *N*-(L-3-*trans*-carboxyoxiran-2-carbonyl)-L-leucyl-3-methylbutanamide; EDC, 1-(3-dimethylaminopropyl)-3-ethylcarbodiimide hydrochloride; EDTA, ethylenediaminetetraacetic acid; EtOAc, ethyl acetate; EtOH, ethanol; FMK, fluoromethyl ketone; HEPES, *N*-2-hydroxyethylpiperazine-*N*′-2-ethanesulfonic acid; HOBt, *N*-hydroxybenzotriazole; *i*BCF, isobutyl chloroformate; *i*Bu, isobutyl; MeOH, methanol; NMM, *N*-methylmorpholine; OBzl, benzyloxy; Orn, ornithine; PIPES, 1,4-piperazinediethanesulfonic acid; *p*NA, *p*-nitroanilide; *t*Bu, *tert*-butyl; TFA, trifluoroacetic acid.

10.1021/jm0601405 CCC: $33.50
Published on Web 08/23/2006

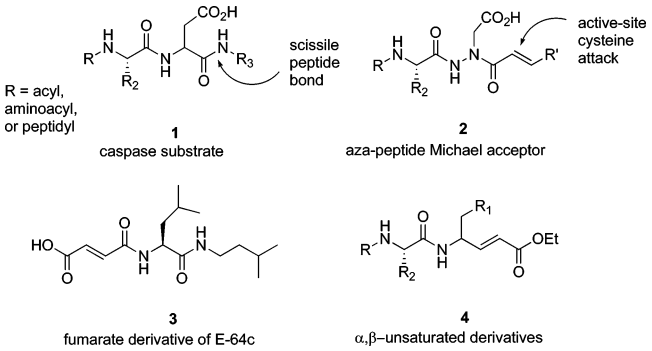

Figure 1. Aza-peptide Michael acceptor design.

tosis, suggesting that other proteases may be involved in the processes previously designated only to caspases. Furthermore, several lysosomal cysteine proteases were shown to be involved in various apoptosis models, although the mechanisms are not yet clear.[12,13] Thus, there is a considerable need for potent and selective caspase inhibitors to elucidate the roles of individual caspases in apoptosis and as potential therapeutics.

A variety of other inhibitors with electrophilic warheads have been reported as irreversible inhibitors effective for clan CA cysteine proteases.[9] One of the first Michael acceptors described in the literature is the fumarate derivative of E-64c (**3**, Figure 1).[14] This inhibitor contains an α,*β*-unsaturated carbonyl moiety and was found to be an irreversible inhibitor of cathepsin B, cathepsin H, and cathepsin L. Vinyl sulfones and α,*β*-unsaturated carbonyl derivatives (**4**, Figure 1) have been developed as highly potent inhibitors for exopeptidases such as DPPI and many clan CA cysteine endopeptidases including papain, cathepsins B, L, S, and K, calpains, and cruzain.[15,16] Michael acceptor inhibitors have great potential for use as drugs. One Michael acceptor CRA-3316 developed by Celera as a cruzain inhibitor to treat Chagas's disease is also in clinical trials.[17] Another Michael acceptor AG7088 (Ruprintrivir) has entered phase II clinical studies with humans as a potential nasally delivered antirhinoviral agent.[18−21] Recently, Michael acceptor inhibitors based on the AG7088 structure drew considerable attention in the treatment of SARS (Severe Acute Respiratory Syndrome) due to their potential as antiviral agents against the SARS coronavirus.[22]

Our laboratory has recently reported aza-peptide Michael acceptor inhibitors (**2**, Figure 1) that are highly specific for clan CD cysteine proteases.[23] The aza-peptide Michael acceptor structure resembles the substrate peptide sequence (**1**, Figure 1), where the carbonyl group of the double bond moiety replaces the carbonyl group of the scissile bond. Replacement of the α-carbon of the P1 amino acid with a nitrogen results in the formation of the aza-peptide, which allows the ready synthesis of a variety of derivatives. In the fumarate derivative **3**, the Michael acceptor is on the N-terminus of the amino acid residue, while in our aza-peptide design, the warhead is at the C-terminal end of the inhibitor. On the other hand, the design of vinyl sulfones and α,*β*-unsaturated carbonyl derivatives was based on the optimal peptide sequence of the target enzyme, where the carbonyl of the scissile bond was replaced by the double bond moiety.

In an effort to obtain greater potency and selectivity, we elaborated our aza-peptide Michael acceptor design in the P′ portion of the inhibitor. Although considerable effort has been devoted to the optimization of interactions of caspase inhibitors at the S1−S4 sites,[24,25] interactions of substrates or inhibitors at the S1' site in the past were analyzed in only very few studies.[26,27] Recently, a few peptidomimetic compounds binding to the groove located near the S1′ site of caspase-3 were identified and characterized structurally.[26] We were particularly interested in designing inhibitors for the key executioner caspases-3, -6, and -7 and initiator caspases-2, -8, -9, and -10. Here we also report crystal structures of caspase-3 and caspase-8 in complex with aza-peptide Michael acceptors with different P1′ substitutions to elucidate the structural determinants for the preference and discrimination at this site. The analysis of the crystal structures of the caspase:Michael acceptor inhibitor complexes also provide insights into the difference in reactivity of cis (**18g**) and trans (**18h**) isomers.

Chemistry. We synthesized a variety of aza-peptide Michael acceptors with P1 Asp residue as potential inhibitors for caspases. We previously reported the general method to prepare aza-peptide Michael acceptors in our preliminary communication.[23] Aza-peptide Michael acceptors for caspases were synthesized by coupling the appropriate substituted peptidyl hydrazides with P1 Asp side chain with the desired fumarate derivative.

A variety of fumarate esters and fumarate mono- and diamides have been synthesized in order to couple to the substituted peptidyl hydrazides (Figure 2). The monobenzyl fumarate **7** was

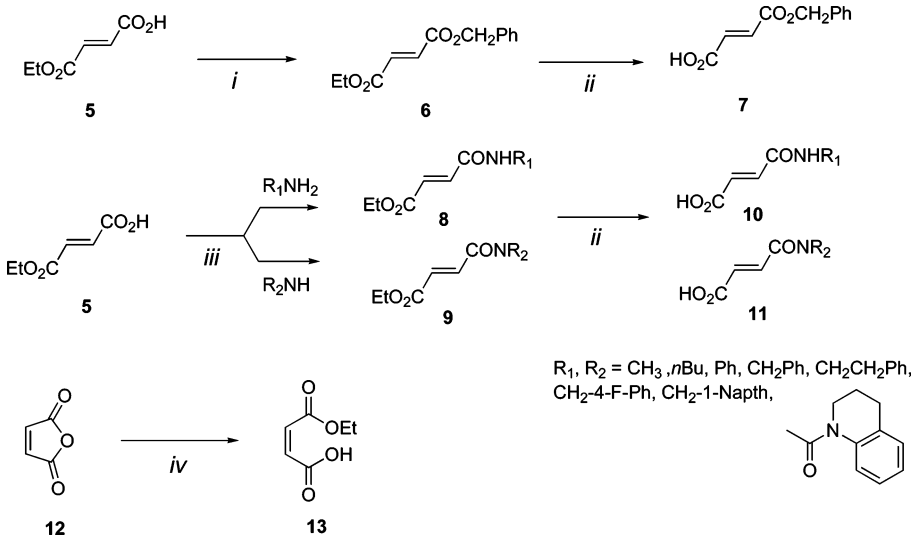

Figure 2. Synthesis of fumarate and maleate derivatives. Reagents used: (i) NMM, EDC, BzlOH, DMF; (ii) KOH, EtOH, r.t.; (iii) NMM, iBCF, CH_2Cl_2; (iv) EtOH, r.t.

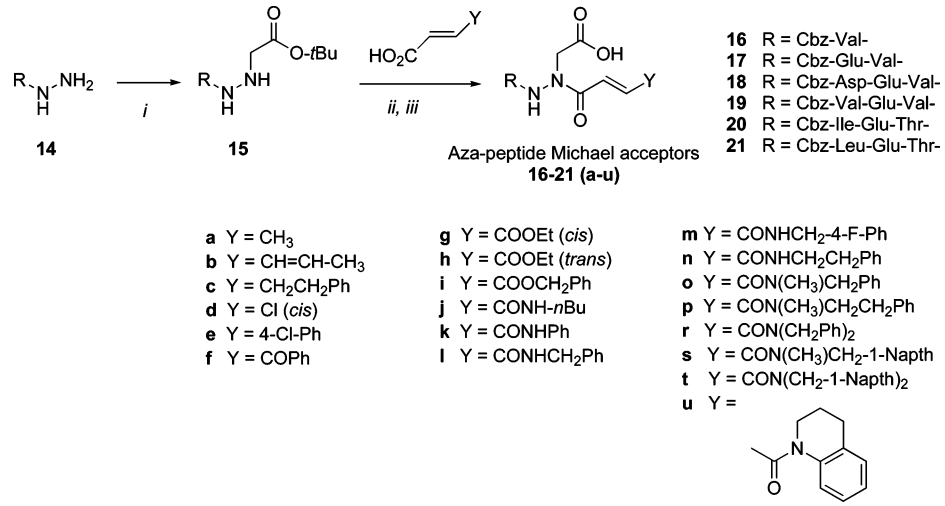

Figure 3. Synthesis of Aza-Asp Michael acceptors. Reagents used: (i) $BrCH_2COO$-*t*Bu, NMM, DMF; (ii) EDC, HOBt, DMF or NMM, iBCF, DMF; (iii) TFA, CH_2Cl_2.

obtained by the addition of 1 eq of benzyl alcohol to monoethyl fumarate **5** using EDC and NMM as coupling reagents followed by the hydrolysis of the ethyl ester **6** in methanol by aqueous NaOH. Mono- and disubstituted amide derivatives **10** and **11** were obtained by coupling the desired primary or secondary amine to monoethyl fumarate **5** and subsequent hydrolysis of the ethyl ester **8** or **9** with 1.2 eq of KOH in ethanol. Monoethyl maleate **13** was synthesized by the alcoholysis reaction of maleic anhydride **12** with ethanol.

Peptidyl hydrazides **14** were obtained by reacting blocked mono-, di-, or tripeptidyl methyl esters with excess hydrazine in methanol. The aza-Asp side chain was introduced by alkylation of the peptidyl hydrazide with *tert*-butyl bromoacetate to form the substituted peptidyl hydrazide **15**.

The final aza-peptide Michael acceptors (**16**−**21 (a**−**u)**, Figure 3), were synthesized primarily by the EDC/HOBt coupling method with the peptide sequences Cbz-Val-NH−NH−CH_2COO-*t*Bu, Cbz-Asp(O-*t*Bu)-Glu(O-*t*Bu)-Val-NH−NH−CH_2COO-*t*Bu, Cbz-Val-Glu(O-*t*Bu)-Val-NH−NH−CH_2-COO-*t*Bu, Cbz-Ile-Glu(O-*t*Bu)-Thr-NH−NH−CH_2COO-*t*Bu, and Cbz-Leu-Glu(O-*t*Bu)-Thr-NH−NH−CH_2COO-*t*Bu using an excess of the desired fumarate derivative. To simplify the purification process and maximize the yield, some aza-peptide Michael acceptors were synthesized by the mixed anhydride method using the peptide sequences Cbz-Glu(O-*t*Bu)-Val-NH−NH−CH_2COO-*t*Bu, Cbz-Ile-Glu(O-*t*Bu)-Thr-NH−NH−CH_2-COO-*t*Bu, and Cbz-Leu-Glu(O-*t*Bu)-Thr-NH−NH−CH_2COO-*t*Bu. In the final step of the aza-peptide Michael acceptor synthesis, the *tert*-butyl protecting groups on the aza-Asp, Glu, and Asp residues were deprotected using TFA in CH_2Cl_2 at 0 °C.

Results and Discussion

The optimal peptide sequences of the target caspases were utilized in the design of the aza-peptide Michael acceptors. The optimal sequences were derived either from natural caspase cleavage sites or from peptide mapping of caspases with libraries of AMC substrates.[28] On the basis of their S4 subsite preferences, Thornberry and co-workers divided the caspases into three groups: group I caspases (1, 4, and 5) prefer aromatic amino acid residues, group II caspases (6, 8, 9, and 10) have a preference for branched apolar residues, and group III caspases (2, 3, and 7) prefer an aspartic acid residue at their P4 positions. The DEVD and LETD sequences are optimal sequences for caspase-3 and caspase-8, respectively, as determined by positional scanning of a synthetic combinatorial library.[29,30] The IETD sequence for caspases-6 and -8 is the cleavage sequence of a natural caspase-8 substrate, the caspase-3 proenzyme.[28] The VEVD sequence was chosen as the optimal substrate for caspase-6 in accordance with the branched amino acid preference of this enzyme. The EVD sequence was selected to obtain a truncated caspase-3 inhibitor. Similarly, the VD sequence was chosen to represent a general inhibitor for all the caspases (caspases-2, -3, -6, -7, -8, -9, and -10).

The aza-peptide Michael acceptors with an aza-Asp residue at P1 position and designed with the appropriate target sequences were tested against various caspases for kinetic activity. The aza-peptide Michael acceptors exhibit excellent inhibitory potency against caspases-2, -3, -6, -7, -8, -9, and -10 (Table 1). The second-order inhibition rates are as high as 10^6 M^{-1} s^{-1}. Generally, the DEVD sequence is the most reactive with caspases-2, -3, and -7. The IETD and LETD sequences are more reactive with the caspases-6, -8, and -9. The VEVD sequence is equally potent as IETD for caspases-6 and -8. Interestingly, the DEVD sequence is the best sequence for caspase-10 although this enzyme was originally included into group II along with caspases-6,-8, and -9. Also the most potent caspase-8 inhibitor has the DEVD sequence. Its favorable interaction with caspase-8 has been demonstgrated in a crystal structure.[31] Similarly, the most potent caspase-9 inhibitor is the one with the EVD tripeptide sequence. This result seems to be an exception to the requirement of the tetrapeptide sequence of caspases for efficient substrate cleavage.

Aza-peptide Michael acceptors are easily extended at their P′ site. To gain more insight about the potency and selectivity of the aza-peptide Michael acceptor inhibitors, we modified the substituents on the fumarate moiety extending into the P′ site. We utilized various groups such as simple alkyl, alkenyl, and aryl groups, as well as halogens, esters, and amides in the hopes of obtaining selectivity in the P′ site among the various caspases.

Caspase-2. In contrast to the other caspases, caspase-2 requires a P5 residue for efficient substrate cleavage. The optimal sequence of caspase-2 is VDVAD, but the caspase-3 specific DEVD sequence still worked best for caspase-2. Because of the P5 requirement, the second-order rates of inhibition with caspase-2 remained in the range of 10^2 M^{-1} s^{-1}, except for the inhibitors **18g** and **18h**. The most potent inhibitor of caspase-2 was the cis isomer **18g** with a k_2 value of 26200

Table 1. Inhibition of Caspases by Aza-Peptide Michael Acceptors

Inhibitor	k_2 [a] ($M^{-1} s^{-1}$)						
	Caspase-2	Caspase-3	Caspase-6	Caspase-7	Caspase-8	Caspase-9	Caspase-10
16a Cbz-Val-AAsp-CH═CH−CH_3	ND	NI	NI	ND	NI	ND	ND
16b Cbz-Val-AAsp-CH═CH−CH═CH−CH_3	NI	NI	NI	NI	NI	NI	NI
16c Cbz-Val-AAsp-CH═CH−CH_2CH_2Ph	ND	NI	NI	ND	NI	ND	ND
16d Cbz-Val-AAsp-CH═CH−Cl	NI	NI	NI	NI	NI	NI	NI
16e Cbz-Val-AAsp-CH═CH-4-Cl−Ph	NI	NI	NI	NI	NI	NI	NI
16h Cbz-Val-AAsp-CH═CH−COOEt	NI	8000	NI	2680 ± 60	NI	5240 ± 380	389 ± 87
16j Cbz-Val-AAsp-CH═CH−CONH-*n*Bu	NI	184 ± 9	NI	55 ± 5	NI	32 ± 13	NI
16l Cbz-Val-AAsp-CH═CH−$CONHCH_2Ph$	NI	185	NI	60 ± 1	NI	20 ± 2	NI
17h Cbz-Glu-Val-AAsp-CH═CH−COOEt	90 ± 10	38600 ± 4200	3540 ± 4200	52400 ± 10600	244000 ± 30000	32900 ± 10250	8940 ± 5250
18f Cbz-Asp-Glu-Val-AAsp-CH═CH−COPh	165 ± 85	122000	1800 ± 13	10800 ± 2000	9720 ± 500	ND	930 ± 80
18g Cbz-Asp-Glu-Val-AAsp-CH═CH−COOEt (cis)	26200 ± 6000	1060000 ± 92500	11000 ± 515	139000 ± 4500	181000 ± 13700	ND	13500 ± 2300
18h Cbz-Asp-Glu-Val-AAsp-CH═CH−COOEt (trans)	2640 ± 10	2130000 ± 99130	35575 ± 0	239000 ± 55600	272960 ± 18370	ND	49900 ± 7000
18i Cbz-Asp-Glu-Val-AAsp-CH═CH−$COOCH_2Ph$	ND	1700000 ± 106000	8470	114000 ± 15900	121000 ± 13700	ND	28300 ± 7700
18l Cbz-Asp-Glu-Val-AAsp-CH═CH−$CONHCH_2Ph$	130 ± 20	1750000 ± 18500	3210 ± 105	249000 ± 52500	78235 ± 8000	2010 ± 150	19400 ± 400
18m Cbz-Asp-Glu-Val-AAsp-CH═CH−$CONHCH_2$-4-F-Ph	130 ± 20	2100000 ± 26400	4400 ± 361	329000 ± 53300	85100 ± 9700	900 ± 70	37700 ± 2550
18n Cbz-Asp-Glu-Val-AAsp-CH═CH−$CONHCH_2CH_2Ph$	120 ± 10	1950000 ± 53000	3470 ± 52	267000 ± 15000	129000 ± 27400	655 ± 50	31400 ± 3600
18o Cbz-Asp-Glu-Val-AAsp-CH═CH−$CON(CH_3)CH_2Ph$	660 ± 240	2640000 ± 397000	9500 ± 210	275000 ± 11300	90300 ± 18250	820 ± 215	29400 ± 830
18p Cbz-Asp-Glu-Val-AAsp-CH═CH−$CON(CH_3)CH_2CH_2Ph$	320 ± 25	1180000 ± 264000	4000 ± 413	172000 ± 72000	31900 ± 2800	425 ± 10	9570 ± 5240
18r Cbz-Asp-Glu-Val-AAsp-CH═CH−$CON(CH_2Ph)_2$	110 ± 25	3000000 ± 80000	5100 ± 0	359000 ± 8400	8600 ± 1600	450 ± 30	6300 ± 50
18t Cbz-Asp-Glu-Val-AAsp-CH═CH−$CON(CH_2$-1-Naphth$)_2$	410 ± 60	5620000 ± 1120000	29700 ± 540	875000 ± 106000	9460 ± 880	150 ± 10	32500 ± 5250
18u Cbz-Asp-Glu-Val-AAsp-CH═CH−CON-tetrahydroquinoline	390 ± 90	2300000 ± 26500	5700 ± 0	137000 ± 25000	118000 ± 14800	340 ± 120	8330 ± 1400
19h Cbz-Val-Glu-Val-AAsp-CH═CH−COOEt	115 ± 20	41200 ± 8600	83600 ± 8400	3650 ± 1330	175800 ± 6800	340 ± 120	6600 ± 690
20h Cbz-Ile-Glu-Thr-AAsp-CH═CH−COOEt	300 ± 160	6740 ± 1650	88700 ± 33700	530 ± 10	56500 ± 3800	ND	6900 ± 250
20i Cbz-Ile-Glu-Thr-AAsp-CH═CH−$COOCH_2Ph$	110 ± 40	2300 ± 77	23350 ± 1650	660 ± 210	148400	ND	15200 ± 2500
20k Cbz-Ile-Glu-Thr-AAsp-CH═CH−CONHPh	365 ± 20	7030 ± 720	99200 ± 10800	920 ± 60	245000 ± 22800	940 ± 275	9210 ± 377
20l Cbz-Ile-Glu-Thr-AAsp-CH═CH−$CONHCH_2Ph$	15 ± 3	2250 ± 560	16800 ± 1030	100 ± 20	61300 ± 2300	440 ± 160	503 ± 209
20n Cbz-Ile-Glu-Thr-AAsp-CH═CH−$CONHCH_2CH_2Ph$	30 ± 0	4750 ± 565	18700 ± 1250	440 ± 95	71000 ± 13700	615 ± 160	8290 ± 1560
20o Cbz-Ile-Glu-Thr-AAsp-CH═CH−$CON(CH_3)CH_2Ph$	95 ± 8	6000 ± 100	45900 ± 5000	390 ± 90	59700 ± 4500	845 ± 190	8500 ± 300
20p Cbz-Ile-Glu-Thr-AAsp-CH═CH−$CON(CH_3)CH_2CH_2Ph$	38 ± 1	5480 ± 26	ND	1020 ± 440	60500 ± 8000	760 ± 335	8770 ± 1780
20r Cbz-Ile-Glu-Thr-AAsp-CH═CH−$CON(CH_2Ph)_2$	76 ± 1	9570 ± 1230	83900 ± 29000	1140 ± 210	39500 ± 0	1930 ± 35	7930 ± 2510
21h Cbz-Leu-Glu-Thr-AAsp-CH═CH−COOEt	NI	5560 ± 290	18700 ± 1040	NI	237000 ± 52700	37 ± 0	NI
21i Cbz-Leu-Glu-Thr-AAsp-CH═CH−$COOCH_2Ph$	480 ± 170	4600 ± 330	47600 ± 2500	1570 ± 135	98400 ± 9130	ND	18900 ± 1580
21k Cbz-Leu-Glu-Thr-AAsp-CH═CH−CONHPh	290 ± 150	4700 ± 308	11400 ± 2060	730 ± 200	176000 ± 2280	1190 ± 230	6050 ± 1380
21l Cbz-Leu-Glu-Thr-AAsp-CH═CH−$CONHCH_2Ph$	66 ± 25	1120	1550 ± 50	340 ± 15	70170 ± 13700	1400 ± 260	14400 ± 1900
21m Cbz-Leu-Glu-Thr-AAsp-CH═CH−$CONHCH_2$-4-F-Ph	70 ± 1	4490 ± 410	3100 ± 465	410 ± 60	171000 ± 36500	1695 ± 30	9380 ± 1560
21n Cbz-Leu-Glu-Thr-AAsp-CH═CH−$CONHCH_2CH_2Ph$	110 ± 40	5400 ± 51	2150 ± 52	440 ± 60	121000 ± 2300	1760 ± 190	17900 ± 2300
21o Cbz-Leu-Glu-Thr-AAsp-CH═CH−$CON(CH_3)CH_2Ph$	140 ± 25	6000 ± 100	10800 ± 410	520 ± 60	169000	4320 ± 930	8430 ± 710
21p Cbz-Leu-Glu-Thr-AAsp-CH═CH−$CON(CH_3)CH_2CH_2Ph$	50 ± 10	2620 ± 26	2550 ± 413	290 ± 170	65300 ± 5700	960 ± 30	6190 ± 820
21r Cbz-Leu-Glu-Thr-AAsp-CH═CH−$CON(CH_2Ph)_2$	110 ± 10	8630 ± 1330	14100 ± 1440	760 ± 100	129000 ± 13700	1105 ± 460	8080 ± 1660
21s Cbz-Leu-Glu-Thr-AAsp-CH═CH−$CON(CH_3)CH_2$-1-Naphth	290 ± 110	11200 ± 1130	21700 ± 206	1100 ± 35	179000 ± 38800	5030 ± 555	13600 ± 970
21t Cbz-Leu-Glu-Thr-AAsp-CH═CH−CON-tetrahydroquinoline	92 ± 51	12100 ± 720	13000 ± 1850	540 ± 30	216000 ± 4600	1660 ± 710	9000 ± 500
Cbz-Val-Ala-Asp-CH_2F (Z-VAD-FMK)[b]	290	16000	7100	18000	280000	180000	ND

NI = no inhibition, ND = not determined, Cbz = $PhCH_2$-OCO-. [a]Assay buffer for caspase-2, -3, -6, -7, and -8 was 20 mM PIPES, 100 mM NaCl, 0.1% (w/v) CHAPS, sucrose 10% (w/v), and 10 mM DTT, at pH 7.2. Caspase-9 assays were performed in 100 mM HEPES, 50 mM NaCl, 0.05% (w/v) CHAPS, sucrose 10% (w/v), and 10 mM DTT, at pH 7.0. Caspase 10 assays were performed in 100 mM HEPES, 0.1% (w/v) CHAPS, PEG 10% (w/v), and 10 mM DTT at pH 7.0. [b] Inhibition data for the widely use fluoromethyl ketone capase inhibitor Z-VAD-FMK from Garcia-Calvo et al.[38] is shown for comparison.

M^{-1} s^{-1}. **18g** was 10-fold more reactive than the trans isomer **18h** (k_2 = 2640 M^{-1} s^{-1}). This result was interesting since for the other caspases (3, 6, 7, 8, 9, and 10) **18g** was less potent when compared to its trans isomer **18h**. The order of reactivity of the inhibitors with the DEVD sequence according to the substituent Y is as follows: COOEt (cis) > COOEt (trans) > $CON(CH_3)CH_2Ph$ > $CON(CH_2$-1-Naphth$)_2$ > CON-tetrahydroquinoline > $CON(CH_3)CH_2CH_2Ph$ > COPh > $CONHCH_2$-Ph > $CONHCH_2$-4-F-Ph > $CONHCH_2CH_2Ph$ > $CON(CH_2Ph)_2$. It seems that the esters are the best substitutents and the disubstituted amides are more preferred over the monosubstituted amides.

Caspase-3. Considerably high rates were obtained for the inhibitors with the caspase-3 specific DEVD sequence against caspase-3. The most potent caspase-3 inhibitor was **18t** (Cbz-Asp-Glu-Val-AAsp-*trans*-CH═CH−$CON(CH_2$-1-Naphth$)_2$) with a second-order inhibition rate of 5620000 M^{-1} s^{-1}. With caspase-3, the order of reactivity of the inhibitors with various substituents on the double bond moiety is $CON(CH_2$-1-Naphth$)_2$ > $CON(CH_2Ph)_2$ > $CON(CH_3)CH_2Ph$ > CON-tetrahydroquinoline > CO_2Et (trans) > $CONHCH_2$-4-F-Ph > $CONHCH_2CH_2Ph$ > $CONHCH_2Ph$ > CO_2CH_2Ph > $CON(CH_3)CH_2CH_2Ph$ > CO_2Et (cis) > COPh. Generally, the bulky aromatic groups were preferred in the prime site of this enzyme. The disubstituted amide derivatives worked better than the monosubstituted ones and the ester derivatives. Replacement of the amide or the ester group by a carbonyl group caused a decrease in potency by 10-fold. The ketone **18f** (Cbz-Asp-Glu-Val-AAsp-*trans*-CH═CH−COPh) inhibits caspase-3 more slowly with a k_2 value of 122000 M^{-1} s^{-1}. The ester **18g**, the inhibitor with the cis configuration of the double bond moiety is a potent inhibitor of caspase-3 (k_2 = 1060000 M^{-1} s^{-1}). However, the trans ethyl ester derivative **18h** is twice as potent against caspase-3 (k_2 = 2130000 M^{-1} s^{-1}). Considerable decrease in potency was observed with the EVD sequence based inhibitor **17h** (k_2 = 38600 M^{-1} s^{-1}) with caspase-3, which emphasizes the importance of an acidic P4 residue for increased potency. In addition, our caspase-3 inhibitors are equally if not more potent than chloromethyl ketone inhibitors such as Cbz-DEVD-CMK which has a k_2/K_I value of 1000000 M^{-1} s^{-1}.[11] More importantly, the aza-peptide Michael acceptors are much more selective (see the Cross-Reactivity Section).

Caspase-7. The DEVD sequence worked also best with caspase-7. The second-order rate constants were in the range of 10^5 M^{-1} s^{-1}. Cbz-Asp-Glu-Val-AAsp-*trans*-CH═CH−$CON(CH_2$-1-Naphth$)_2$ (**18t**) is the most potent inhibitor with a second-order rate constant of 875000 M^{-1} s^{-1}. The order of reactivity with the substituted Y (Figure 3) group among the DEVD series is as follows: $CON(CH_2$-1-Naphth$)_2$ > $CON(CH_2Ph)_2$ > $CONHCH_2$-4-F-Ph > $CON(CH_3)CH_2Ph$ > $CONHCH_2CH_2Ph$ > $CONHCH_2Ph$ > CO_2Et (trans) > $CON(CH_3)CH_2CH_2Ph$ > CO_2Et (cis) > CON-tetrahydroquinoline > CO_2CH_2Ph > COPh. Similar to caspase-3, bulky aromatic groups such as benzyl or naphthyl groups which extend deep into the pocket are preferred at the caspase-7 S′ subsite. There is no distinct preference for disubstituted amide group preference as in the case of caspase-3. However, amide substituents still work generally better than the esters. The fluorophenyl derivative **18m** (Cbz-Asp-Glu-Val-AAsp-*trans*-CH═CH−$CONHCH_2$-4-F-Ph) is still the best monosubstituted amide inhibitor for both caspase-3 and caspase-7. There is also a decrease in potency with the tripeptide inhibitor **17h** (k_2 = 52400 M^{-1} s^{-1}) indicating that the P4 amino acid is an important factor in potency with caspase-7.

Caspases-6 and -8. The IETD sequence works best with caspase-6, whereas the LETD sequence is ideal for caspase-8. Caspase-8 prefers leucine > valine > aspartic acid at its P4 position. This preference offers some room for obtaining selectivity of caspase-8 over caspase-6, where caspase-6 prefers valine > threonine > leucine at the same position (P4).[27] The best caspase-6 inhibitor is **20k** (Cbz-Ile-Glu-Thr-AAsp-CH═CH−CONPh) with a k_2 value of 99200 M^{-1} s^{-1}. Unfortunately, this inhibitor also potently inactivates caspase-8 (k_2 = 245000 M^{-1} s^{-1}). The order of reactivity with differing Y groups for caspase-6 within the IETD sequence is as follows: CONHPh > CO_2Et (trans) > $CON(CH_2Ph)_2$ > $CON(CH_3)CH_2Ph$ > CO_2CH_2Ph > $CONHCH_2CH_2Ph$ > $CONHCH_2Ph$. There is no distinct preference for any substitution pattern at the caspase-6 S′ subsite. The monosubstituted amide derivative **20k** is the most preferred, but the disubstituted amide derivatives **20o**, **20p**, and **20r** are also potent inhibitors. The other caspase-6 specific sequence (VEVD) also yielded very potent inhibition. The inhibitor **19h** (Cbz-Val-Glu-Val-AAsp-CH═CH−COOEt) inhibits caspase-6 with a k_2 value of 83600 M^{-1} s^{-1}. However, the VEVD sequence seems to be less selective. Not only does it inhibits caspase-8 potently (k_2 = 175800 M^{-1} s^{-1}), it also inhibits caspase-3 with a k_2 of 41200 M^{-1} s^{-1}.

Although the LETD sequence is determined to be the best one for caspase-8, other caspase-specific sequences are also preferred by this enzyme. The most potent caspase-8 inhibitor is the one that is actually designed for caspase-3 with the DEVD sequence. Hence, **18h** (Cbz-Asp-Glu-Val-AAsp-*trans*-CH═CH−COOEt) has a second-order rate constant of 272960 M^{-1} s^{-1} with caspase-8. Also, the inhibitor **20k** with the IETD sequence is a very potent caspase-8 inhibitor (k_2 = 245000 M^{-1} s^{-1}). The same Y group (CONHPh) when attached to a LETD sequence (**21k**) makes a less potent inhibitor with caspase-8 (k_2 = 176000 M^{-1} s^{-1}). For the inhibitors with the LETD sequence the order of reactivity with caspase-8 with differing Y groups is as follows: COOEt (trans) > CON-tetrahydroquinoline > $CON(CH_3)CH_2$-1-Naphth > CONHPh > $CONHCH_2$-4-F-Ph > $CON(CH_3)CH_2Ph$ > $CON(CH_2Ph)_2$ > $CONHCH_2CH_2Ph$ > $COOCH_2Ph$ > $CON(CH_3)CH_2CH_2Ph$ > $CONHCH_2Ph$. The inhibitor **21h** (Cbz-Leu-Glu-Thr-AAsp-*trans*-CH═CH−COOEt) is the best one among this series with a k_2 value of 237000 M^{-1} s^{-1}. The tetrahydroquinoline derivative **21u** (Cbz-Leu-Glu-Thr-AAsp-*trans*-CH═CH−CON-tetrahydroquinoline) is less potent than the ethyl ester derivative **21h**, but it is more selective over caspase-6. Interestingly, one of the most potent caspase-8 inhibitors is the tripeptide derivative **17h** (Cbz-Glu-Val-AAsp-*trans*-CH═CH−COOEt) with a k_2 value of 244000 M^{-1} s^{-1}. In general, higher rates were obtained with caspase-8 where Y is a small sized group such as ethyl and when Y is not extending deeply into the S′ subsite.

Caspase-9. The rates of inhibition of caspase-9 by the aza-peptide Michael acceptors are not as high as the other members of the caspase family we have tested. However, the LETD is still the best sequence with rates in the range of $10-10^3$ M^{-1} s^{-1}. The best inhibitors are **21s** and **21o** with k_2 values of 5030 M^{-1} s^{-1} and 4320 M^{-1} s^{-1}, respectively. However, the most potent caspase-9 inhibitor is the tripeptide derivative **17h** (Cbz-Glu-Val-AAsp-*trans*-CH═CH−COOEt) with a k_2 value of 32900 M^{-1} s^{-1}. Surprisingly, a considerable decrease in potency is observed with the same Y group (ethyl) when attached to a tetrapeptide sequence. The inhibitor **21h** (Cbz-Leu-Glu-Thr-AAsp-*trans*-CH═CH−COOEt) inhibits caspase-9 very weakly (k_2 = 37 M^{-1} s^{-1}).

Table 2. Cross Reactivity of Caspase Inhibitors with Clan CA and Other Clan CD Enzymes[a]

		k_2 (M^{-1} s^{-1})					
	Inhibitor	Cathepsin B	Papain	Calpain	Legumain	Clostripain	Gingipain K
18h	Cbz-Asp-Glu-Val-AAsp-CH═CH−COOEt	NI	NI	NI	NI	NI	NI
18i	Cbz-Asp-Glu-Val-AAsp-CH═CH−$COOCH_2Ph$	NI	ND	ND	ND	NI	NI
18l	Cbz-Asp-Glu-Val-AAsp-CH═CH−$CONHCH_2Ph$	NI	ND	ND	ND	NI	NI
21i	Cbz-Leu-Glu-Thr-AAsp-CH═CH−$COOCH_2Ph$	<10	NI	<10	NI	NI	NI

[a] NI = No inhibition, ND = not determined. Enzymes: human liver cathepsin B, papaya latex papain, calpain I from porcine erythrocytes, *S. mansoni* legumain, clostripain from *Clostridium histolyticum*, gingipain K from *Porphyromonas gingivalis*.

Caspase-10. The best inhibitors of caspase-10 have the caspase-3 optimal sequence DEVD. The rates of inhibition are in the range of 10^3-10^4 M^{-1} s^{-1} and the best inhibitor is Cbz-Asp-Glu-Val-AAsp-*trans*-CH═CH−COOEt (**18h**, k_2 = 49900 M^{-1} s^{-1}). The order of reactivity with differing Y groups with the DEVD sequence is as follows: COOEt (trans) > CON-HCH_2-4-F-Ph > $CON(CH_2$-1-Naphth$)_2$ > $CONHCH_2CH_2Ph$ > $CON(CH_3)CH_2Ph$ > $COOCH_2Ph$ > $CONHCH_2Ph$ > COOEt (cis) > $CON(CH_3)CH_2CH_2Ph$ > CON-tetrahydroquinoline > $CON(CH_2Ph)_2$. The tripeptide inhibitor **17h** works equally well as some of the tetrapeptide inhibitors with caspase-10 (k_2 = 8940 M^{-1} s^{-1}). Once again, this result indicates that with group II caspases (6, 8, 9, 10) the absence of the P4 residue is not as crucial as for group III caspases (2, 3, 7) for potency and selectivity.

Caspase Selectivity. In general, the most potent inhibitors of a target caspase were the ones that were designed with its ideal substrate sequence, although caspases-8, -9, and -10 were exceptions in some cases. Interestingly, the most specific inhibitors while still very potent were not the most potent ones. The most specific inhibitor for caspase-3 was Cbz-Asp-Glu-Val-AAsp-*trans*-CH═CH−$CON(CH_2Ph)_2$ (**18r**, k_2 = 3000000 M^{-1} s^{-1}), which is 27300, 588, 8.4, 348, 6670, and 476-fold more selective for caspase-3 over caspases-2, -6, -7, -8, -9, and -10, respectively. The most specific caspase-6 inhibitor was Cbz-Ile-Glu-Thr-AAsp-*trans*-CH═CH−COOEt (**20h**, k_2 = 88,700 M^{-1} s^{-1}). It is 296, 13.2, 167, 1.6, and 12.9-fold more selective for caspase-6 over caspases-2, -3, -7, -8, and -10, respectively. The most selective caspase-8 inhibitor was Cbz-Leu-Glu-Thr-AAsp-*trans*-CH═CH−COOEt (**21h**, k_2 = 237000 M^{-1} s^{-1}), which is 42.6, 12.6, and 6400-fold more selective for caspase-8 over caspases-3, -6, and -9, respectively.

The selectivity of the aza-peptide Michael acceptor inhibitors with the DEVD sequence for caspase-3 over caspase-7 is 6.9−17-fold. Selectivity between caspase-3 and caspase-7 was hard to achieve, since the DEVD sequence is ideal for both enzymes. The selectivity of caspase-3 over caspase-2 is as high as 10^5 fold, because of the P5 requirement of caspase-2. The selectivity for caspase-3 over caspase-6 is usually around 500-fold. However, when one obtained selectivity over caspase-6, it was difficult to obtain selectivity also for caspase-8. The range of selectivity for caspase-3 over caspase-8 was only up to 37-fold, except in the case of the inhibitor **18r**. It has been previously shown that the prime site of caspase-8 differs from that of the other caspases by the presence of a helix-turn-helix insertion ranging from residues 245−253, which is unique to caspase-8.[32] Clearly, we have taken advantage of this structural difference by designing an inhibitor with a dibenzyl amide substituent on the double bond moiety, which resulted in optimal selectivity. Generally, caspase-10 behaved similarly to caspase-8; however, it yielded less potent inhibitors. Last, the rates of inhibition of caspase-9 were quite low when compared to the other caspases (3, 6, 7, 8, and 10).

In addition to the tri- and tetrapeptidyl aza-peptide Michael acceptors we also made several dipeptidyl derivatives with the VD sequence in the hopes of obtaining a potent and broad spectrum inhibitor for caspases. Due to enhanced aqueous solubility, it has been previously shown that the fluoromethyl ketone inhibitor Z-VD-fmk was more active than the tri- and tetrapeptide based inhibitors such as Z-VAD-fmk in certain cell culture models of apoptosis.[33] Unfortunately, our dipeptide inhibitor Cbz-Val-AAsp-*trans*-CH═CH−COOEt (**16h**) weakly inactivated caspase-3 (k_2 = 8000 M^{-1} s^{-1}), caspase-7 (k_2 = 2680 M^{-1} s^{-1}), caspase-9 (k_2 = 5260 M^{-1} s^{-1}) and caspase-10 (k_2 = 389 M^{-1} s^{-1}). It did not show any inhibition of caspases-2, -6, or -8. The two amide derivatives **16j** and **16l** showed little potency toward caspase-3 (k_2 values are 184 M^{-1} s^{-1} and 185 M^{-1} s^{-1}, respectively), caspase-7 (k_2 values are 55 M^{-1} s^{-1} and 60 M^{-1} s^{-1}, respectively), caspase-9 (k_2 values are 32 M^{-1} s^{-1} and 20 M^{-1} s^{-1}, respectively), but no activity against caspases-2, -6, -8 or -10. The dipeptidyl aza-peptide Michael acceptors with simple alkyl, alkenyl or halogen substituents remained unreactive toward all the caspases (2, 3, 6, 7, 8, 9, and 10). The decreased potency of the dipeptide derivatives toward caspases is in accordance with the previous observation of the requirement of at least tripeptides for effective binding and recognition.

Cross Reactivity with Clan CA and Other Clan CD Proteases. The aza-peptide Michael acceptors designed for caspases show little to no inhibition of the clan CA cysteine proteases papain, cathepsin B, and calpain, where the specificity is determined primarily by the S2 subsite. The inhibitors **18h**, **18i**, **18l**, and **21i** showed essentially no inhibition against papain, cathepsin B, and calpain after an incubation period of 1 h (Table 2).

We also tested the cross reactivity of our inhibitors with other members of clan CD proteases such as legumain, clostripain, and gingipain K. Legumain has a strict requirement for Asn at P1, whereas clostripain and gingipain K prefer Orn and Lys at the same position. Aza-peptide Michael acceptors designed for caspases did not show any activity against those enzymes after being incubated for 1 h. Likewise, the aza-peptide Michael acceptor inhibitors with legumain, clostripain, and gingipain K specific sequences did not show any cross reactivity with clan CA enzymes or with each other.[23] Clearly, the aza-peptide Michael acceptor design is highly specific for clan CD enzymes.

Stability Studies. We tested the stability of the aza-peptide Michael acceptors toward simple thiol nucleophiles such as thiol DTT contained in the caspase assay buffer. A representative group of inhibitors (2.5−4 mM) were treated with 10 mM DTT in the caspase assay buffer with a pH of 7.2 at 25 °C. The reactivity of the Michael acceptor double bond was monitored by UV spectrum at 250 nm for a period of 15 h. The half-lives were obtained from first-order rate plots of $\ln(A_t/A_0)$ versus time.

We observed that the ester derivative **18h** (Cbz-Asp-Glu-Val-AAsp-CH═CH−COOEt) had a half-life of 10 min. The amide substituted Michael acceptors appeared to be less reactive toward DTT under the same conditions. The monosubstituted amide derivative **18l** (Cbz-Asp-Glu-Val-AAsp-CH═CH−$CONHCH_2Ph$) had a half-life of 58 min, where the disubstituted

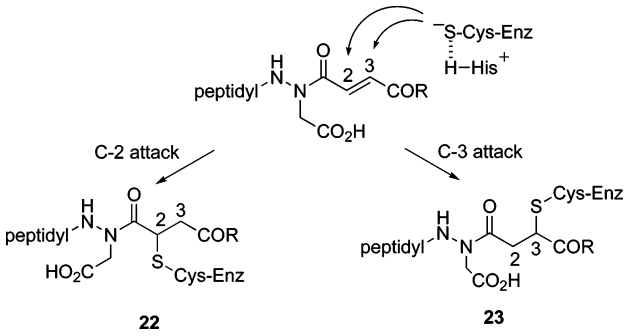

Figure 4. Proposed mechanism of inhibition of caspases by aza-peptide Michael acceptors.

amide derivative **18o** (Cbz-Asp-Glu-Val-AAsp-CH═CH−CON-$(CH_3)CH_2Ph$) was twice as long stable with a half-life of 116 min. The dienyl derivative **16b** (Cbz-Val-AAsp-CH═CH−CH═CH−CH_3) was essentially stable over the period of 15 h of monitoring.

Aza-peptide Michael acceptors designed for other clan CD proteases such as legumain, gingipain, and clostripain specific sequences were also tested for stability against DTT.[23] The half-life of the legumain inhibitor Cbz-Ala-Ala-AAsn-CH═CH−COOEt in the legumain assay buffer (pH = 5.8) with excess DTT was 19 min. When tested at a higher pH (6.8) the half-life of the same inhibitor was shortened to 3.7 min.

It should be noted that the pH of the assay buffer has a considerable effect on the stability of the inhibitors against DTT. The DTT thiol has a pK_a value of 9.2. The lower the pH, the lower is the concentration of the deprotonated thiol group of DTT. Hence, a nucleophilic attack on the Michael acceptor double bond is more favored at higher pH values.

We also anticipate that the nature of the P′ substituent on the double bond contributes significantly to the overall stability of the inhibitor. In general, the order of stability of our inhibitors is as follows: alkyl > amide > ester. It has been previously demonstrated by Freidig and co-workers that simple acrylates are more reactive than simple acrylamides to thiol nucleophiles such as glutathione.[34] Ethyl acrylate reacts with glutathione 85 times faster than ethyl acrylamide with second-order rate constants of 0.66 M^{-1} s^{-1} and 7.8 × 10^{-3} M^{-1} s^{-1}, respectively. Our results of the reactivity of the ester and amide substituted inhibitors indicate a strong correlation with the observed reactivity of acrylates and acrylamides with glutathione.

Mechanism of Inhibition. In general, the inactivation of cysteine proteases by Michael acceptor inhibitors proceeds through the nucleophilic attack of the active site cysteine thiol group on the C3-carbon of the Michael acceptor double bond. The mechanism of inhibition of caspases by aza-peptide Michael acceptors could involve irreversible thioalkylation of the active site Cys by the two pathways shown in Figure 4. Theoretically, if the substituent on the double bond is an acyl derivative such as ester or amide, the formation of both thioether adducts **22** and **23** is possible upon a nucleophilic attack taking place either at the C-2 or C-3 carbon on the double bond moiety. If the substituent is a simple alkyl or halogen, only the C-3 carbon is the possible site for the Michael addition reaction.

On the basis of the results of the NMR study and the stability studies of our inhibitors with DTT, we previously hypothesized that a nucleophilic attack of the active site thiol group at the C-2 would be more favorable.[23] However, to determine conclusively the point of attack, crystal structures of five caspase-double bond complexes were determined.

X-ray Structure Analysis of Caspase−Inhibitor Complexes. We have determined four crystal structures of caspase-3−inhibitor complexes and the structure of one caspase-8−inhibitor complex (Tables 3 and 4). The Michael acceptors used for the structural studies with caspase-3 are the two stereoisomers (cis and trans) of the ethyl ester derivative (**18g** and **18h**), a benzyl ester derivative (**18i**), and a *N*-methyl-*N*-benzyl amide derivative (**18o**). We have determined the structure of caspase-8 complexed with **21t** which is a tetrahydroisoquinoline derivative. These inhibitor complexes are unique since they have inhibitor moieties which interact with S′ subsites of the enzyme unlike most caspase−inhibitor complex structures published to date.

The overall structures of the polypeptide chain in the complexes are quite similar to the other known crystal structures of the caspase family.[35−38] The superposition of the Cα atoms

Table 3. X-ray Data Collection Statistics of the Caspase:Michael Acceptor Complex Crystals

	Caspase-3: Cbz-DEVaD-CH═CH−CO_2Et (trans) **18h**	Caspase-3: Cbz-DEVaD-CH═CH−CO_2Et (cis) **18g**	Caspase-3: Cbz-DEVaD-CH═CH−CO_2Bzl **18i**	Caspase-3: Cbz-DEVaD-CH═CH−CON(CH_3)Bzl **18o**	Caspase-8: Cbz-LETaD-CH═CH−CO-tetrahydroquinoline **21t**
Resolution range (Å)	20−1.76	20−1.86	20−1.93	20−2.45	10−1.95
(last shell)	(1.86−1.76)	(1.96−1.86)	(2.03−1.93)	(2.58−2.45)	(2.05−1.95)
Unique reflections	25781 (3441)	22830 (2606)	19537 (2531)	10094 (1402)	21841 (1561)
Redundancy	4.3 (4.0)	5.0 (4.7)	3.3 (3.1)	5.8 (5.4)	12 (13)
R_{merge} (%)	5.4 (20.8)	7.6 (43.9)	7.8 (26.2)	7.9 (24.3)	5.2 (9.0)
Completeness (%)	95.3 (87.8)	97.8 (84.1)	94.3 (85)	99.2 (95.8)	98.5 (99.5)
Average I/σ	19.1 (6.6)	17.3 (4.5)	12.8 (4.2)	19.6 (7.0)	36.4 (24.7)

Table 4. Refinement Statistics of Caspase:Michael Acceptor Crystal Structures

	Caspase-3: Cbz-DEVaD-CH═CH−CO_2Et (trans) **18h**	Caspase-3: Cbz-DEVaD-CH═CH−CO_2Et (cis) **18g**	Caspase-3: Cbz-DEVaD-CH═CH−CO_2Bzl **18i**	Caspase-3: Cbz-DEVaD-CH═CH−CON(CH_3) Bzl **18o**	Caspase-8: Cbz-LETaD-CH═CH−CO-tetrahydroquinoline **21t**
Resolution (Å)	20−1.76	20−1.86	20−1.93	20−2.45	10−1.95
R_{cryst}	15.9	18.4	16.1	16.8	16.8
R_{free}	18.4	21.5	19.7	21.0	20.1
			Number of Atoms		
Protein	1996	1996	1996	1996	1912
Ligand	49	49	54	55	56
Water	419	303	363	303	411
			Average *B*-Factors		
Protein (Å^2)	11.94	15.47	13.4	19.73	17.3
Ligand (Å^2)	18.98	30.7	29.5	42.5	23.1
Water (Å^2)	33.61	31.8	33.3	27.0	37.0
PDB accession code	2C1E	2C2K	2C2M	2C2O	2C2Z

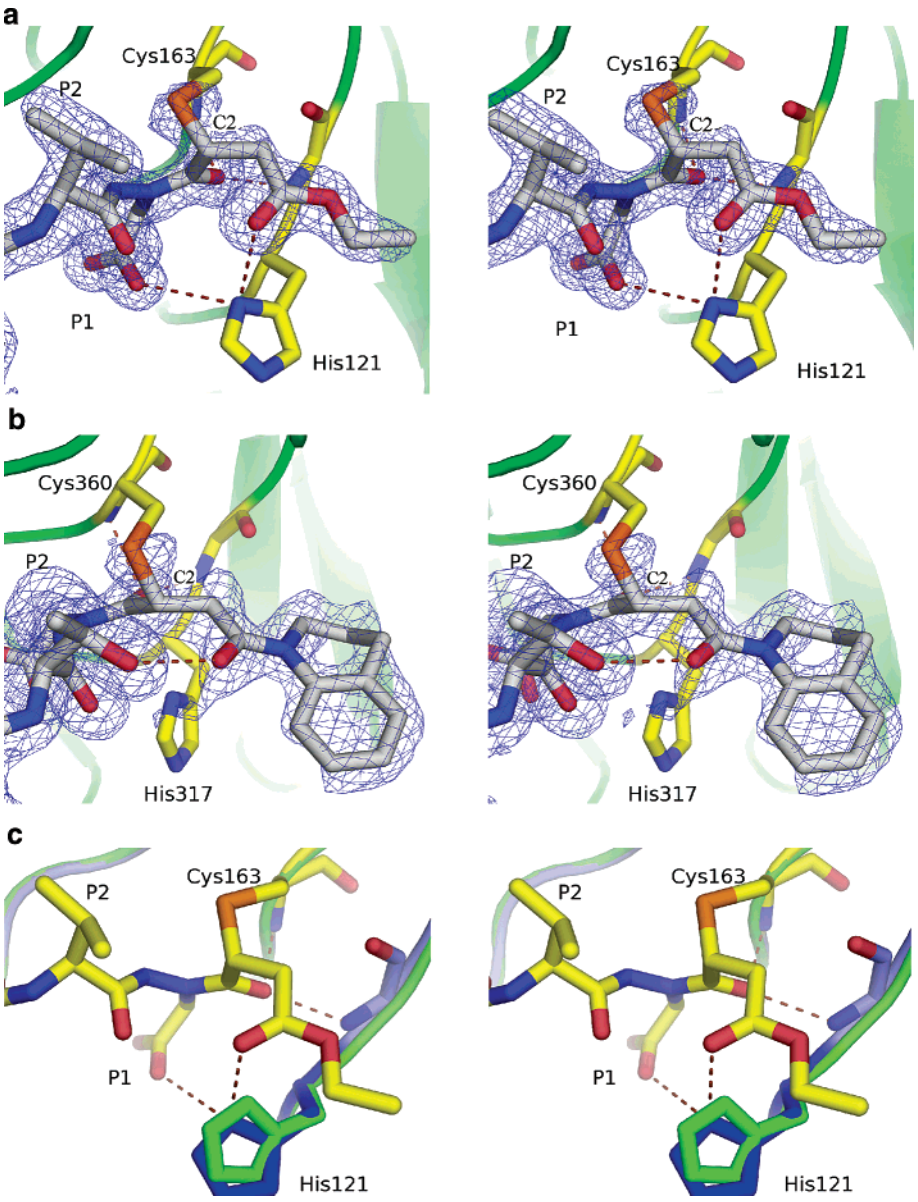

Figure 5. Stereoview of the atomic model of (a) caspase-3 in complex with the trans Cbz-Asp-Glu-Val-AAsp-CH═CH−CO_2Et (**18h)** and (b) caspase-8 in complex with Cbz-Leu-Glu-Thr-AAsp-CH═CH−CO-tetrahydroisoquinoline (**21t)** overlaided with an electron density map contoured at 1.0 s. Potential hyrdogen bond interaction are drawn in brown dashed lines. The residues involved in interaction with the inhibitor and catalytic dyad Cys163/His121 are highlighted. (c) Stereoview of the active site residues of caspase-3 in complex with the trans ethyl ester **18h** (blue) overlaided on top of structure of caspase-3:peptidyl aldehyde Ac-DEVD-CHO complex (green pdb code: 1PAU). The atoms of the inhibitor (**18h**) are highlighted in yellow. The catalytic His121 of **18h** complex is rotated approximately 20° about its Chi2 angle, which enables it to form a hydrogen bond with P1-Asp and P1′ carbonyl groups.

of the subunits result in a root-mean-square deviation of 0.2 Å for caspase-8 and 0.35 Å for caspase-3−inhibitor complexes. This indicates that large scale conformational transitions do not occur upon binding of the P′ portion of the inhibitor structure; however, conformational changes do occur in parts of the enzyme directly interacting with the inhibitor to improve the fit. The interactions of the P1−P4 moieties of the Michael acceptor inhibitors bind to the substrate binding cleft of the caspase active site similar to the structures previously observed in peptidyl aldehyde or peptidyl halogen methyl ketone inhibitor complexes[35−38] and closely mimick substrate binding from P1 to P4.

The high resolution crystal structures clearly demonstrate that the nucleophilic attack takes place at the C-2 carbon more precisely on the *re* face. This results in a covalent thioether bond between the C-2 carbon and the sulfur atom of the active site Cys residue. As a result of the nucleophilic attack, the hybridization of both the C-2 and C-3 carbons change from sp^2 to sp^3 yielding a tetrahedral C-3 carbon and a chiral tetrahedral C-2 carbon with the *R*-configuration (Figure 5a,b).

Caspase-3−Inhibitor Complexes. As observed in the crystal structures of caspases complexed with halomethyl ketones,[26,37] the P1 azapeptide carbonyl points toward the "oxyanion hole" and it is stabilized by the amide protons of Gly122 and Cys163. A unique feature of all the crystal structures of caspase-3 Michael acceptor complexes is the rotation of the catalytic His121 about Chi2 by approximately 20 deg. In this new orientation the imidazole ring is ideally placed to form a hydrogen bond to the carboxylate of P1−Asp (Figure 5c). The distance of this hydrogen bond ranges from 3.3 to 3.6 Å in our complexes. This interaction between the catalytic His121 and P1−Asp is not observed in any other caspase crystal structure reported so far. Apart from this interaction, His121 also forms a hydrogen bond to the azapeptide P1′ carbonyl. The interactions

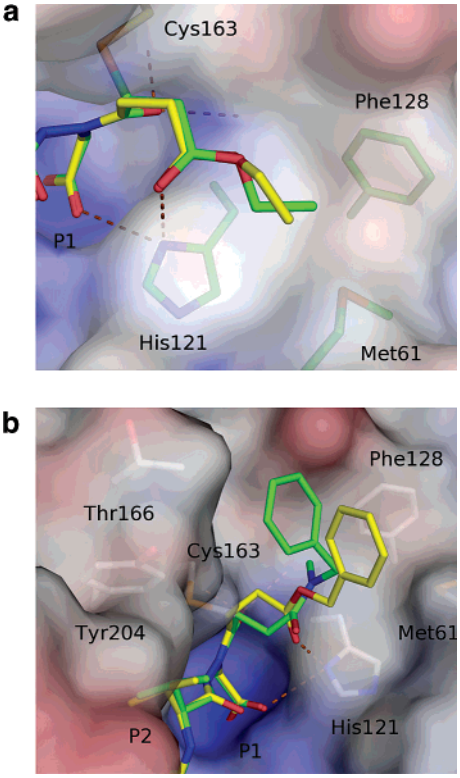

Figure 6. Surface representation of the active site of caspase-3 with the active site and prime site residues are highlighted. (a) Superposition of atoms of the ethyl ester inhibitor Cbz-Asp-Glu-Val-AAsp-CH═CH−COOEt (**18g**, cis isomer in yellow) and the ethyl ester **18h** (trans isomer in green). (b) Superposition of atoms of the trans benzyl ester inhibitor Cbz-Asp-Glu-Val-AAsp-CH═CH−$COOCH_2$Ph **18i** (in yellow) and the *N*-methylbenzyl amide derivative Cbz-Asp-Glu-Val-AAsp-CH═CH−$CON(CH_3)CH_2$Ph (**18o** (in green). The inhibitor **18i** is able to form a hydrogen bond with the catalytic His121 while **18o** is not involved in such an interaction.

of the P2 and P3 residues are similar to those reported in other caspase-3 structures.[35, 37]

The P1′ site in caspase-3 is predominantly hydrophobic, and it is defined by four loop regions. The 179-loop (between strand β1 and helix α2), the 240-loop (between strand β3 and helix α3), and the C-terminal loop belong to the alpha subunit, whereas the fourth loop (between strand β4 and helix α3) is from the β subunit. The approximate solvent accessible volume of the prime site cavity is 900 $Å^3$. In the Michael acceptor **18o**, the P1′ moiety is a *N*-methyl-benzyl amide derivative. The phenyl ring points toward the one side of the S1′ pocket and stabilized by hydrophobic contacts with Thr166 and Tyr204 while the *N*-methyl group is stabilized by Phe128 (Figure 6b). This is most reactive caspase-3 inhibitor of those studied crystallographically. In the case of the benzyl derivative **18i**, the electron density for the phenyl ring is not well defined as indicated by high *B* values. In the ethyl ester derivative formed from the cis and trans isomers **18h** and **18g**, the ethyl group interacts with the side chains of Phe128 and His121. To avoid steric hindrance and in tandem to maintain the hydrophobic contact with the ethyl group of the inhibitor, the side chain of Met61 of the 179-loop adopts a different conformation. This conformation is quite different from that observed in all other known caspase-3 structures. As expected, the atoms of the products formed from the two stereoisomers (**18g** and **18h**) of the ethyl ester overlay well on superposition. Additionally, in both structures, the C-2 carbon adopts a *R*-configuration indicating the attack is on the *re* face of the inhibitor (Figure 6a).

Caspase-8. Unlike in caspase-3:Michael acceptor inhibitor complexes, in the caspase-8 complex the P1′ carbonyl is stabilized by the side chain of P2-Thr instead of the catalytic His317. The P4-Leu is stabilized in the manner similar to the P4-Ile as exemplified in the crystal structure of caspase-8 complex with the peptidyl aldehyde Ac-IETD-CHO.[36] The phenyl ring of the capping residue Cbz in **21t** stacks favorably on top of Pro415, subsequently the puckering of this Pro is different from the one which is observed in other caspase-8−inhibitor complex structures.[36,38,39]

The S1′ site of caspase-8 is different from all other caspases due to the helix-turn-helix insertion in the 179-loop.[38] We have determined the structure of caspase-8 in complex with **21t**. This compound is a tetrahydroisoquinoline derivative in which the tetrahydroisoquinoline occupies the hydrophobic S1′ pocket defined by the residues Leu254, Ile257, and Tyr324 (Figure 7). As a consequence, this bulky hydrophobic moiety displaces the 179-loop by about 1.0 Å when compared to other caspase-8−inhibitor complexes. More importantly, significant changes in the side chain conformation of Arg258 are observed. Arg258 recognizes P3-Glu, and its backbone carbonyl is critical for maintaining a hydrogen bond with Nϵ1 of the catalytic His317. In the complex with **21t** the side chain of Arg258 is pointing toward Ser175 and in addition is involved in a hydrogen bond with the backbone carbonyl of Ser175. Such conformational

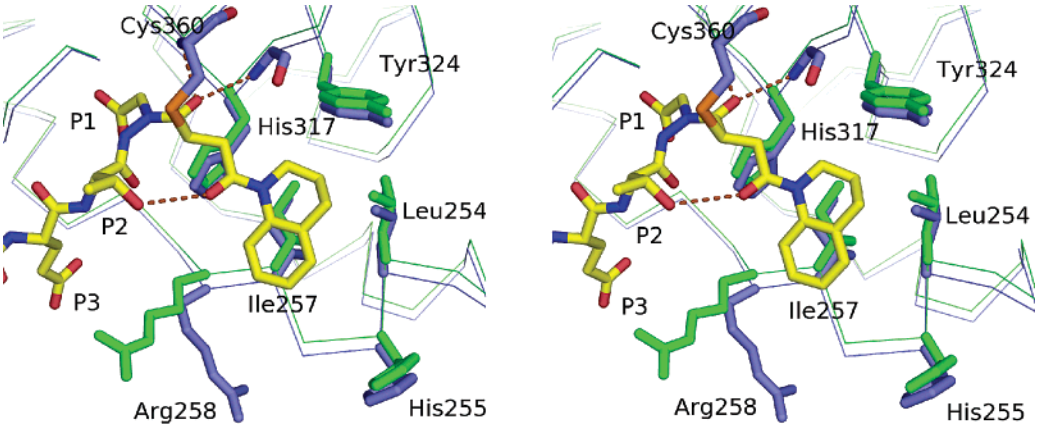

Figure 7. Superposition of the crystal structure of complex of caspase-8 with the inhibitor Cbz-Leu-Glu-Thr-AAsp-CH═CH−CON-tetrahydroquinoline (**21t** in blue) with the crystal structure of caspase-8:peptidyl aldehyde Ac-IETD-CHO (in green, pdb code 1QTN). Large scale movement of the 179-loop apart from the different conformation of Arg 258 are depicted. The hydrogen bond between the P1′ carbonyl and the side chain of P2-Thr is shown as a brown dashed line.

changes might cost binding energy, which in turn is compensated by the formation of favorable hydrogen bonds or by hydrophobic interactions. Such differences are particularly observed in caspase-8, as it has a unique helix-turn-helix insertion loop at that site.[38]

Stereochemistry. In our design of the aza-peptide Michael acceptors the double bond moiety has two different substitutents. One is the peptide chain and the other is the differing Y group, which consists of various groups such as alkyl, alkenyl, aryl, halogen, ester, or amide. Therefore, the double bond in aza-peptide Michael acceptors has two isomers: the cis isomer and the trans isomer. We focused our attention of making mainly fumarate analogues. However, we made one inhibitor with the cis configuration on the double bond moiety (**18g**). This inhibitor turned out to be the most potent inhibitor of caspase-2 (k_2 = 26200 M^{-1} s^{-1}), when compared to the fumarate analogues. **18g** was also quite potent with the other caspases as well (Table 1). It was less potent than the trans isomer **18h**, but overall it was more reactive than some of the fumarate analogues. The weaker inhibition by the cis isomer (**18g**) compared to the trans isomer (**18h**) could be due to an inherent difference in chemical reactivity of the two isomers and/or to weaker binding of the cis isomer to the enzyme. In an attempt to search for some structural reasons for this behavior, we have cocrystallized both the isomers with caspase-3. The crystal structure of the cis and trans isomer complexes were determined at 1.76 Å and 1.86 Å resolution, respectively. In the cis complex the *B*-factor values of the inhibitor in general and P1′ atoms in particular are higher than the trans complex, indicating higher mobility and/or lower occupancy in the active site. Consequently, the difference in electron density for the bound inhibitor in the active sites of the caspase-3 cis complex is weaker than for the trans isomer. Nonetheless the electron density maps were good enough to fit the inhibitor model into the active site. The superposition of the cis and the trans complexes reveals that the bound covalent adducts overlap well with similar side chain rearrangements in the two complex structures. From structural considerations alone one would argue that both compounds bind with equal potency which is confirmed by kinetic data (1060000 M^{-1} s^{-1} for the cis and 2130000 M^{-1} s^{-1} for the trans isomer). But, with larger P1′ substituents, there is likely to be a more significant difference between the cis and trans isomers.

Conclusion. Aza-peptide Michael acceptors with the Asp residue at P1 are a novel class of inhibitors for caspases-2, -3, -6, -7, -8, -9, and -10. The inhibitors have excellent inhibitory potency and selectivity for clan CD cysteine proteases, where the second-order rate constants are as high as 5620000 M^{-1} s^{-1}. Aza-peptide Michael acceptors designed for caspases have been tested with a variety of other cysteine proteases for cross reactivity. They do not show cross reactivity with the clan CA proteases such as papain, cathepsin B, and calpain. Aza-peptide Michael acceptors designed for caspases show little to no cross reactivity with legumain which has a specifity for Asn at P1. They do not react with other clan CD proteases gingipain K and clostripain with specificities Lys and Orn at P1, respectively.

Analysis of our crystal structures reveals that the nucleophilic attack takes place on the C2-carbon of the double bond; thus, additional substitution might be tolerated in the C3-carbon. In an effort to obtain greater selectivity among caspases-2, -3, -6, -7, -8, -9, and -10, we modified the P′ substituent on the double bond for each appropriate caspase sequence. Our results indicate that caspases-3 and -7 can tolerate bulky and aromatic residues in the prime site. Caspases-6 and -10 can accommodate a variety of different substituents at the same position, whereas caspase-8 prefers smaller P′ substituents such as the ethyl group. Currently, we are continuing to refine our design on the P′ site, where we would like exploit the further possibilities for some polar interactions in the prime site. By introducing substituents on the double bond with a variety of different electron-withdrawing characters, we are also hoping to improve the stability of aza-peptide Michael acceptors toward thiol nucleophiles such as the thiol DTT.

Aza-peptide Michael acceptors' potency and selectivity for caspases make them great candidates for potential use as probes in cellular function studies and as drugs. Due to the strict requirement of the negatively charged Asp residue at P1 and the peptide chain itself, the hydrophobic character of our inhibitors is significantly low. By introducing nonpeptide moieties to replace the peptide backbone and shielding the side chain carboxylic acid group with certain isosteres, one can increase the hydrophobicity and hence the bioavailability of our caspase inhibitors.

Experimental Section

Materials and Methods. Amino acid methyl esters were purchased from Bachem Bioscience Inc., King of Prussia, PA. Tripeptides were synthesized using standard coupling procedures such as the mixed anhydride method. The ^{1}H NMR spectra were obtained using a Varian Mercury Vx 400 MHz spectrometer. Electrospray ionization (ESI), fast-atom-bombardment (FAB) and high-resolution mass spectrometry were performed using Micromass Quattro LC and VG Analytical 70-SE instruments. Elemental analysis was performed by Atlantic Microlab Inc., Norcross, GA.

Peptidyl Hydrazides. Anhydrous hydrazine (10 equiv) was added to a stirred solution of a peptidyl methyl ester (1 equiv) in MeOH and the reaction mixture was stirred vigorously for 16 h at room temperature. Excess hydrazine and solvent were removed under vacuum and the residue was washed with ether several times to give the peptidyl hydrazide as a white solid. Compounds were purified further on silica gel column using the eluent 2:18:5 MeOH:CH_2Cl_2:EtOAc when needed. MS and ^{1}H NMR ($CDCl_3$ or DMSO-d_6) were consistent with the proposed structures.

Cbz-Val-NH−NH_2, white solid, yield 92%; Cbz-Glu(O-*t*Bu)-Val-NH−NH_2, white solid, yield 47−53%; Cbz-Asp(O-*t*Bu)-Glu(O-*t*Bu)-Val-NH−NH_2, white solid, yield 43%; Cbz-Leu-Glu(O-*t*Bu)-Thr-NH−NH_2, white solid, yield 92%; Cbz-Ile-Glu(O-*t*Bu)-Thr-NH−NH_2, white solid, yield 91%; Cbz-Val-Glu(O-*t*Bu)-Val-NH−NH_2, white solid, yield 75%.

Peptidyl-AA_2-NH−NH−CH_2COO*t*Bu. General Procedure. To a stirred solution of a peptidyl hydrazide (1 equiv) in DMF, NMM (1.1 equiv) and neat *tert*-butyl bromoacetate (1.1 equiv) were added dropwise at −15 °C and the mixture was allowed to react for 16 h at room temperature. The solvent was removed under vacuum and the residue was dried in vacuo. Purification on a silica gel column with the proper eluent gave the product with yields of 18−68%. MS and ^{1}H NMR ($CDCl_3$ or DMSO-d_6) were consistent with the proposed structures.

Cbz-Val-NH−NH−CH_2COO*t*Bu was purified by column chromatography on silica gel using 1:20:4.2 MeOH:CH_2Cl_2:EtOAc as the eluent; white solid, yield 64%. ^{1}H NMR (DMSO-d_6): 0.90 (t, 6H, Val), 1.40 (s, 9H, *t*Bu), 1.86 (m, 1H, Val), 3.37 (d, 2H, NHCH_2-COOH), 3.72 (t, 1H, α-H), 4.99 (s, 2H, Cbz), 5.13 (d, 1H, NH), 7.30 (s, 5H, Ph), 9.38 (d, 1H, NH).

Cbz-Glu(O-*t*Bu)-Val-NH−NH−CH_2COO*t*Bu was purified by column chromatography on silica gel using 2:18:5 MeOH:CH_2Cl_2:EtOAc as the eluent; white solid, yield 78%. MS (ESI) *m*/*z* 565.3 [$(M + 1)^+$]. ^{1}H NMR ($CDCl_3$): 0.95 (t, 6H, Val), 1.49 (s, 18H, *t*Bu), 1.85−2.20 (m, 3H, Val and Glu), 2.21 (m, 2H, Glu), 3.45−3.70 (m, 3H, NHCH_2 and *NH*CH_2), 4.25−4.30 (m, 2H, α-H), 5.05 (m, 2H, Cbz), 5.85 (d, 1H, NH), 7.05 (d, 1H, NH), 7.20−7.40 (m, 5H, Ph), 8.00 (m, 1H, NH).

Cbz-Asp(O-*t*Bu)-Glu(O-*t*Bu)-Val-NH−NH−CH_2COO*t*Bu was purified by column chromatography on silica gel using 2:18:5

MeOH:CH_2Cl_2:EtOAc as the eluent, and then rechromatographed using 1:9:5 MeOH:CH_2Cl_2:EtOAc as the eluent; white solid, yield 54%. ^{1}H NMR (DMSO-d_6): 0.81 (d, 6H, Val), 1.35−1.41 (t, 27H, *t*Bu), 1.71 (m, 1H, Val), 1.84 (m, 2H, Glu), 2.17 (m, 2H, Glu), 2.44 (dd, 1H, Asp), 2.49 (dd, 1H, Asp), 4.02 (t, 1H, α-H), 4.26−4.35 (dm, 2H, α-H), 5.02 (q, 2H, Cbz), 7.32 (s, 5H, Ph), 7.61 (d, 1H, NH), 7.79 (d, 1H, NH), 7.91 (d, 1H, NH), 9.43 (d, 1H, NH).

Cbz-Ile-Glu(O-*t*Bu)-Thr-NH−NH−CH_2COO*t*Bu was purified by column chromatography on silica gel using 1:9 MeOH:CH_2Cl_2 as the eluent; white solid, yield 26%. MS (ESI) *m*/*z* 680 [(M + 1)$^+$]. ^{1}H NMR (DMSO-d_6): 0.7−0.9 (t, 6H, Ile CH_3), 0.9−1.0 (d, 3H, Thr CH_3), 1−1.2 (m, 2H, Ile CH_2), 1.3−1.5 (s, 18H, *t*Bu), 1.6−1.8 (m, 2H, Ile CH and Glu CH_2), 1.8−1.9 (m, 1H, Glu CH_2), 2.1−2.3 (m, 2H, Glu CH_2), 3.4 (d, 2H, NCH_2), 3.9 (m, 2H, α-H), 4.1 (m, 1H, α-H), 4.35 (m, 1H, Thr C*H*-OH), 4.8 (d, 1H, NH), 5.03 (s, 2H, Cbz), 5.05 (d, 1H, NH), 7.3−7.4 (m, 5H, phenyl), 7.7 (d, 1H, NH), 8.05 (d, 1H, NH), 9.2 (s, 1H, NH).

Cbz-Leu-Glu(O-*t*Bu)-Thr-NH−NH−CH_2COO*t*Bu was purified by column chromatography on silica gel using 2:18:5 MeOH:CH_2Cl_2:EtOAc as the eluent, white solid, yield 68%. ^{1}H NMR (DMSO-d_6): 0.84 (t, 6H, Leu), 0.98 (d, 3H, Thr), 1.37−1.44 (m, 20H, *t*Bu and Leu), 1.62−1.73 (dm, 2H, Glu), 1.88 (m, 1H, Leu), 2.22 (m, 2H, Glu), 3.94 (m, 1H, α-H), 4.03−4.13 (dm, 2H, α-H), 4.37 (m, 1H, Thr), 4.99 (s, 2H, Cbz), 6.65 7.33 (m, 5H, Ph), 7.42 (d, 1H, NH), 7.63 (d, 1H, NH), 8.03 (d, 1H, NH), 9.26 (s, 1H, NH).

Cbz-Val-Glu(O-*t*Bu)-Val-NH−NH−CH_2COO*t*Bu was purified by column chromatography on silica gel using 1:9:5 MeOH:CH_2Cl_2:EtOAc as the eluent, and then rechromatographed using 1:9:5 MeOH:CH_2Cl_2:EtOAc as the eluent; white solid, yield 18%. ^{1}H NMR (DMSO-d_6): 0.78−0.85 (dd, 12H, Val), 1.40 (d, 18H, *t*Bu), 1.71 (m, 1H, Val), 1.83 (m, 2H, Glu), 1.91 (m, 1h, Val), 2.17 (m, 2H, Glu), 3.86 (t, 1H, α-H), 4.04 (t, 1H, α-H), 4.32 (m, 1H, α-H), 5.01 (s, 2H, Cbz), 5.12 (m, 1H, NH), 7.33 (s, 5H, Ph), 7.76 (d, 1H, NH), 8.00 (d, 1H, NH), 9.43 (d, 1H, NH).

Monoethyl Maleate (HOOC−CH=CH−COOEt). Monoethyl maleate was obtained as a colorless oil from the reaction of maleic anhydride with absolute ethanol at room temperature for 18 h (yield = 86%).[40] ^{1}H NMR (DMSO-d_6): 1.19 (t, 3H, OCH_2CH_3), 4.11 (q, 2H, OCH_2CH_3), 6.33 (s, 2H, C*H*=C*H*).

***trans*-3-Benzyloxycarbonylacrylic Acid (HOOC−CH=CH−$COOCH_2$Ph).** Equimolar amounts of fumaric acid and benzyl alcohol were dissolved in anhydrous DMF. NMM (1 equiv) was added at 0 °C followed by EDC after 15 min. The reaction was stirred overnight at room temperature. DMF was evaporated and the crude residue was redissolved in EtOAc. The product was extracted with saturated aqueous $NaHCO_3$. The aqueous layer was then acidified with 1N HCl to pH 2. The product was extracted with EtOAc, and the organic layer was washed with water and dried ($MgSO_4$). The solvent was evaporated and the crude residue was subjected to column chromatography (MeOH/CH_2Cl_2) to give a white powder (51% yield). ^{1}H NMR (DMSO-d_6): 5.21 (s, 2H, CH=CH−COOCH_2Ph), 6.73 (s, 2H, *CH*=*CH*-$COOCH_2$Ph), 7.29−7.43 (m, 5H, Ph). MS (ESI) *m*/*z* 207 [(M + 1)$^+$].

***trans*-3-Butylcarbamoylacrylic Acid (HOOC−CH=CH−CONH-*n*Bu).** This compound was obtained by EDC/HOBt coupling in $CHCl_3$ followed by standard NaOH hydrolysis (white solid, yield = 60%). ^{1}H NMR (DMSO-d_6): 0.86 (t, 3H, $NHCH_2CH_2CH_2CH_3$), 1.28 (m, 2H, $NHCH_2CH_2CH_2CH_3$), 1.41 (m, 2H, $NHCH_2CH_2CH_2CH_3$), 3.12 (m, 2H, $NHCH_2CH_2CH_2CH_3$), 6.49 (d, 1H, CH=*CH*-CONH), 6.87 (d, 1H, CH=*CH*-COOH), 8.43 (t, 1H, NH).

***trans*-3-Phenylcarbamoylacrylic Acid (HOOC−CH=CH−CONHPh).** *trans*-3-Phenylcarbamoylacrylic acid ethyl ester was obtained by mixed anhydride coupling of equimolar amounts of monoethyl fumarate and aniline to give a white solid (59% yield). EtOOC−CH=CH−CONHPh was hydrolyzed in MeOH using NaOH (1M aqueous, 1.1 equiv) under standard deblocking conditions to give a white solid (81% yield). ^{1}H NMR (DMSO-d_6): 6.61−6.65 (d, 1H, *J* = 15.2 Hz, *CH*=CHCON), 7.02−7.14 (m, 1H, CH=*CH*CON), 7.14−7.31 (m, 2H, Ph), 7.32 (t, 2H, Ph), 7.66 (d, 2H, Ph), 10.47 (s, 1H, NH).

***trans*-3-Benzylcarbamoylacrylic Acid (HOOC−CH=CH−$CONHCH_2$Ph).** To a stirred solution of benzylamine (1 equiv), HOBt (1.1 equiv), and monoethyl fumarate (1.1 equiv) in DMF was added EDC (1.1 equiv) and the mixture was allowed to react for 16 h at room temperature. The DMF was removed under vacuum and the residue was treated with EtOAc. The organic layer was then washed with 2% citric acid, saturated $NaHCO_3$, and brine. The organic layer was dried over Na_2SO_4, filtered, and concentrated. Column chromatography on silica gel with 1:1 EtOAc:hexanes as the eluent gave the *trans*-3-benzylcarbamoylacrylic acid ethyl ester as a white solid with a 63% yield. Hydrolysis of the ethyl ester with NaOH (1.1 equiv) followed by acidic workup gave the *trans*-3-benzylcarbamoylacrylic acid as a white solid in 65% yield. ^{1}H NMR (DMSO-d_6): 4.37 (d, 2H, CH_2Ph), 6.55 (d, 1H, CH=*CH*-CONH), 6.93 (d, 1H, CH=*CH*-COOH), 7.29 (m, 5H, Ph), 8.96 (t, 1H, NH). In general, carbamoylacrylic acids were obtained in 60−79% yield.

***trans*-3-(4-Fluorobenzylcarbamoyl)acrylic Acid (HOOC−CH=CH−$CONHCH_2$-4-F-Ph).** *trans*-3-(4-Fluorobenzylcarbamoyl)acrylic acid ethyl ester was obtained by mixed anhydride coupling of equimolar amounts of monoethyl fumarate and 4-fluorobenzylamine to give a pink solid (66% yield). EtOOC−CH=CH−$CONHCH_2$-4-F-Ph was hydrolyzed in MeOH using NaOH (1M aqueous, 1.1 equiv) under standard deblocking conditions to give a clear, colorless syrup (45% yield). ^{1}H NMR (DMSO-d_6): 4.34−4.35 (d, 2H, N-CH_2−Ph), 6.52−6.55 (d, 1H, *J* = 15.2 Hz, *CH*=CHCON), 6.93−6.94 (d, 1H, *J* = 15.6 Hz, CH=*CH*CON), 7.14−7.16 (t, 2H, Ph), 7.27−7.31 (t, 2H, Ph), 8.99 (t, 1H, NH).

***trans*-3-Phenethylcarbamoylacrylic Acid (HOOC−CH=CH−$CONHCH_2CH_2$Ph).** Monoethyl fumarate (1 equiv) was dissolved in dry THF and cooled to −15 °C. NMM (1 equiv) and IBCF were added dropwise and the mixture was allowed to react for 20 min. Phenethylamine was added to the above mixture at −15 °C. The mixture was stirred for 1 h at −15 °C and was allowed to react for 16 h at room temperature. The solvent was evaporated and the residue was treated with EtOAc and H_2O. The organic layer was washed with 1 M HCl, saturated $NaHCO_3$, and brine, dried over Na_2SO_4, filtered, and concentrated to give *trans*-3-phenethylcarbamoylacrylic acid ethyl ester. Hydrolysis of the ethyl ester with NaOH (1.1 equiv) followed by acidic workup gave the *trans*-3-phenethylcarbamoylacrylic acid as a yellow solid in 79% yield. ^{1}H NMR (DMSO-d_6): 2.75 (t, 2H, $NHCH_2CH_2$Ph), 3.38 (q, 2H, $NHCH_2CH_2$Ph), 6.55 (d, 1H, CH=*CH*-CONH), 6.98 (d, 1H, CH=*CH*-COOH), 7.20 (m, 5H, Ph), 8.59 (t, 1H, NH).

***trans*-3-Benzylmethylcarbamoylacrylic Acid (HOOC−CH=CH−$CON(CH_3)CH_2$Ph).** *trans*-3-Benzylmethylcarbamoylacrylic acid ethyl ester was obtained by mixed anhydride coupling of equimolar amounts of monoethyl fumarate and *N*-methylbenzylamine to give a clear, pink syrup (76% yield). EtOOC−CH=CH−$CON(CH_3)CH_2$Ph was hydrolyzed in MeOH using NaOH (1M aqueous, 1.1 equiv) under standard deblocking conditions to give a clear, colorless syrup (77% yield). ^{1}H NMR ($CDCl_3$): 3.03 (s, 3H, N−CH_3), 4.62−4.67 (d, 2H, N-CH_2−Ph), 6.83−6.87 (d, 1H, *J* = 16 Hz, *CH*=CHCON), 7.15−7.17 (d, 1H, *J* = 8 Hz, CH=*CH*CON), 7.25−7.50 (m, 5H, Ph).

***trans*-3-(Methylphenethylcarbamoyl)acrylic Acid (HOOC−CH=CH−$CON(CH_3)CH_2CH_2$Ph).** *trans*-3-(Methylphenethylcarbamoyl)acrylic acid ethyl ester was obtained by mixed anhydride coupling of equimolar amounts of monoethyl fumarate and *N*-methylphenethylamine to give a clear colorless syrup (64% yield). EtOOC−CH=CH−$CON(CH_3)CH_2CH_2$Ph was hydrolyzed in MeOH using NaOH (1M aqueous, 1.1 equiv) under standard deblocking conditions to give a clear, colorless syrup (81% yield). ^{1}H NMR (DMSO-d_6): 2.82 (s, 3H, N−CH_3), 3.54 (t, 2H, N−CH_2-CH_2−Ph), 3.61 (t, 2H, N-CH_2−CH_2−Ph), 6.43−6.47 (d, 1H, *J* = 15.2 Hz, *CH*=CHCON), 6.98−6.7.02 (d, 1H, *J* = 15.6 Hz, CH=*CH*CON), 7.14−7.31 (m, 5H, Ph).

***trans*-3-Dibenzylcarbamoylacrylic Acid (HOOC−CH=CH−$CON(CH_2Ph)_2$).** *trans*-3-Dibenzylcarbamoylacrylic acid ethyl ester

was obtained by mixed anhydride coupling of equimolar amounts of monoethyl fumarate and dibenzylamine to give a clear, pink syrup (87% yield). EtOOC−CH═CH−CON(CH_2Ph)$_2$ was hydrolyzed in MeOH using NaOH (1M aqueous, 1.1 equiv) under standard deblocking conditions to give a clear, colorless syrup which was recrystallized overnight from hexane/EtOAc (30% yield). ^{1}H NMR (DMSO-d_6): 4.57 (s, 2H, N-CH_2−Ph), 4.65 (s, 2H, N-CH_2−Ph), 6.59−6.63 (d, 1H, J = 15.2 Hz, *CH*═CHCON), 7.15−7.17 (d, 1H, J = 8 Hz, CH═*CH*CON), 7.25−7.50 (m, 10H, 2 ? Ph).

***trans*-3-(3,4-Dihydro-2*H*-quinolin-1-ylcarbonyl)acrylic Acid (HOOC−CH═CH−CO-tetrahydroquinoline).** *trans*-3-(3,4-Dihydro-2H-quinolin-1-ylcarbonyl)acrylic acid ethyl ester was obtained by mixed anhydride coupling of equimolar amounts of monoethyl fumarate and 1,2,3,4-tetrahydroquinoline to give a brown syrup (83% yield). EtOOC−CH═CH−CO-tetrahydroquinoline was hydrolyzed in MeOH using NaOH (1M aqueous, 1.1 equiv) under standard deblocking conditions to give a clear syrup, which was recrystallized using cold EtOAc to give a yellow powder (68% yield).

***trans*-3-(Methyl-1-naphthylmethylcarbamoyl)acrylic Acid (HOOC−CH═CH−CON(CH_3)CH_2-1-Naphth).** *trans*-3-(Methyl-1-naphthylmethylcarbamoyl)acrylic acid ethyl ester was obtained by mixed anhydride coupling of equimolar amounts of monoethyl fumarate and *N*-methyl-1-naphthylmethylamine hydrochloride to give a clear, colorless syrup (99% yield). EtOOC−CH═CH−CON-(CH_3)CH_2-1-Naphth was hydrolyzed in MeOH using NaOH (1M aqueous, 1.1 equiv) under standard deblocking conditions to give a white solid after recrystallization from cold EtOAc (13% yield). ^{1}H NMR (DMSO-d_6): 3.01 (s, 3H, CH_3), 5.01 (s, 2H, CH_2), 6.61−6.65 (d, 1H, J = 15.2 Hz, *CH*═CHCON), 7.17−7.21 (d, 1H, CH═*CH*CON), 7.37−7.60 (m, 4H, naphthyl), 7.85−8.01 (m, 3H, naphthyl).

***trans*-3-Di-1-Naphthylcarbamoylacrylic Acid (HOOC−CH═CH−CON(CH_2-1-Naphth)$_2$).** *trans*-3-Di-1-Naphthylcarbamoylacrylic acid ethyl ester was obtained by mixed anhydride coupling of equimolar amounts of monoethyl fumarate and di-1-naphthylamine(Ref.) to give a clear, yellow syrup (71% yield). EtOOC−CH═CH−CON(CH_2-1-Naph)$_2$ was hydrolyzed in EtOH using NaOH (1M aqueous, 1.5 equiv) under standard deblocking conditions to give a light tan solid. (52% yield). ^{1}H NMR (DMSO-d_6): 5.21 (s, 4H, N-CH_2-1-Naph), 6.61−6.62 (d, 1H, J = 1.2 Hz, CH═*CH*CON), 6.69−6.72 (d, 1H, J = 14 Hz, *CH*═CHCON), 7.17−8.11 (m, 14H, N(CH_2-*1-Naph*)$_2$).

Cbz-Val-AAsp(O-*t*Bu)-CH═CH−COOEt. EDC/HOBt Coupling Method. To a stirred solution of Cbz-Val-NH−NH−CH_2−COO*t*Bu (0.34 mM, 1 equiv), HOBt (0.37 mM, 1.1 equiv), and monoethyl fumarate (0.37 mM, 1.1 equiv) in DMF was added EDC (0.37 mM, 1.1 equiv) and the mixture was allowed to react for 16 h at room temperature (2 eq of EDC/HOBt were used with the tetrapeptides). The DMF was removed under vacuum and the residue was treated with 10 mL EtOAc. The organic layer was then washed with 2 × 10 mL 2% citric acid, 1 × 15 mL saturated $NaHCO_3$, and 2 × 10 mL brine. The organic layer was dried over Na_2SO_4, filtered, and concentrated. Column chromatography on silica gel with 1:49:50 MeOH:CH_2Cl_2:EtOAc as the eluent gave the product as a white solid with 63% yield. MS and ^{1}H NMR (DMSO-d_6) were consistent with the proposed structure. MS (ESI) m/z 506.3 [(M + 1)$^+$]. ^{1}H NMR ($CDCl_3$): 0.97−1.02 (dd, 6H, Val), 1.28 (t, 3H, OCH$_2$*CH*$_3$), 1.46 (s, 9H, *t*Bu), 2.18 (m, 1H, Val), 3.98 (t, 1H, α-H), 4.21 (q, 2H, O*CH*$_2$CH$_3$), 5.11 (s, 2H, Cbz), 5.21 (d, 1H, NH), 6.86 (d, 1H, db), 7.33 (s, 6H, Ph and db), 8.49 (s, 1H, NH−N).

Cbz-Val-AAsp(O-*t*Bu)-CH═CH−CH_3 was obtained by the EDC/HOBt coupling method, and purified by column chromatography on silica gel with 0.5:49.5:50 MeOH:CH_2Cl_2:EtOAc as the eluent; white solid, yield 53%. MS (ESI) m/z 448.4 [(M + 1)$^+$]. ^{1}H NMR (DMSO-d_6): 0.85−0.89 (dd, 6H, Val), 1.39 (s, 9H, *t*Bu), 1.94 (m, 1H, Val), 3.83 (t, 1H, α-H), 5.02 (q, 2H, Cbz), 6.41 (m, 1H, db), 6.72 (m, 1H, db), 7.32 (s, 5H, Ph), 7.58 (d, 1H, NH).

Cbz-Val-AAsp(O-*t*Bu)-CH═CH−CH═CH−CH_3 was obtained by the EDC/HOBt coupling method, and purified by column chromatography on silica gel with 0.5:49.5:50 MeOH:CH_2Cl_2: EtOAc as the eluent; white solid, yield 8%. MS (ESI) m/z 474.3 [(M + 1)$^+$]. ^{1}H NMR (DMSO-d_6): 0.83−0.89 (dd, 6H, Val), 1.39 (s, 9H, *t*Bu), 1.75 (d, 3H, CH_3), 1.92 (m, 1H, Val), 3.83 (t, 1H, α-H), 5.02 (q, 2H, Cbz), 6.14 (m, 2H, db), 6.40 (m, 1H, db), 7.09 (m, 1H, db), 7.33 (s, 5H, Ph), 7.58 (d, 1H, NH), 10.77 (s, 1H, NH−N).

Cbz-Val-AAsp(O-*t*Bu)-CH═CH−CH_2CH_2Ph was obtained by the EDC/HOBt coupling method, and purified by column chromatography on silica gel with 0.5:49.5:50 MeOH:CH_2Cl_2:EtOAc as the eluent; white solid, yield 53%. MS (ESI) m/z 538.3 [(M + 1)$^+$].

Cbz-Val-AAsp(O-*t*Bu)-*cis*-CH═CH−Cl was obtained by the EDC/HOBt coupling method, and purified by column chromatography on silica gel with 0.5:49.5:50 MeOH:CH_2Cl_2:EtOAc as the eluent; white solid, yield 25%. MS (ESI) m/z 468.4 [(M + 1)$^+$]. ^{1}H NMR (DMSO-d_6): 0.89 (d, 6H, Val), 1.43 (s, 9H, *t*Bu), 1.95 (m, 1H, Val), 3.84 (t, 1H, α-H), 5.04 (s, 2H, Cbz), 6.59 (s, 1H, db), 6.81 (d, 1H, db), 7.35 (s, 5H, Ph), 7.56 (d, 1H, NH), 10.81 (s, 1H, NH−N).

Cbz-Val-AAsp(O-*t*Bu)-CH═CH−Ph-4-Cl was obtained by the EDC/HOBt coupling method, and purified by column chromatography on silica gel with 0.5:49.5:50 MeOH:CH_2Cl_2:EtOAc as the eluent; white solid, yield 62%. MS (ESI) m/z 544.3 [(M + 1)$^+$]. ^{1}H NMR (DMSO-d_6): 0.86−0.93 (dd, 6H, Val), 1.41 (s, 9H, *t*Bu), 1.98 (m, 1H, Val), 3.80 (t, 1H, α-H), 5.03 (q, 2H, Cbz), 7.30 (s, 5H, Ph), 7.40 (d, 1H, db), 7.52 (d, 1H, db), 7.76 (m, 4H, Ph-Cl), 10.95 (s, 1H, NH−N).

Cbz-Val-AAsp(O-*t*Bu)-CH═CH−CONH-*n*Bu was obtained by the EDC/HOBt coupling method, and purified by column chromatography on silica gel with 1:9:10 MeOH:CH_2Cl_2:EtOAc as the eluent; white solid, yield 53%. MS (ESI) m/z 533.2 [(M + 1)$^+$]. ^{1}H NMR (DMSO-d_6): 0.83−0.87 (m, 9H, Val and NHCH$_2$CH$_2$-CH$_2$*CH*$_3$), 1.27 (m, 2H, NHCH$_2$CH$_2$*CH*$_2$CH$_3$), 1.41 (s, 11H, *t*Bu and NHCH$_2$*CH*$_2$CH$_2$CH$_3$), 1.96 (m, 1H, Val), 3.12 (dd, 2H, NH*CH*$_2$-CH$_2$CH$_2$CH$_3$), 3.90 (t, 1H, α-H), 5.03 (q, 2H, Cbz), 6.91 (d, 1H, db), 7.08 (d, 1H, db), 7.28−7.34 (m, 5H, Ph), 7.47 (d, 1H, NH), 8.37 (t, 1H, *NH*CH$_2$CH$_2$CH$_2$CH$_3$), 10.93 (s, 1H, NH−N).

Cbz-Val-AAsp(O-*t*Bu)-CH═CH−CONHCH$_2$Ph was obtained by the EDC/HOBt coupling method, and purified by column chromatography on silica gel with 1:49:50 MeOH:CH_2Cl_2:EtOAc as the eluent; white solid, yield 72%. MS (ESI) m/z 567.4 [(M + 1)$^+$]. ^{1}H NMR (DMSO-d_6): 0.85 (d, 6H, Val), 1.40 (s, 9H, *t*Bu), 1.96 (m, 1H, Val), 3.90 (t, 1H, α-H), 4.33 (d, 2H, NH*CH*$_2$Ph), 5.00 (s, 2H, Cbz), 6.97 (d, 1H, db), 7.14−7.32 (m, 11H, Ph and db), 7.49 (d, 1H, NH), 8.90 (t, 1H, *NH*CH$_2$Ph), 10.92 (s, 1H, NH−N).

Mixed Anhydride Coupling Method. Coupling of some of the bulky peptides, such as Cbz-Asp(O-*t*Bu)-Glu(O-*t*Bu)-Val-NH−NH−CH_2COO-*t*Bu and Cbz-Leu-Glu(O-*t*Bu)-Thr-NH−NH−CH_2-COO-*t*Bu, with the monoethyl fumarate, was accomplished using the mixed anhydride coupling method. To a solution of the monoethyl fumarate (5 equiv) in DMF at 0 °C was added *N*-methylmorpholine (NMM, 5 equiv) followed by isobutyl chloroformate (IBCF, 5 equiv). After the reaction mixture was allowed to stir for 30 min, the substituted hydrazide (1 equiv) dissolved in DMF, was added to the mixture. After 10 min the ice bath was removed and the reaction mixture was stirred for 16 h at room temperature. The DMF was evaporated and the residue was washed and purified using the same procedure as described above for the EDC/HOBt coupling method. MS and ^{1}H NMR (DMSO-d_6, $CDCl_3$ or acetone-d_6) were consistent with the proposed structures.

Cbz-Glu(O-*t*Bu)-Val-AAsp(O-*t*Bu)-CH═CH−COOEt was obtained using the mixed anhydride method and was purified using column chromatography on silica gel using 1:9:10 MeOH:CH_2Cl_2: EtOAc as the eluent, white solid, yield 49%. ^{1}H NMR (DMSO-d_6): 0.90 (m, 6H, Val), 1.20 (t, 3H, OCH$_2$*CH*$_3$), 1.41 (m, 18H, *t*Bu), 1.60−2.00 (m, 3H, Val, Glu), 2.21 (m, 2H, Glu), (m, 4H, N*CH*$_2$COOH, and O*CH*$_2$CH$_3$), 4.20−4.40 (m, 2H, α-H), 5.05 (m, 2H, Cbz), 7.10 (−CO-*CH*═CH−COOEt), 7.20−7.40 (m, 5H, Ph), 8.00 (m, 2H, NH). ESI (M+1) Calcd. for $C_{34}H_{51}N_4O_{11}$: 691.35 Observed m/z 691.30.

Cbz-Asp(O-*t*Bu)-Glu(O-*t*Bu)-Val-AAsp(O-*t*Bu)-CH═CH−COPh was obtained by the EDC/HOBt coupling method, and purified by column chromatography on silica gel with 1:499:500 MeOH:CH_2Cl_2:EtOAc as the eluent; white solid, yield 40%. MS (ESI) *m*/*z* 894.4 [$(M + 1)^+$]. ^{1}H NMR (DMSO-d_6): 0.82 (t, 6H, Val), 1.34−1.42 (m, 27H, *t*Bu), 1.70 (m, 1H, Glu), 1.85 (m, 1H, Glu), 1.96 (m, 1H, Val), 2.15 (m, 2H, Glu), 2.44 (dd, 1H, Asp), 2.58−2.60 (dd, 1H, Asp), 4.14 (t, 1H, α-H), 4.26−4.33 (dm, 2H, α-H), 5.02 (q, 2H, Cbz), 7.23 (d, 1H, db), 7.31 (s, 5H, Cbz), 7.51 (m, 3H, Ph), 7.66 (t,1H, NH), 7.80 (d, 1H, db), 7.99 (d, 2H, Ph), 11.02 (s, 1H, NH−N).

Cbz-Asp(O-*t*Bu)-Glu(O-*t*Bu)-Val-AAsp(O-*t*Bu)-*cis*-CH═CH−COOEt was obtained using the EDC/HOBt coupling method from monoethyl maleate, purified by column chromatography on silica gel with 1:19:20 MeOH:CH_2Cl_2:EtOAc as the eluent; white solid, yield 53%. MS (ESI) *m*/*z* 862.5 [$(M + 1)^+$]. ^{1}H NMR (DMSO-d_6): 0.85 (d, 6H, Val), 1.18 (t, 3H, OCH_2CH_3), 1.33−1.39 (m, 27H, *t*Bu), 1.74 (m, 1H, Glu), 1.86 (m, 1H, Glu), 1.95 (m, 1H, Val), 2.18 (m, 2H, Glu), 2.45 (dd, 1H, Asp), 2.61 (dd, 1H, Asp), 4.09 (t, 1H, α-H), 4.16 (q, 2H, OCH_2CH_3), 4.33 (m, 2H, α-H), 5.01 (q, 2H, Cbz), 6.61 (d, 1H, db), 7.25 (d, 1H, db), 7.33 (s, 5H, Ph), 7.62 (d, 1H, NH), 7.93 (t, 2H, NH), 11.05 (s, 1H, NH−N).

Cbz-Asp(O-*t*Bu)-Glu(O-*t*Bu)-Val-AAsp(O-*t*Bu)-*trans*-CH═CH−COOEt was obtained using the EDC/HOBt coupling method from monoethyl fumarate, purified by column chromatography on silica gel with 50:45:5 CH_2Cl_2:EtOAc:MeOH as the eluent; white solid, yield 68%. ^{1}H NMR ($CDCl_3$): 1.00 (d, 6H, Val CH_3), 1.29 (t, 3H, OEt), 1.45 (s, 27H, *t*-Bu), 1.90 (m, 1H, Val CH), 2.10 (d of m, 2H, Glu CH_2), 2.40 (d of m, 2H, Glu CH_2), 2.80 (d of m, 2H, Asp CH_2), 3.20 (s, 2H, AAsp CH_2), 4.19 (q, 3H, OEt and α-H), 4.30 (b, 1H, α-H), 4.45 (b, 1H, α-H), 5.12 (q, 2H, Cbz), 6.05 (d, 1H, NH), 6.81 and 7.20 (d of d, 2H, CH═CH), 7.33 (m, 6H, Ph and NH), 7.90 (d, 1H, NH), 9.00 (s, 1H, NH).

Cbz-Asp(O-*t*Bu)-Glu(O-*t*Bu)-Val-AAsp(O-*t*Bu)-CH═CH−COOCH$_2$Ph was obtained by the EDC/HOBt coupling method, and purified by column chromatography on silica gel with 1:499:500 MeOH:CH_2Cl_2:EtOAc as the eluent; white solid, yield 49%. MS (ESI) *m*/*z* 924.5 [$(M + 1)^+$]. ^{1}H NMR (DMSO-d_6): 0.80 (t, 6H, Val), 1.35−1.41 (m, 27H, *t*Bu), 1.75 (m, 1H, Glu), 1.84 (m, 1H, Glu), 1.94 (m, 1H, Val), 2.17 (m, 2H, Glu), 2.45 (dd, 1H, Asp), 2.60 (dd, 1H, Asp), 4.13 (t, 1H, α-H), 4.28−4.35 (dm, 2H, α-H), 5.02 (q, 2H, Cbz), 5.19 (s, 2H, Bzl), 6.70 (d, 1H, db), 7.25−7.37 (m, 11H, Ph and db), 7.57 (d,1H, NH), 7.92 (d, 1H, NH), 7.98 (d, 1H, NH), 11.02 (s, 1H, NH−N).

Cbz-Asp(O-*t*Bu)-Glu(O-*t*Bu)-Val-AAsp(O-*t*Bu)-CH═CH−CONHCH$_2$Ph was obtained by the EDC/HOBt coupling method, and purified by column chromatography on silica gel with 1:9:10 MeOH:CH_2Cl_2:EtOAc as the eluent; white solid, yield 49%. MS (ESI) *m*/*z* 923.5 [$(M + 1)^+$]. ^{1}H NMR (DMSO-d_6): 0.85 (t, 6H, Val), 1.35−1.41 (m, 27H, *t*Bu), 1.72 (m, 1H, Glu), 1.84 (m, 1H, Glu), 1.96 (m, 1H, Val), 2.17 (m, 2H, Glu), 2.44 (dd, 1H, Asp), 2.60 (dd, 1H, Asp), 4.17 (t, 1H, α-H), 4.28 (m, 2H, α-H), 4.36 (d, 2H, NHCH_2Ph), 5.02 (q, 2H, Cbz), 6.95 (d, 1H, db), 7.12 (d, 1H, db), 7.22−7.31 (m, 10H, Ph), 7.57 (d, 1H, NH), 7.94 (d, 1H, NH), 8.92 (t, 1H, *NH*CH_2Ph), 10.96 (s, 1H, NH−N).

Cbz-Asp(O-*t*Bu)-Glu(O-*t*Bu)-Val-AAsp(O-*t*Bu)-CH═CH−CONHCH$_2$-4-F-Ph was obtained by the EDC/HOBt coupling method, and purified by column chromatography on silica gel with 1:19:20 MeOH:CH_2Cl_2:EtOAc as the eluent; white solid, yield 67%. MS (ESI) *m*/*z* 941.4 [$(M + 1)^+$]. ^{1}H NMR (DMSO-d_6): 0.86 (t, 6H, Val), 1.34−1.41 (m, 27H, *t*Bu), 1.75 (m, 1H, Glu), 1.88 (m, 1H, Glu), 2.01 (m, 1H, Val), 2.20 (m, 2H, Glu), 2.48 (dd, 1H, Asp), 2.65 (dd, 1H, Asp), 4.18 (t, 1H, α-H), 4.34 (m, 4H, α-H and NHCH_2Ph-4-F), 5.01 (q, 2H, Cbz), 6.93 (d, 1H, db), 7.12 (d, 2H, NHCH$_2$*Ph*-4-F), 7.25−7.32 (m, 8H, Cbz-Ph, NHCH$_2$*Ph*-4-F, and db), 7.59 (d, 1H, NH), 7.90−7.99 (dd, 2H, NH), 8.94 (t, 1H, *NH*CH_2Ph-4-F), 10.98 (s, 1H, NH−N).

Cbz-Asp(O-*t*Bu)-Glu(O-*t*Bu)-Val-AAsp(O-*t*Bu)-CH═CH−CONHCH$_2$CH$_2$Ph was obtained by the EDC/HOBt coupling method, and purified by column chromatography on silica gel with 1:9:5 MeOH:CH_2Cl_2:EtOAc as the eluent, and then rechromatographed using 1:1 EtOAc:CH_2Cl_2 as the eluent; white solid, yield 29%. MS (ESI) *m*/*z* 937.5 [$(M + 1)^+$]. ^{1}H NMR (DMSO-d_6): 0.85 (t, 6H, Val), 1.35−1.41 (m, 27H, *t*Bu), 1.72 (m, 1H, Glu), 1.86 (m, 1H, Glu), 2.00 (m, 1H, Val), 2.17 (m, 2H, Glu), 2.43 (dd, 1H, Asp), 2.61−2.64 (dd, 1H, Asp), 2.73 (t, 2H, NHCH$_2$*CH$_2$*Ph), 3.35 (q, 2H, NH*CH$_2$*CH$_2$Ph), 4.17 (t, 1H, α-H), 4.29−4.35 (m, 2H, α-H), 5.02 (q, 2H, Cbz), 6.89 (d, 1H, db), 7.07 (d, 1H, db), 7.17−7.31 (m, 10H, Ph), 7.59 (d,1H, NH), 7.94 (d, 1H, NH), 8.51 (t, 1H, *NH*CH$_2$CH$_2$Ph), 10.95 (s, 1H, NH−N).

Cbz-Asp(O-*t*Bu)-Glu(O-*t*Bu)-Val-AAsp(O-*t*Bu)-CH═CH−CON(CH$_3$) CH$_2$Ph was obtained by the EDC/HOBt coupling method, and purified by column chromatography on silica gel with 1:9:5 MeOH:CH_2Cl_2:EtOAc as the eluent, and then rechromatographed using 1:1 EtOAc:hexanes as the eluent; white solid, yield 34%. MS (ESI) *m*/*z* 937.5 [$(M + 1)^+$]. ^{1}H NMR (DMSO-d_6): 0.86 (t, 6H, Val), 1.34−1.41 (m, 27H, *t*Bu), 1.65 (m, 1H, Glu), 1.88 (m, 1H, Glu), 1.97 (m, 1H, Val), 2.17 (m, 2H, Glu), 2.43 (dd, 1H, Asp), 2.59 (dd, 1H, Asp), 2.88−2.98 (d, 3H, N(*CH$_3$*)CH$_2$Ph), 4.16 (t, 1H, α-H), 4.29−4.34 (dm, 2H, α-H), 4.54 (q, 1H, N(CH$_3$)*CH$_2$*-Ph), 4.67 (s, 1H, N(CH$_3$)*CH$_2$*Ph), 5.02 (q, 2H, Cbz), 7.14 (d, 1H, db), 7.20 (d, 1H, db), 7.28−7.37 (m, 10H, Ph), 7.56 (d,1H, NH), 7.94 (t, 1H, NH), 10.97 (s, 1H, NH−N).

Cbz-Asp(O-*t*Bu)-Glu(O-*t*Bu)-Val-AAsp(O-*t*Bu)-CH═CH−CON(CH$_3$)CH$_2$CH$_2$Ph was obtained by the EDC/HOBt coupling method, and purified by column chromatography on silica gel with 1:19:20 MeOH:CH_2Cl_2:EtOAc as the eluent, and then rechromatographed using 1:1 EtOAc:CH_2Cl_2 as the eluent; white solid, yield 45%. MS (ESI) *m*/*z* 951.5 [$(M + 1)^+$]. ^{1}H NMR (acetone-d_6): 0.86 (t, 6H, Val), 1.41−1.48 (m, 27H, *t*Bu), 1.75 (m, 1H, Glu), 1.89 (m, 1H, Glu), 2.01 (m, 1H, Val), 2.21 (m, 2H, Glu), 2.46 (dd, 1H, Asp), 2.62 (dd, 1H, Asp), 2.80 (t, 2H, N(CH$_3$)CH$_2$*CH$_2$*Ph), 2.85−2.98 (d, 3H, N(*CH$_3$*)CH$_2$CH$_2$Ph), 3.73 (m, 2H, N(CH$_3$)*CH$_2$*CH$_2$-Ph), 4.18 (t, 1H, α-H), 4.32 (dm, 2H, α-H), 5.00 (q, 2H, Cbz), 6.88 (t, 1H, NH), 7.17−7.34 (m, 12H, Cbz-Ph, N(CH$_3$)CH$_2$CH$_2$*Ph*, and C*H*═C*H*), 7.59 (d, 1H, NH), 7.85 (d, 1H, NH), 7.97 (d, 1H, NH), 9.89 (d, 1H, NH−N).

Cbz-Asp(O-*t*Bu)-Glu(O-*t*Bu)-Val-AAsp(O-*t*Bu)-CH═CH−CON(CH$_2$Ph)$_2$ was obtained by the EDC/HOBt coupling method, and purified by column chromatography on silica gel with 2:1 EtOAc:hexane as the eluent, and then rechromatographed using 1:1 EtOAc:hexanes as the eluent; white solid, yield 62%. MS (ESI) *m*/*z* 1013.4 [$(M + 1)^+$]. ^{1}H NMR (DMSO-d_6): 0.87 (t, 6H, Val), 1.35−1.39 (m, 27H, *t*Bu), 1.73 (m, 1H, Glu), 1.87 (m, 1H, Glu), 2.02 (m, 1H, Val), 2.23 (m, 2H, Glu), 2.48 (dd, 1H, Asp), 2.65 (dd, 1H, Asp), 4.19 (t, 1H, α-H), 4.33 (m, 2H, α-H), 4.55 (d, 2H, N(*CH$_2$*Ph)$_2$), 4.63 (s, 2H, N(*CH$_2$*Ph)$_2$), 5.00 (q, 2H, Cbz), 7.14 (d, 1H, db), 7.21−7.34 (m, 16H, db, Cbz-Ph, and N(CH$_2$*Ph*)$_2$), 7.60 (d, 1H, NH), 7.91−7.98 (dd, 2H, NH), 11.00 (s, 1H, NH−N).

Cbz-Asp(O-*t*Bu)-Glu(O-*t*Bu)-Val-AAsp(O-*t*Bu)-CH═CH−CON(CH$_2$-1-Naphth)$_2$ was obtained by the EDC/HOBt coupling method, and purified by column chromatography on silica gel with 2:1 EtOAc:hexane as the eluent; white solid, yield 17%. ^{1}H NMR (acetone-d_6): 1.04 (d, 6H, Val), 1.35−1.43 (m, 27H, *t*Bu), 1.97 (m, 2H, Glu), 2.17−2.38 (m, Glu, Val, Asp), 2.71 (dd, 1H, Asp), 4.30 (t, 1H, α-H), 4.51 (m, 2H, α-H), 5.10 (dd, 2H, N(*CH$_2$*-1-Naph)$_2$), 5.24 (s, 2H, N(*CH$_2$*-1-Naph)$_2$), 5.33 (s, 2H, Cbz), 6.85 (d, 1H, db), 7.29−7.95 (m, 16H, db, Cbz-Ph, and N(CH$_2$-*1-Naph*)$_2$), 8.18 (d, 1H, NH), 9.81 (s, 1H, NH−N).

Cbz-Asp(O-*t*Bu)-Glu(O-*t*Bu)-Val-AAsp(O-*t*Bu)-CH═CH−CO-tetrahydroquinoline was obtained by the EDC/HOBt coupling method, and purified by column chromatography on silica gel with 1:2 CH_2Cl_2:EtOAc as the eluent; yellow solid, yield 54%. MS (ESI) *m*/*z* 949.4 [$(M + 1)^+$]. ^{1}H NMR (DMSO-d_6): 0.89 (t, 6H, Val), 1.35−1.42 (m, 27H, *t*Bu), 1.75 (m, 1H, Glu), 1.87 (m, 3H, Glu and NCH$_2$CH$_2$*CH$_2$*), 2.02 (m, 1H, Val), 2.20 (m, 2H, Glu), 2.48 (dd, 1H, Asp), 2.65 (dd, 1H, Asp), 2.70 (t, 2H, NCH$_2$*CH$_2$*CH$_2$), 3.73 (t, 2H, N*CH$_2$*CH$_2$CH$_2$), 4.19 (t, 1H, α-H), 4.33 (m, 2H, α-H), 5.01 (q, 2H, Cbz), 6.95 (m, 1H, db), 7.04 (d, 1H, db), 7.14−7.33 (m, 9H, Cbz-Ph, and quinoline), 7.60 (d, 1H, NH), 7.96 (dd, 2H, NH), 11.02 (s, 1H, NH−N).

Cbz-Val-Glu(O-*t*Bu)-Val-AAsp(O-*t*Bu)-CH═CH−COOEt was obtained by the EDC/HOBt coupling method, and purified by column chromatography on silica gel with 1:9:5 MeOH:CH_2Cl_2:EtOAc as the eluent; white solid, yield 71%. MS (ESI) *m*/*z* 790.3 [$(M + 1)^+$]. ^{1}H NMR (DMSO-d_6): 0.81−0.87 (dd, 12H, Val), 1.22 (t, 3H, OCH_2CH_3), 1.24−1.41 (d, 18H, *t*Bu), 1.72 (m, 1H, Glu), 1.83 (m, 1H, Glu), 1.96 (m, 1H, Val), 2.19 (m, 2H, Glu), 3.86 (t, 1H, α-H), 4.17 (m, 3H, α-H and OCH_2CH_3), 4.32 (m, 1H, α-H), 5.01 (s, 2H, Cbz), 6.64 (d, 1H, db), 7.20 (d, 1H, db), 7.30−7.33 (m, 5H, Ph), 7.97 (t, 2H, NH), 11.02 (s, 1H, NH−N).

Cbz-Ile-Glu(O-*t*Bu)-Thr-AAsp(O-*t*Bu)-CH═CH−COOEt was synthesized using the mixed anhydride coupling method and purified by column chromatography using 4:1 (1:9 MeOH:CH_2Cl_2):EtOAc as an eluent, and then rechromatographed using 4:1 (1:19 MeOH:CH_2Cl_2):EtOAc as the eluent; white solid, yield 36%. MS (ESI) *m*/*z* 806 [$(M + 1)^+$].

Cbz-Ile-Glu(O-*t*Bu)-Thr-AAsp(O-*t*Bu)-CH═CH−$COOCH_2$-Ph was obtained using the EDC/HOBt coupling method, purified by column chromatography on silica gel with 50:45:5 CH_2Cl_2:EtOAc:MeOH as the eluent; white solid, yield 37%. ^{1}H NMR ($CDCl_3$): 0.91 and 0.94 (m, 6H, Ile CH_3), 1.20 (m, 5H, Ile CH_2 and Thr CH_3), 1.45 (s, 19H, *t*-Bu and Ile CH), 2.05 and 2.20 (d of m, 2H, Glu CH_2), 2.35 and 2.50 (d of m, 2H, Glu CH_2), 3.21 (s, 2H, AAsp CH_2), 4.12 (m, 2H, α-H), 4.30 (m, 1H, α-H), 4.44 (m, 1H, Thr CH), 5.10 (m, 4H, Cbz and CH_2Ph), 5.40 (d, 1H, NH), 6.85 and 7.20 (d of d, 2H, CH═CH), 7.20−7.40 (m, 10H, Ph), 7.50 (d, 1H, NH), 8.00 (d, 1H, NH), 9.40 (s, 1H, NH).

Cbz-Ile-Glu(O-*t*Bu)-Thr-AAsp(O-*t*Bu)-CH═CH−CONHPh was obtained using the EDC/HOBt coupling method, purified by column chromatography on silica gel with 50:45:5 CH_2Cl_2:EtOAc:MeOH as the eluent; white solid, yield 67%. ^{1}H NMR (acetone-d_6): 0.89 and 0.99 (m, 6H, Ile CH_3), 1.24 (m, 5H, Thr CH_3 and Ile CH_2), 1.45 (s, 18H, *t*-Bu), 1.60 (m, 1H, Ile CH), 1.95 and 2.15 (d of m, 2H, Glu CH_2), 2.39 (m, 2H, Glu CH_2), 2.86 (s, 2H, AAsp CH_2), 4.16 (m, 1H, α-H), 4.35 (m, 1H, α-H), 4.45 (m, 2H, α-H and Thr CH), 5.10 (q, 2H, Cbz), 6.70 (d, 1H, NH), 6.80 and 7.20 (d of d, 2H, CH═CH), 7.08 (m, 2H, Ph), 7.35 (m, 6H, Ph), 7.52 (m, 1H, NH), 7.78 (t, 2H, Ph), 7.90 (b, 1H, NH), 9.60 (s, 1H, NH), 9.70 (s, 1H, NH).

Cbz-Ile-Glu(O-*t*Bu)-Thr-AAsp(O-*t*Bu)-CH═CH−CONHC-H_2Ph was obtained using the EDC/HOBt coupling method, purified by column chromatography on silica gel with 50:45:5 CH_2Cl_2:EtOAc:MeOH as the eluent; white solid, yield 30%. ^{1}H NMR ($CDCl_3$): 0.92 and 0.95 (m, 6H, Ile CH_3), 1.19 (m, 5H, Ile CH_2 and Thr CH_3), 1.45 (s, 18H, *t*-Bu), 1.80 (m, 1H, Ile CH), 1.90 (m, 2H, Glu CH_2), 2.30 and 2.40 (d of m, 2H, Glu CH_2), 3.20 (s, 2H, AAsp CH_2), 4.12 (m, 1H, α-H), 4.38 (m, 3H, α-H, Thr CH and CH_2Ph), 4.52 (m, 1H, CH_2Ph), 5.10 (s, 2H, Cbz), 5.53 (d, 1H, NH), 6.85 (d, 1H, CH═CH), 7.15−7.40 (m, 11H, CH═CH and Ph), 7.70 (s, 1H, NH), 8.05 (b, 1H, NH), 8.35 (b, 1H, NH), 9.45 (s, 1H, NH).

Cbz-Ile-Glu(O-*t*Bu)-Thr-AAsp(O-*t*Bu)-CH═CH−CONHC-H_2CH_2Ph was obtained using the EDC/HOBt coupling method, purified by column chromatography on silica gel with 50:45:5 CH_2Cl_2:EtOAc:MeOH as the eluent; white solid, yield 77%. ^{1}H NMR ($CDCl_3$): 0.92 and 0.98 (m, 6H, Ile CH_3), 1.19 (m, 5H, Ile CH_2 and Thr CH_3), 1.45 (s, 18H, *t*-Bu), 1.80 (m, 1H, Ile CH), 1.95 and 2.10 (d of m, 2H, Glu CH_2), 2.35 and 2.50 (d of m, 2H, Glu CH_2), 2.80 (m, 2H, CH_2Ph), 3.20 (s, 2H, AAsp CH_2), 3.52 (m, 2H, NCH_2), 4.15 (m, 2H, α-H), 4.25 (m, 1H, α-H), 4.40 (m, 1H, Thr CH), 5.11 (s, 2H, Cbz), 5.45 (d, 1H, NH), 6.85 (d, 1H, CH═CH), 7.15−7.40 (m, 12H, CH═CH, Ph and NH), 7.70 (b, 1H, NH), 8.05 (b, 1H, NH), 9.40 (s, 1H, NH).

Cbz-Ile-Glu(O-*t*Bu)-Thr-AAsp(O-*t*Bu)-CH═CH−CON(CH_3)-CH_2CH_2Ph was obtained using the EDC/HOBt coupling method, purified by column chromatography on silica gel with 50:45:5 CH_2Cl_2:EtOAc:MeOH as the eluent; white solid, yield 77%. ^{1}H NMR (acetone-d_6): 0.90 and 0.99 (m, 6H, Ile CH_3), 1.21 (m, 3H, Thr CH_3), 1.45 (s, 18H, *t*-Bu), 1.60 (m, 3H, Ile CH and CH_2), 1.96 (m, 2H, Glu CH_2), 2.38 (m, 2H, Glu CH_2), 2.84 (s, 2H, AAsp CH_2), 2.95 and 3.08 (d, 3H, NCH_3), 4.15−4.30 (m, 3H, α-H), 4.42 (m, 1H, Thr CH), 4.65 (s, 2H, CH_2Ph), 5.08 (q, 2H, Cbz), 6.63 (d, 1H, NH), 7.20−7.40 (m, 13H, CH═CH, Ph and NH), 7.52 (d, 1H, NH), 7.84 (d, 1H, NH), 9.75 (s, 1H, NH).

Cbz-Ile-Glu(O-*t*Bu)-Thr-AAsp(O-*t*Bu)-CH═CH−CON(CH_3)-CH_2CH_2Ph was obtained using the EDC/HOBt coupling method, purified by column chromatography on silica gel with 50:45:5 CH_2Cl_2:EtOAc:MeOH as the eluent; white solid, yield 71%. ^{1}H NMR ($CDCl_3$): 0.90 (m, 3H, Ile CH_3), 0.96 (m, 3H, Ile CH_3), 1.20 (m, 3H, Thr CH_3), 1.45 (s, 18H, *t*-Bu), 1.80−1.90 (m, 3H, Ile CH and CH_2), 2.10 (m, 2H, Glu CH_2), 2.40 (m, 2H, Glu CH_2), 2.85 (m, 2H, CH_2Ph), 2.97 (d, 3H, NCH_3), 3.30 (m, 2H, AAsp CH_2), 3.54 (m, 2H, NCH_2), 4.20 (m, 2H, α-H), 4.41 (m, 2H, α-H and Thr CH), 5.11 (q, 2H, Cbz), 5.60 (d, 1H, NH), 7.10−7.40 (m, 13H, CH═CH, Ph and NH), 7.85 (b, 1H, NH), 9.50 (d, 1H, NH).

Cbz-Ile-Glu(O-*t*Bu)-Thr-AAsp(O-*t*Bu)-CH═CH−CON(CH_2Ph)$_2$ was obtained using the EDC/HOBt coupling method, purified by column chromatography on silica gel with 50:45:5 CH_2Cl_2:EtOAc:MeOH as the eluent; white solid, yield 46%. ^{1}H NMR (acetone-d_6): 0.89 and 0.99 (m, 6H, Ile CH_3), 1.21 (m, 3H, Thr CH_3), 1.45 (s, 18H, *t*-Bu), 1.60 (m, 3H, Ile CH and CH_2), 1.95 and 2.10 (d of m, 2H, Glu CH_2), 2.39 (m, 2H, Glu CH_2), 2.84 (s, 2H, AAsp CH_2), 4.15 (t, 1H, α-H), 4.35 (m, 1H, α-H), 4.45 (m, 2H, α-H and Thr CH), 4.67 (m, 4H, CH_2Ph), 5.09 (q, 2H, Cbz), 5.60 (d, 1H, NH), 7.20−7.40 (m, 17H, CH═CH and Ph), 7.55 (d, 1H, NH), 7.85 (d, 1H, NH), 9.75 (s, 1H, NH).

Cbz-Leu-Glu(O-*t*Bu)-Thr-AAsp(O-*t*Bu)-CH═CH−COOEt was synthesized using the mixed anhydride coupling method and purified by column chromatography using 4:1 (1:19 MeOH:CH_2Cl_2):EtOAc as the eluent; white solid, yield 35%. MS (ESI) *m*/*z* 806 [$(M + 1)^+$]. ^{1}H NMR (DMSO-d_6): 0.85 (t, 6H, Leu CH_3), 1.1 (d, 3H, Thr CH_3), 1.2−1.3 (t, 3H, OCH_2CH_3), 1.3−1.5 (d, 20H, *t*Bu and Leu CH_2), 1.6 (m, 1H, CH Leu), 1.7 (m, 1H, Glu CH_2), 1.9 (m, 1H, Glu CH_2), 2.2 (m, 2H, Glu CH_2), 3.9−4.1 (m, 4H, NCH_2COOH and α-H), 4.1−4.2 (m, 3H, OCH_2CH_3 and *CH*-OH), 4.3 (m, 2H, α-H), 5.0 (s, 2H, Cbz), 6.6 (d, 1H, CH═CH), 7.20−7.40 (m, 6H, Ph and CH═CH), 7.50 (d, 1H, NH), 7.75 (d, 1H, NH), 8.0 (d, 1H, NH).

Cbz-Leu-Glu(O-*t*Bu)-Thr-AAsp(O-*t*Bu)-CH═CH−COOCH-$_2$Ph was obtained by the EDC/HOBt coupling method, and purified by column chromatography on silica gel with 1:499:500 MeOH:CH_2Cl_2:EtOAc as the eluent; white solid, yield 52%. MS (ESI) *m*/*z* 868.4 [$(M + 1)^+$]. ^{1}H NMR (DMSO-d_6): 0.83 (t, 6H, Leu), 1.02 (d, 3H, Thr), 1.36−1.40 (t, 20H, *t*Bu and Leu), 1.60 (m, 1H, Glu), 1.72 (m, 1H, Glu), 1.88 (m, 1H, Leu), 2.21 (m, 2H, Glu), 3.92 (m, 1H, α-H), 4.03 (m, 1H, α-H), 4.17 (m, 1H, α-H), 4.34 (m, 1H, Thr), 4.99 (s, 2H, Cbz), 5.19 (s, 2H, Bzl), 6.67−6.71 (d, 1H, db), 7.32−7.38 (m, 10H, Ph), 7.40 (d, 1H, db), 7.76 (d, 1H, NH), 8.04 (d, 1H, NH), 10.80 (s, 1H, NH−N).

Cbz-Leu-Glu(O-*t*Bu)-Thr-AAsp(O-*t*Bu)-CH═CHCONHPh was obtained using the EDC/HOBt coupling method, purified by column chromatography on silica gel with 50:45:5 CH_2Cl_2:EtOAc:MeOH as the eluent; white solid, yield 80%. ^{1}H NMR (acetone-d_6): 0.93 (d, 6H, Leu CH_3), 1.22 (m, 3H, Thr CH_3), 1.44 (s, 18H, *t*-Bu), 1.67 (t, 2H, Leu CH_2), 1.78 (m, 1H, Leu CH), 1.95 and 2.15 (d of m, 2H, Glu CH_2), 2.38 (m, 2H, Glu CH_2), 2.87 (s, 2H, AAsp CH_2), 4.30−4.35 (m, 3H, α-H), 4.42 (m, 1H, Thr CH), 5.09 (q, 2H, Cbz), 6.75 (d, 1H, NH), 6.80 and 7.20 (d of d, 2H, CH═CH), 7.08 (m, 2H, Ph), 7.35 (m, 6H, Ph), 7.52 (m, 1H, NH), 7.78 (t, 2H, Ph), 7.88 (b, 1H, NH), 9.63 (s, 1H, NH), 9.72 (s, 1H, NH).

Cbz-Leu-Glu(O-*t*Bu)-Thr-AAsp(O-*t*Bu)-CH═CHCONHC-H_2Ph was obtained using the EDC/HOBt coupling method, purified by column chromatography on silica gel with 50:45:5 CH_2Cl_2:EtOAc:MeOH as the eluent; white solid, yield 38%. ^{1}H NMR ($CDCl_3$): 0.94 (d, 6H, Leu CH_3), 1.20 (m, 3H, Thr CH_3), 1.45 (s, 18H, *t*-Bu), 1.64 (m, 3H, Leu CH and CH_2), 2.00 (m, 2H, Glu CH_2), 2.34 and 2.42 (d of m, 2H, Glu CH_2), 3.20 (s, 2H, AAsp CH_2), 4.10 (m, 1H, α-H), 4.21 (m, 2H, α-H), 4.40−4.50 (m, 3H, Thr CH and CH_2Ph), 5.05 (q, 2H, Cbz), 5.42 (d, 1H, NH), 6.85 (d, 1H, CH═CH), 7.15−7.40 (m, 11H, CH═CH and, Ph), 7.55 (b, 1H, NH), 7.70 (b, 1H, NH), 8.20 (b, 1H, NH), 9.40 (s, 1H, NH).

Cbz-Leu-Glu(O-*t*Bu)-Thr-AAsp(O-*t*Bu)-CH═CHCONHCH$_2$-4-F-Ph was obtained using the EDC/HOBt coupling method, purified by column chromatography on silica gel with 50:45:5 CH_2Cl_2:EtOAc:MeOH as the eluent; white solid, yield 46%. ^{1}H NMR (acetone-d_6): 0.92 (d, 6H, Leu CH_3), 1.21 (d, 3H, Thr CH_3), 1.45 (s, 18H, *t*-Bu), 1.66 (t, 2H, Leu CH_2), 1.76 (m, 1H, Leu CH), 1.95 and 2.10 (d of m, 2H, Glu CH_2), 2.36 (m, 2H, Glu CH_2), 3.20 (s, 2H, AAsp CH_2), 4.29 (m, 3H, α-H), 4.40 (m, 1H, Thr CH), 4.50 (d, 2H, C*H*$_2$Ph), 5.10 (q, 2H, Cbz), 6.76 (d, 1H, NH), 6.91 (d, 1H, CH═CH), 7.07 (d. 2H, CH═CH and Ph), 7.25−7.40 (m, 8H, Ph), 7.50 (b, 1H, NH), 7.95 (b, 1H, NH), 8.23 (b, 1H, NH), 9.70 (s, 1H, NH).

Cbz-Leu-Glu(O-*t*Bu)-Thr-AAsp(O-*t*Bu)-CH═CHCONHCH$_2$CH$_2$Ph was obtained using the EDC/HOBt coupling method, purified by column chromatography on silica gel with 50:45:5 CH_2Cl_2:EtOAc:MeOH as the eluent; white solid, yield 55%. ^{1}H NMR ($CDCl_3$): 0.94 (d, 6H, Leu CH_3), 1.20 (m, 3H, Thr CH_3), 1.45 (s, 18H, *t*-Bu), 1.65 (m, 3H, Leu CH and CH_2), 2.05 (m, 2H, Glu CH_2), 2.40 (m, 2H, Glu CH_2), 2.78 (m, 2H, *CH*$_2$Ph), 3.20 (s, 2H, AAsp CH_2), 3.50 (m, 2H, NCH_2), 4.24 (m, 3H, α-H), 4.41 (m, 1H, Thr CH), 5.05 (s, 2H, Cbz), 5.62 (d, 1H, NH), 6.80 and 7.10 (d of d, 2H, CH═CH), 7.15−7.40 (m, 12H, Ph and NH), 8.00 (b, 1H, NH), 9.45 (s, 1H, NH).

Cbz-Leu-Glu(O-*t*Bu)-Thr-AAsp(O-*t*Bu)-CH═CH−CON(CH$_3$)-CH$_2$Ph was obtained using the EDC/HOBt coupling method, purified by column chromatography on silica gel with 50:45:5 CH_2Cl_2:EtOAc:MeOH as the eluent; white solid, yield 77%. ^{1}H NMR (acetone-d_6): 0.94 (d, 6H, Leu CH_3), 1.20 (m, 3H, Thr CH_3), 1.45 (s, 18H, *t*-Bu), 1.65 (m, 2H, Leu CH_2), 1.80 (m, 1H, Leu CH), 1.95−2.10 (d of m, 2H, Glu CH_2), 2.38 (d of m, 2H, Glu CH_2), 2.85 (s, 2H, AAsp CH_2), 2.95 and 3.08 (d, 3H,NCH_3), 4.30 (m, 3H, α-H), 4.42 (m, 1H, Thr CH), 4.65 (s, 2H, *CH*$_2$Ph), 5.08 (q, 2H, Cbz), 6.75 (d, 1H, NH), 7.20−7.40 (m, 12H, CH═CH and Ph), 7.44 (d, 1H, NH), 7.90 (d, 1H, NH), 9.75 (s, 1H, NH).

Cbz-Leu-Glu(O-*t*Bu)-Thr-AAsp(O-*t*Bu)-CH═CH−CON(CH$_3$)-CH$_2$CH$_2$Ph was obtained using the EDC/HOBt coupling method, purified by column chromatography on silica gel with 50:45:5 CH_2Cl_2:EtOAc:MeOH as the eluent; white solid, yield 76%. ^{1}H NMR ($CDCl_3$): 0.94 (m, 6H, Leu CH_3), 1.21 (m, 3H, Thr CH_3), 1.45 (s, 18H, *t*-Bu), 1.55 (m, 2H, Leu CH_2), 1.70 (m, 1H, Leu CH), 2.13 (m, 2H, Glu CH_2), 2.43 (m, 2H, Glu CH_2), 2.81 (m, 2H, *CH*$_2$Ph), 2.88 and 2.92 (d, 3H, NCH_3), 3.56 (m, 4H, NCH_2 and AAsp CH_2), 4.30 (m, 2H, α-H), 4.43 (m, 2H, α-H and Thr CH), 5.10 (q, 2H, Cbz), 5.55 (m, 1H, NH), 7.10−7.40 (m, 12H, CH═CH and Ph), 7.45 (d, 1H, NH), 7.95 (b, 1H, NH), 9.42 (d, 1H, NH).

Cbz-Leu-Glu(O-*t*Bu)-Thr-AAsp(O-*t*Bu)-CH═CH−CON(CH$_2$-Ph)$_2$ was obtained using the EDC/HOBt coupling method, purified by column chromatography on silica gel with 50:45:5 CH_2Cl_2:EtOAc:MeOH as the eluent; white solid, yield 85%. ^{1}H NMR (acetone-d_6): 0.93 (d, 6H, Leu CH_3), 1.21 (m, 3H, Thr CH_3), 1.45 (s, 18H, *t*-Bu), 1.67 (m, 2H, Leu CH_2), 1.80 (m, 1H, Leu CH), 1.95 and 2.10 (d of m, 2H, Glu CH_2), 2.39 (m, 2H, Glu CH_2), 2.88 (s, 2H, AAsp CH_2), 4.25−4.35 (m, 3H, α-H), 4.43 (m, 1H, Thr CH), 4.66 (m, 4H, *CH*$_2$Ph), 5.09 (q, 2H, Cbz), 6.75 (d, 1H, NH), 7.20−7.40 (m, 17H, CH═CH and Ph), 7.55 (d, 1H, NH), 7.90 (b, 1H, NH), 9.75 (s, 1H, NH).

Cbz-Leu-Glu(O-*t*Bu)-Thr-AAsp(O-*t*Bu)-CH═CH−CO-tetrahydroquinoline was obtained using the EDC/HOBt coupling method, purified by column chromatography on silica gel with 50:45:5 CH_2Cl_2:EtOAc:MeOH as the eluent; white solid, yield 85%. ^{1}H NMR ($CDCl_3$): 0.94 (m, 6H, Leu CH_3), 1.21 (m, 3H, Thr CH_3), 1.45 (s, 18H, *t*-Bu), 1.60 (m, 2H, Leu CH_2), 1.70 (m, 1H, Leu CH), 1.90 (m, 2H, quinoline CH_2), 2.10 (m, 2H, Glu CH_2), 2.45 (m, 2H, Glu CH_2), 2.67 (t, 2H, quinoline CH_2), 3.40 (m, 2H, AAsp CH_2), 3.90 (m, 2H, NCH_2), 4.30 (m, 2H, α-H), 4.45 (m, 2H, α-H and Thr CH), 5.10 (q, 2H, Cbz), 5.55 (b, 1H, NH), 6.90 (b, 1H, NH), 7.10−7.40 (m, 10H, CH═CH and Ph), 7.50 (d, 1H, Ph), 7.95 (d, 1H, NH), 9.40 (d, 1H, NH).

Cbz-Leu-Glu(O-*t*Bu)-Thr-AAsp(O-*t*Bu)-CH═CH−CON(CH$_3$)-CH$_2$-1-Naphth was obtained using the EDC/HOBt coupling method, purified by column chromatography on silica gel with 50:45:5 CH_2Cl_2:EtOAc:MeOH as the eluent; white solid, yield 66%. ^{1}H NMR ($CDCl_3$): 0.95 (m, 6H, Leu CH_3), 1.22 (m, 3H, Thr CH_3), 1.45 (s, 18H, *t*-Bu), 1.55 (m, 2H, Leu CH_2), 1.70 (m, 1H, Leu CH), 2.15 (m, 2H, Glu CH_2), 2.45 (m, 2H, Glu CH_2), 2.92 and 2.99 (d, 3H, NCH_3), 3.30 (m, 2H, AAsp CH_2), 4.31 (m, 2H, α-H), 4.47 (m, 2H, α-H and Thr CH), 5.09 (m, 4H, *CH*$_2$-naphth and Cbz), 5.50 (b, 1H, NH), 7.10 (d, 1H, NH), 7.20−7.40 (m, 10H, CH═CH and Ph), 7.52 (m, 2H, naphth), 7.79 (d, 1H, NH), 7.90 (m, 2H, naphth), 9.45 (d, 1H, NH).

Deblocking of the *t*-Butyl Protecting Group in the Aza-Asp Peptide Inhibitors. The aza-peptide inhibitors were treated with 1:1 TFA: CH_2Cl_2 at 0 °C for 1 h and at room temperature for 2 h. TFA and CH_2Cl_2 were removed under vacuum and the final products were recrystallized from ether/hexanes mostly as white solids.

***N*^{2}-(*N*-Benzyloxycarbonylvalyl)-*N*^{1}-*trans*-(but-2-enoyl)-*N*^{1}-carboxymethylhydrazine (Cbz-Val-AAsp-CH═CH−CH$_3$, 16a).** HRMS (ESI) Calcd. for $C_{19}H_{25}N_3O_6$; 391.1822; Observed *m*/*z*: 391.1797. ***N*^{2}-(*N*-Benzyloxycarbonylvalyl)-*N*^{1}-carboxymethyl-*N*^{1}-*trans*-(hexa-2,4-dienoyl)hydrazine (Cbz-Val-AAsp-CH═CH−CH═CH−CH$_3$, 16b).** ^{1}H NMR (DMSO-d_6): 0.90 (d, 6H, Val), 1.78 (d, 3H, CH_3), 1.97 (m, 1H, Val), 3.87 (t, 1H, α-H), 5.05 (q, 2H, Cbz), 6.14 (m, 2H, db), 6.38 (m, 1H, db), 7.09 (dd, 2H, db), 7.33 (m, 5H, Ph), 7.59 (d, 1H, NH), 10.81 (s, 1H, *NH*-N). HRMS (ESI) Calcd. for $C_{21}H_{27}N_3O_6$: 417.1978; Observed *m*/*z*: 417.1974. Anal. ($C_{21}H_{27}N_3O_6$·1.43H_2O·0.05TFA) C, H, N.

***N*^{2}-(*N*-Benzyloxycarbonylvalyl)-*N*^{1}-carboxymethyl-*N*^{1}-*trans*-(3-phenethylacryloyl)hydrazine (Cbz-Val-AAsp-CH═CH−CH$_2$CH$_2$Ph, 16c).** HRMS (ESI) Calcd. for $C_{26}H_{31}N_3O_6$: 482.2291; Observed *m*/*z*: 482.2301. Anal. ($C_{26}H_{31}N_3O_6$·0.84H_2O) C, H, N.

***N*^{2}-(*N*-Benzyloxycarbonylvalyl)-*N*^{1}-carboxymethyl-*N*^{1}-*cis*-(3-chloroacryloyl)hydrazine (Cbz-Val-AAsp-*cis*-CH═CH−Cl, 16d).** ^{1}H NMR (DMSO-d_6): 0.86 (d, 6H, Val), 1.93 (m, 1H, Val), 3.84 (t, 1H, α-H), 5.01 (s, 2H, Cbz), 6.57 (s, 1H, db), 6.76 (d, 1H, db), 7.29−7.34 (m, 5H, Ph), 7.53 (d, 1H, NH), 10.80 (s, 1H, NH−N). HRMS (ESI) Calcd. for $C_{18}H_{22}N_3O_6Cl$: 411.1275; Observed *m*/*z*: 411.1195. Anal. ($C_{18}H_{22}N_3O_6Cl$·0.04H_2O) C, H, N.

***N*^{2}-(*N*-Benzyloxycarbonylvalyl)-*N*^{1}-carboxymethyl-*N*^{1}-*trans*-(3-(4-chlorophenyl) acryloyl)hydrazine (Cbz-Val-AAsp-CH═CH−Ph-4-Cl, 16e).** ^{1}H NMR (DMSO-d_6): 0.86−0.95 (dd, 6H, Val), 1.94 (m, 1H, Val), 3.84 (t, 1H, α-H), 5.03 (q, 2H, Cbz), 7.27−7.32 (m, 5H, Ph), 7.42 (d, 1H, db), 7.55 (d, 1H, db), 7.77 (m, 4H, Ph-Cl), 10.97 (s, 1H, NH−N). HRMS (ESI) Calcd. for $C_{24}H_{26}N_3O_6$-Cl: 488.1588; Observed *m*/*z*: 488.1563. Anal. ($C_{24}H_{26}N_3O_6Cl$·0.29H_2O) C, H, N.

***N*^{2}-(*N*-Benzyloxycarbonylvalyl)-*N*^{1}-carboxymethyl-*N*^{1}-*trans*-(3-ethoxycarbonylacryloyl)hydrazine (Cbz-Val-AAsp-CH═CH−COOEt, 16h).** ^{1}H NMR (DMSO-d_6): 0.87 (d, 6H, Val), 1.15−1.23 (m, 3H, OCH_2CH_3), 1.98 (m, 1H, Val), 3.89 (t, 1H, α-H), 4.13 (q, 2H, O*CH*$_2$CH$_3$), 5.03 (s, 2H, Cbz), 6.65 (d, 1H, db), 7.28−7.34 (m, 6H, db and Ph), 7.54 (d, 1H, NH), 11.00 (s, 1H, NH). HRMS (FAB) Calcd. for $C_{21}H_{27}N_3O_8$: 449.1798; Observed *m*/*z*: 449.1876. Anal. ($C_{21}H_{27}N_3O_8$·0.29H_2O) C, H, N.

***N*^{2}-(*N*-Benzyloxycarbonylvalyl)-*N*^{1}-*trans*-(3-butylcarbamoylacryloyl)-*N*^{1}-carboxymethylhydrazine (Cbz-Val-AAsp-CH═CH−CONH-*n*Bu, 16j).** ^{1}H NMR (DMSO-d_6): 0.83−0.87 (m, 9H, Val and $NHCH_2CH_2CH_2CH_3$), 1.27 (m, 2H, $NHCH_2CH_2CH_2CH_3$), 1.37−1.41 (m, 2H, $NHCH_2CH_2CH_2CH_3$), 1.97 (m, 1H, Val), 3.12 (dd, 2H, $NHCH_2CH_2CH_2CH_3$), 3.93 (t, 1H, α-H), 5.03 (q, 2H, Cbz), 6.91 (d, 1H, db), 7.08 (d, 1H, db), 7.28−7.34 (m, 5H, Ph), 7.47 (d, 1H, NH), 8.37 (t, 1H, *NH*$CH_2CH_2CH_2CH_3$), 10.93 (s, 1H, NH−N). HRMS (ESI) Calcd. for $C_{23}H_{32}N_4O_7$: 477.2349; Observed *m*/*z*: 477.2357. Anal. ($C_{23}H_{32}N_4O_7$·0.46H_2O) C, H, N.

***N*^{1}-*trans*-(3-Benzylcarbamoylacryloyl)-*N*^{2}-(*N*-benzyloxycarbonylvalyl)-*N*^{1}-carboxymethylhydrazine (Cbz-Val-AAsp-CH═CH−CONHCH$_2$Ph, 16l).** ^{1}H NMR (DMSO-d_6): 0.85 (d, 6H, Val), 1.97 (m, 1H, Val), 3.96 (t, 1H, α-H), 4.35 (d, 2H, NH*CH*$_2$Ph), 5.01 (s, 2H, Cbz), 6.97 (d, 1H, db), 7.15 (d, 1H, db), 7.19−7.32 (m, 10H, Ph), 7.47 (d, 1H, NH), 8.91 (t, 1H, *NH*CH_2Ph), 10.94 (s, 1H, NH−N). HRMS (ESI) Calcd. for $C_{26}H_{30}N_4O_7$: 510.2193; Observed *m*/*z*: 510.2208. Anal. ($C_{26}H_{30}N_4O_7$·0.56H_2O) C, H, N.

***N*²-(*N*-Benzyloxycarbonylglutamylvalyl)-*N*¹-carboxymethyl-*N*¹-*trans*-(3-ethoxycarbonylacryloyl) hydrazine (Cbz-Glu-Val-AAsp-CH=CH−COOEt, 17h).** ^{1}H NMR (DMSO-d_6): 0.84 (m, 6H, Val), 1.20−1.21 (t, 3H, OCH_2CH_3), 1.70−2.10 (m, 3H, Val, Glu), 2.21 (m, 2H, Glu), 2.40 (CH=*CH*-COOEt) 4.05−4.22 (m, 4H, NCH_2COOH and OCH_2CH_3), 4.50−4.60 (m, 2H, α-H), 5.05 (m, 2H, Cbz), 7.12 (CO-*CH*=CH−COOEt) 7.20−7.40 (m, 5H, Ph), 7.60 (1H, NH), 7.85 (m, 2H, NH), 11.00 (m, COOH). HRMS (FAB, M+1)) Calcd. for $C_{26}H_{35}N_4O_{11}$: 579.2302; Observed *m*/*z* 579.2342. Anal. ($C_{26}H_{34}N_4O_{11}$) C, H, N.

***N*²-(*N*-Benzyloxycarbonylaspartylglutamylvalyl)-*N*¹-*trans*-(3-benzoylacryloyl)-*N*¹-carboxymethylhydrazine (Cbz-Asp-Glu-Val-AAsp-CH=CH−COPh, 18f).** ^{1}H NMR (DMSO-d_6): 0.82 (d, 6H, Val), 1.73 (m, 1H, Glu), 1.85 (m, 1H, Glu), 1.98 (m, 1H, Val), 2.20 (m, 2H, Glu), 2.48 (dd, 1H, Asp), 2.62 (dd, 1H, Asp), 4.16 (t, 1H, α-H), 4.33 (m, 2H, α-H), 5.01 (s, 2H, Cbz), 7.24 (d, 1H, db), 7.32 (s, 5H, Ph), 7.54 (t, 3H, Ph), 7.67 (t, 1H, NH), 7.79 (d, 1H, NH), 7.93 (t, 1H, NH), 7.97 (d, 2H, Ph), 11.06 (s, 1H, NH−N). HRMS (ESI) Calcd. for $C_{34}H_{39}N_5O_{13}$: 725.2623; Observed *m*/*z*: 725.2543. Anal. ($C_{34}H_{39}N_5O_{13}\cdot H_2O\cdot 0.61$TFA) C, H, N.

***N*²-(*N*-Benzyloxycarbonylaspartylglutamylvalyl)-*N*¹-carboxylmethyl-*N*¹-*cis*-(3-ethoxycarbonylacryloyl)hydrazine (Cbz-Asp-Glu-Val-AAsp-*cis*-CH=CH−COOEt, 18g).** ^{1}H NMR (DMSO-d_6): 0.85 (d, 6H, Val), 1.18 (t, 3H, OCH_2CH_3), 1.74 (m, 1H, Glu), 1.86 (m, 1H, Glu), 1.95 (m, 1H, Val), 2.18 (m, 2H, Glu), 2.45 (dd, 1H, Asp), 2.61 (dd, 1H, Asp), 4.09 (t, 1H, α-H), 4.16 (q, 2H, OCH_2CH_3), 4.33 (m, 2H, α-H), 5.01 (s, 2H, Cbz), 6.61 (d, 1H, db), 7.25 (d, 1H, db), 7.33 (s, 5H, Ph), 7.62 (d, 1H, NH), 7.93 (t, 2H, NH), 11.05 (s, 1H, NH−N). HRMS (ESI) Calcd. for $C_{30}H_{39}N_5O_{14}$: 693.2566; Observed *m*/*z*: 693.2516. Anal. ($C_{30}H_{39}N_5O_{14}\cdot 1H_2O$) C, H, N.

***N*²-(*N*-Benzyloxycarbonylaspartylglutamylthreonyl)-*N*¹-carboxylmethyl-*N*¹-*trans*-(3-ethoxycarbonylacryloyl)hydrazine (Cbz-Asp-Glu-Val-AAsp-CH=CH−COOEt, 18h).** ^{1}H NMR (DMSO-d_6): 0.86 (d, 6H, Val CH_3), 1.21 (t, 3H, OEt), 1.75 and 1.98 (d of m, 2H, Glu CH_2), 1.85 (m, 1H, Val CH), 2.18 (m, 2H, Glu CH_2), 2.47 and 2.60 (d of m, 2H, Asp CH_2), 3.32 (s, 2H, AAsp CH_2), 4.15 (q, 2H, OEt), 4.31 (m, 3H, α-H), 5.00 (s, 2H, Z), 6.58 (d, 1H, CH=CH), 7.20−7.35 (m, 7H, CH=CH, Ph and NH), 7.58 (d, 1H, NH), 7.97 (m, 2H, NH), 10.95 (b, 3H, COOH). HRMS (FAB, M+1) calcd. for $C_{30}H_{40}N_5O_{14}$: 694.2572; Observed *m*/*z* 694.2599. Anal. ($C_{30}H_{39}N_5O_{14}$) C, H, N.

***N*¹-*trans*-(3-Benzyloxycarbonylacryloyl)-*N*²-(*N*-benzyloxycarbonylaspartylglutamylvalyl)-*N*¹-carboxymethylhydrazine (Cbz-Asp-Glu-Val-AAsp-CH=CH−COOCH₂Ph, 18i).** ^{1}H NMR (DMSO-d_6): 0.81 (d, 6H, Val), 1.74 (m, 1H, Glu), 1.86 (m, 1H, Glu), 1.95 (m, 1H, Val), 2.18 (m, 2H, Glu), 2.45 (dd, 1H, Asp), 2.61 (dd, 1H, Asp), 4.13 (t, 1H, α-H), 4.29 (m, 2H, α-H), 4.99 (s, 2H, Cbz), 5.18 (s, 2H, Bzl), 6.69 (d, 1H, db), 7.25−7.37 (m, 11H, Ph, and db), 7.60 (d, 1H, NH), 7.93 (t, 2H, NH), 11.02 (s, 1H, *NH*-N). HRMS (ESI) Calcd. for $C_{35}H_{41}N_5O_{14}$: 755.2728; Observed *m*/*z*: 755.2631. Anal. ($C_{35}H_{41}N_5O_{14}\cdot 0.59H_2O$) C, H, N.

***N*¹-*trans*-(3-Benzylcarbamoylacryloyl)-*N*²-(*N*-benzyloxycarbonylaspartylglutamylvalyl)-*N*¹-carboxymethylhydrazine (Cbz-Asp-Glu-Val-AAsp-CH=CH−CONHCH₂Ph, 18l).** ^{1}H NMR (DMSO-d_6): 0.85 (t, 6H, Val), 1.75 (m, 1H, Glu), 1.88 (m, 1H, Glu), 2.01 (m, 1H, Val), 2.19 (m, 2H, Glu), 2.48 (dd, 1H, Asp), 2.61 (dd, 1H, Asp), 4.17 (t, 1H, α-H), 4.30 (m, 2H, α-H), 4.35 (d, 2H, NHCH_2Ph), 5.00 (s, 2H, Cbz), 6.96 (d, 1H, db), 7.12 (d, 1H, db), 7.21−7.32 (m, 10H, Ph), 7.58 (d, 1H, NH), 7.90 (d, 1H, NH), 7.96 (d, 1H, NH), 8.92 (t, 1H, *NH*CH_2Ph), 10.97 (s, 1H, NH−N). HRMS (ESI) Calcd. for $C_{35}H_{42}N_6O_{13}$: 754.2888; Observed *m*/*z*: 754.2853. Anal. ($C_{35}H_{42}N_6O_{13}\cdot 1.63H_2O$) C, H, N.

***N*²-(*N*-Benzyloxycarbonylaspartylglutamylvalyl)-*N*¹-carboxymethyl-*N*¹-*trans*-(3-(4-fluorobenzyl)carbamoylacryloyl)hydrazine (Cbz-Asp-Glu-Val-AAsp-CH=CH−CONHCH₂-4-F-Ph, 18m).** ^{1}H NMR (DMSO-d_6): 0.86 (t, 6H, Val), 1.75 (m, 1H, Glu), 1.88 (m, 1H, Glu), 2.01 (m, 1H, Val), 2.20 (m, 2H, Glu), 2.48 (dd, 1H, Asp), 2.65 (dd, 1H, Asp), 4.18 (t, 1H, α-H), 4.34 (m, 4H, α-H and NHCH_2Ph-4-F), 5.01 (s, 2H, Cbz), 6.93 (d, 1H, db), 7.12 (d, 2H, NHCH$_2$*Ph*-4-F), 7.25−7.32 (m, 8H, Cbz-Ph, NHCH$_2$*Ph*-4-F, and db), 7.59 (d, 1H, NH), 7.90−7.99 (dd, 2H, NH), 8.94 (t, 1H, *NH*CH_2Ph-4-F), 10.98 (s, 1H, NH−N). HRMS (ESI) Calcd. for $C_{35}H_{41}N_6O_{13}F$: 772.2788; Observed *m*/*z*: 772.2747. Anal. ($C_{35}H_{41}N_6O_{13}F\cdot 2.08H_2O$) C, H, N.

***N*²-(*N*-Benzyloxycarbonylaspartylglutamylvalyl)-*N*¹-carboxymethyl-*N*¹-*trans*-(3-phenethylcarbamoylacryloyl)hydrazine (Cbz-Asp-Glu-Val-AAsp-CH=CH−CONHCH₂CH₂Ph, 18n).** ^{1}H NMR (DMSO-d_6): 0.87 (t, 6H, Val), 1.75 (m, 1H, Glu), 1.89 (m, 1H, Glu), 2.01 (m, 1H, Val), 2.21 (m, 2H, Glu), 2.46 (dd, 1H, Asp), 2.62 (dd, 1H, Asp), 2.73 (t, 2H, NHCH$_2$*CH*$_2$Ph), 3.73 (d, 2H, NH*CH*$_2$CH$_2$Ph), 4.18 (t, 1H, α-H), 4.32 (m, 2H, α-H), 5.01 (s, 2H, Cbz), 6.89 (d, 1H, db), 7.08 (d, 1H, db), 7.16−7.32 (m, 10H, Ph), 7.59 (d, 1H, NH), 7.89 (d, 1H, NH), 7.98 (d, 1H, NH), 8.52 (t, 1H, *NH*CH_2CH$_2$Ph), 10.97 (s, 1H, NH−N). HRMS (ESI) Calcd. for $C_{36}H_{44}N_6O_{13}$: 768.3044; Observed *m*/*z*: 768.2949. Anal. ($C_{36}H_{44}N_6O_{13}\cdot 1.22H_2O$) C, H, N.

***N*¹-*trans*-(3-Benzylmethylcarbamoylacryloyl)-*N*²-(*N*-benzyloxycarbonylaspartylglutamylvalyl)-*N*¹-carboxymethylhydrazine (Cbz-Asp-Glu-Val-AAsp-CH=CH−CON(CH₃)CH₂Ph, 18o).** ^{1}H NMR (DMSO-d_6): 0.85 (d, 6H, Val), 1.73 (m, 1H, Glu), 1.87 (m, 1H, Glu), 1.97 (m, 1H, Val), 2.20 (m, 2H, Glu), 2.48 (dd, 1H, Asp), 2.63 (dd, 1H, Asp), 2.88−2.98 (d, 3H, N(*CH*$_3$)CH$_2$Ph), 4.17 (t, 1H, α-H), 4.32 (m, 2H, α-H), 4.47−4.58 (q, 1H, N(CH$_3$)*CH*$_2$-Ph), 4.66 (s, 1H, N(CH$_3$)*CH*$_2$Ph), 5.00 (s, 2H, Cbz), 7.14 (d, 1H, db), 7.20 (d, 1H, db), 7.28−7.36 (m, 10H, Ph), 7.57 (d, 1H, NH), 7.91−7.95 (m, 2H, NH), 10.99 (s, 1H, NH−N). HRMS (ESI) Calcd. for $C_{36}H_{44}N_6O_{13}$: 768.3045; Observed *m*/*z*: 768.3039. Anal. ($C_{36}H_{44}N_6O_{13}\cdot$EtOAc) C, H, N.

***N*²-(*N*-Benzyloxycarbonylaspartylglutamylvalyl)-*N*¹-carboxymethyl-*N*¹-*trans*-(3-phenethylmethylcarbamoylacryloyl)hydrazine (Cbz-Asp-Glu-Val-AAsp-CH=CH−CON(CH₃)CH₂-CH₂Ph, 18p).** ^{1}H NMR (DMSO-d_6): 0.86 (t, 6H, Val), 1.75 (m, 1H, Glu), 1.89 (m, 1H, Glu), 2.01 (m, 1H, Val), 2.21 (m, 2H, Glu), 2.46 (dd, 1H, Asp), 2.62 (dd, 1H, Asp), 2.80 (t, 2H, N(CH$_3$)CH$_2$*CH*$_2$Ph), 2.85−2.98 (d, 3H, N(*CH*$_3$)CH$_2$CH$_2$Ph), 3.73 (d, 2H, N(CH$_3$)*CH*$_2$-CH$_2$Ph), 4.18 (t, 1H, α-H), 4.32 (m, 2H, α-H), 5.00 (s, 2H, Cbz), 6.94 (d, 1H, db), 7.05 (dd, 1H, db), 7.15−7.32 (m, 10H, Ph), 7.59 (d, 1H, NH), 7.91 (d, 1H, NH), 7.97 (d, 1H, NH), 10.93 (d, 1H, NH−N). HRMS (ESI) Calcd. for $C_{37}H_{46}N_6O_{13}$: 783.3196; Observed *m*/*z*: 783.3182. Anal. ($C_{37}H_{46}N_6O_{13}\cdot 1.09H_2O\cdot 0.24$TFA) C, H, N.

***N*²-(*N*-Benzyloxycarbonylaspartylglutamylvalyl)-*N*¹-carboxymethyl-*N*¹-*trans*-(3-dibenzylcarbamoylacryloyl)hydrazine (Cbz-Asp-Glu-Val-AAsp-CH=CH−CON(CH₂Ph)₂, 18r).** ^{1}H NMR (DMSO-d_6): 0.87 (t, 6H, Val), 1.73 (m, 1H, Glu), 1.87 (m, 1H, Glu), 2.02 (m, 1H, Val), 2.23 (m, 2H, Glu), 2.48 (dd, 1H, Asp), 2.65 (dd, 1H, Asp), 4.19 (t, 1H, α-H), 4.33 (m, 2H, α-H), 4.55 (d, 2H, N(*CH*$_2$Ph)$_2$), 4.63 (s, 2H, N(*CH*$_2$Ph)$_2$), 5.00 (s, 2H, Cbz), 7.14 (d, 1H, db), 7.21−7.34 (m, 16H, db, Cbz-Ph, and N(CH$_2$*Ph*)$_2$), 7.60 (d, 1H, NH), 7.91−7.98 (dd, 2H, NH), 11.00 (s, 1H, NH−N). HRMS (ESI) Calcd. for $C_{42}H_{48}N_6O_{13}$: 844.3352; Observed *m*/*z*: 844.3210. Anal. ($C_{42}H_{48}N_6O_{13}\cdot 0.53H_2O\cdot 0.40$TFA) C, H, N.

***N*²-(*N*-Benzyloxycarbonylaspartylglutamylvalyl)-*N*¹-carboxymethyl-*N*¹-*trans*-(3-di-1-naphthylcarbamoylacryloyl)hydrazine (Cbz-Asp-Glu-Val-AAsp-CH=CH−CON(CH₂-1-Naphth)₂, 18t).** ^{1}H NMR (acetone-d_6): 1.03 (d, 6H, Val), 2.04−2.48 (m, 5H, Glu, Val, Asp), 2.88 (dd, 1H, Asp), 2.99 (dd, 1H, Asp), 4.46 (m, 1H, α-H), 4.57 (m, 2H, α-H), 5.09 (d, 2H, N(*CH*$_2$-1-Naph)$_2$), 5.29−5.38 (m, 4H, N(*CH*$_2$-1-Naph)$_2$), Cbz), 6.89 (d, J = 7.2 Hz, 1H, db), 7.30−7.99 (m, 21H, db, NH, Cbz-Ph, and N(CH$_2$-*1-Naph*)$_2$), 8.15 (d, 1H, NH), 9.87 (s, 1H, NH−N). HRMS (ESI) Calcd. for $C_{50}H_{53}N_6O_{13}$: 945.3572; Observed *m*/*z*: 945.3665.

***N*²-(*N*-Benzyloxycarbonylaspartylglutamylvalyl)-*N*¹-carboxymethyl-*N*¹-*trans*-(3-(3,4-dihydro-2*H*-quinolin-1-ylcarbonyl)acryloyl)hydrazine (Cbz-Asp-Glu-Val-AAsp-CH=CH−CO-tetrahydroquinoline, 18u).** ^{1}H NMR (DMSO-d_6): 0.89 (t, 6H, Val), 1.75 (m, 1H, Glu), 1.87 (m, 3H, Glu and NCH$_2$CH$_2$*CH*$_2$), 2.02 (m, 1H, Val), 2.20 (m, 2H, Glu), 2.48 (dd, 1H, Asp), 2.65 (dd, 1H, Asp), 2.70 (t, 2H, NCH$_2$*CH*$_2$CH$_2$), 3.73 (t, 2H, N*CH*$_2$CH$_2$CH$_2$), 4.19 (t, 1H, α-H), 4.33 (m, 2H, α-H), 5.01 (s, 2H, Cbz), 6.95 (m, 1H, db), 7.04 (d, 1H, db), 7.14−7.33 (m, 9H, Cbz-Ph, and quinoline), 7.60

(d, 1H, NH), 7.96 (dd, 2H, NH), 11.02 (s, 1H, NH−N). HRMS (ESI) Calcd. for $C_{37}H_{44}N_6O_{13}$: 780.3039; Observed *m/z*: 780.2954. Anal. ($C_{37}H_{44}N_6O_{13}$·0.48H_2O·0.47TFA) C, H, N.

***N*²-(*N*-Benzyloxycarbonylvalylglutamylvalyl)-*N*¹-carboxy-methyl-*N*¹-*trans*-(3-ethoxycarbonylacryloyl)hydrazine (Cbz-Val-Glu-Val-AAsp-CH═CH−COOEt, 19h).** ¹H NMR (DMSO-d_6): 0.80−0.87 (dd, 12H, Val), 1.21 (t, 3H, OCH_2CH_3), 1.74 (m, 1H, Glu), 1.89 (m, 1H, Glu), 1.94 (m, 1H, Val), 2.20 (m, 2H, Glu), 3.87 (t, 1H, α-H), 4.16 (m, 3H, α-H and OCH_2CH_3), 4.33 (t, 1H, α-H), 5.01 (s, 2H, Cbz), 6.63 (d, 1H, db), 7.20 (d, 1H, db), 7.33 (m, 5H, Ph), 7.97 (t, 2H, NH), 11.02 (s, 1H, NH−N). HRMS (ESI) Calcd. for $C_{31}H_{43}N_5O_{12}$: 677.2986; Observed *m/z*: 677.2978. Anal. ($C_{31}H_{43}N_5O_{12}$·1.41H_2O·0.51hex) C, H, N.

***N*²-(*N*-Benzyloxycarbonylisoleucylglutamylthreonyl)-*N*¹-carboxymethyl-*N*¹-*trans*-(3-ethoxycarbonylacryloyl)hydrazine (Cbz-Ile-Glu-Thr-AAsp-CH═CH−COOEt, 20h).** ¹H NMR (DMSO-d_6): 0.8 (m, 6H, Ile CH_3), 1−1.2 (m, 4H, Thr CH_3 and Ile CH_2), 1.2−1.3 (t, 3H, OCH_2CH_3), 1.4 (m, 1H, Ile CH_2), 1.6−1.8 (m, 2H, CH Ile and Glu CH_2), 1.8−2.0 (m, 1H, Glu CH_2), 2.15−2.35 (m, 2H, Glu CH_2), 3.85−4.05 (m, 3H, NCH_2COOH and *CH*-OH), 4.1−4.3 (m, 3H, OCH_2CH_3 and α-H), 4.4 (m, 2H, α-H), 5.05 (m, 2H, Cbz), 6.6−6.65 (d, 1H, CH═CH), 7.20−7.40 (m, 6H, Ph and CH═CH), 7.80 (m, 1H, NH), 8.1 (m, 1H, NH). HRMS (FAB, M+1) Calcd. for $C_{31}H_{44}N_5O_{13}$: 694.29356; Observed *m/z* 694.29979. Anal. ($C_{31}H_{43}N_5O_{13}$·H_2O) C, H, N.

***N*¹-*trans*-(3-Benzyloxycarbonylacryloyl)-*N*²-(*N*-benzyloxycarbonylisoleucylglutamylthreonyl)-*N*¹-carboxylmethylhydrazine (Cbz-Ile-Glu-Thr-AAsp-CH═CH−$COOCH_2$Ph, 20i).** ¹H NMR (DMSO-d_6): 0.80 (m, 6H, Ile CH_3), 1.02 (m, 3H, Thr CH_3), 1.10 (m, 2H, Ile CH_2), 1.65 (m, 1H, Ile CH), 1.75 and 1.85 (d of m, 2H, Glu CH_2), 2.25 (m, 2H, Glu CH_2), 3.30 (s, 2H, AAsp CH_2), 3.90 (m, 2H, α-H), 4.25 (m, 1H, α-H), 4.39 (m, 1H, Thr CH), 5.00 (s, 2H, Z), 5.20 (s, 2H, CH_2Ph), 6.70 (d, 1H, NH), 7.20−7.40 (m, 12H, Ph and CH═CH), 7.90 (b, 1H, NH), 8.10 (b, 1H, NH), 8.60 (m, 1H, NH), 10.70 (b, 2H, COOH). HRMS (FAB, M+1) Calcd. for $C_{36}H_{46}N_5O_{13}$: 756.3092; Observed *m/z* 756.3037. Anal. ($C_{36}H_{45}N_5O_{13}$·$2H_2O$) C, H, N.

***N*²-(*N*-Benzyloxycarbonylisoleucylglutamylthreonyl)-*N*¹-carboxylmethyl-*N*¹-*trans*-(3-phenylcarbamoylacryloyl)hydrazine (Cbz-Ile-Glu-Thr-AAsp-CH═CH−CONHPh, 20k).** ¹H NMR (DMSO-d_6): 0.84 (t, 6H, Ile CH_3), 1.06 (m, 3H, Thr CH_3), 1.45 (m, 2H, Ile CH_2), 1.70 (m, 1H, Ile CH), 1.80 and 1.90 (d of m, 2H, Glu CH_2), 2.25 (m, 2H, Glu CH_2), 3.33 (s, 2H, AAsp CH_2), 3.88 (t, 1H, α-H), 4.00 (m, 1H, α-H), 4.25 (m, 1H, α-H), 4.39 (m, 1H, Thr CH), 5.00 (s, 2H, Z), 7.00−7.10 (m, 4H, CH═CH and Ph), 7.30 (m, 7H, Ph and NH), 7.64 (d, 2H, Ph), 7.85 (b, 1H, NH), 8.05 (d, 1H, NH), 8.35 (m, 1H, NH), 8.60 (m, 1H, NH), 10.45 (b, 2H, COOH). HRMS (FAB, M+1) Calcd. for $C_{35}H_{45}N_6O_{12}$: 741.3095; Observed *m/z* 741.3106. Anal. ($C_{35}H_{44}N_6O_{12}$·$2H_2O$) C, H, N.

***N*¹-*trans*-(3-Benzylcarbamoylacryloyl)-*N*²-(*N*-benzyloxycarbonylisoleucylglutamylthreonyl)-*N*¹-carboxylmethylhydrazine (Cbz-Ile-Glu-Thr-AAsp-CH═CH−$CONHCH_2$Ph, 20l).** ¹H NMR (DMSO-d_6): 0.75−0.87 (m, 6H, Ile CH_3), 1.02 (m, 3H, Thr CH_3), 1.49 (m, 2H, Ile CH_2), 1.65 (m, 1H, Ile CH), 1.74 and 1.85 (d of m, 2H, Glu CH_2), 2.25 (m, 2H, Glu CH_2), 3.32 (s, 2H, AAsp CH_2), 4.00 (m, 2H, α-H), 4.25 (m, 1H, α-H), 4.40 (m, 3H, Thr CH and CH_2-Ph), 5.00 (s, 2H, Z), 7.00 (d, 1H, CH═CH), 7.40−7.40 (m, 13H, CH═CH, Ph and NH), 7.90 (b, 1H, NH), 8.05 (b, 1H, NH), 8.90 (b, 1H, NH), 10.60 (b, 2H, COOH). HRMS (FAB, M+1) Calcd. for $C_{36}H_{47}N_6O_{12}$: 755.3252; Observed *m/z* 755.3200. Anal. ($C_{36}H_{46}N_6O_{12}$·$2H_2O$) C, H, N.

***N*²-(*N*-Benzyloxycarbonylisoleucylglutamylthreonyl)-*N*¹-carboxylmethyl-*N*¹-*trans*-(3-phenyethylcarbamoylacryloyl)hydrazine (Cbz-Ile-Glu-Thr-AAsp-CH═CH−$CONHCH_2CH_2$Ph, 20n).** ¹H NMR (DMSO-d_6): 0.82 (m, 6H, Ile CH_3), 1.04 (m, 3H, Thr CH_3), 1.45 (m, 2H, Ile CH_2), 1.65 (m, 1H, Ile CH), 1.75 and 1.90 (d of m, 2H, Glu CH_2), 2.24 (m, 2H, Glu CH_2), 2.73 (t, 2H, CH_2-Ph), 3.32 (m, 4H, AAsp CH_2 and NCH_2), 3.95 (m, 2H, α-H), 4.22 (m, 1H, α-H), 4.40 (m, 1H, Thr CH), 5.00 (s, 2H, Z), 6.88 (d, 1H, CH═CH), 7.10−7.45 (m, 13H, CH═CH, Ph and NH), 7.90 (b, 2H, NH), 8.05 (b, 1H, NH), 8.52 (b, 1H, NH), 10.73 (b, 2H, COOH). HRMS (FAB, M+1) Calcd. for $C_{37}H_{49}N_6O_{12}$: 769.3408; Observed *m/z* 769.3332. Anal. ($C_{37}H_{48}N_6O_{12}$·$2H_2O$) C, H, N.

***N*¹-*trans*-(3-Benzylmethylcarbamoylacryloyl)-*N*²-(*N*-benzyloxycarbonylisoleucylglutamylthreonyl)-*N*¹-carboxylmethylhydrazine (Cbz-Ile-Glu-Thr-AAsp-CH═CH−$CON(CH_3)CH_2$Ph, 20o).** ¹H NMR (DMSO-d_6): 0.80 (m, 6H, Ile CH_3), 1.06 (m, 3H, Thr CH_3), 1.49 (m, 2H, Ile CH_2), 1.65 (m, 1H, Ile CH), 1.80 and 1.92 (d of m, 2H, Glu CH_2), 2.24 (m, 2H, Glu CH_2), 2.88 and 2.99 (d, 3H, NCH_3), 3.32 (s, 2H, AAsp CH_2), 4.02 (m, 2H, α-H), 4.20 (m, 1H, α-H), 4.40 (m, 1H, Thr CH), 4.55 (m, 2H, CH_2Ph), 5.00 (s, 2H, Z), 7.10−7.45 (m, 14H, CH═CH, Ph and NH), 7.80 (m, 1H, NH), 8.05 (m, 1H, NH),10.90 (b, 2H, COOH). HRMS (FAB, M+1) Calcd. for $C_{37}H_{49}N_6O_{12}$: 769.3408; Observed *m/z* 769.3394. Anal. ($C_{37}H_{48}N_6O_{12}$·$2H_2O$) C, H, N.

***N*²-(*N*-Benzyloxycarbonylisoleucylglutamylthreonyl)-*N*¹-carboxylmethyl-*N*¹-*trans*-(3-methylphenylethylcarbamoylacryloyl)-hydrazine (Cbz-Ile-Glu-Thr-AAsp-CH═CH−$CON(CH_3)CH_2$-CH_2Ph, 20p).** ¹H NMR (acetone-d_6): 0.88 (m, 3H, Ile CH_3), 0.97 (m, 3H, Ile CH_3), 1.21 (m, 3H, Thr CH_3), 1.60 (m, 3H, Ile CH and CH_2), 2.00 (m, 2H, Glu CH_2), 2.47 (m, 2H, Glu CH_2), 2.88 (m, 4H, CH_2Ph and AAsp CH_2), 2.98 and 3.10 (d, 3H, CH_3), 3.67 (m, 2H, CH_2N), 4.13 (m, 1H, α-H), 4.32 (m, 1H, α-H), 4.50 (m, 2H, α-H and Thr CH), 5.09 (m, 2H, Z), 6.62 (b, 1H, NH), 7.10−7.40 (m, 13H, CH═CH, NH and Ph), 7.65 (b, 1H, NH), 7.90 (b, 1H, NH). HRMS (FAB) Calcd. for $C_{38}H_{51}N_6O_{12}$: 783.3565; Observed *m/z* 783.3569. Anal. ($C_{38}H_{50}N_6O_{12}$·$2H_2O$) C, H, N.

***N*²-(*N*-Benzyloxycarbonylisoleucylglutamylthreonyl)-*N*¹-carboxylmethyl-*N*¹-*trans*-(3-dibenzylcarbamoylacryloyl)hydrazine (Cbz-Ile-Glu-Thr-AAsp-CH═CH−$CON(CH_2Ph)_2$, 20r).** ¹H NMR (DMSO-d_6): 0.80 (m, 6H, Ile CH_3), 1.06 (m, 3H, Thr CH_3), 1.50 (m, 2H, Ile CH_2), 1.65 (m, 1H, Ile CH), 1.78 and 1.90 (d of m, 2H, Glu CH_2), 2.25 (m, 2H, Glu CH_2), 3.32 (s, 2H, AAsp CH_2), 4.00 (m, 2H, α-H), 4.25 (m, 1H, α-H), 4.40 (m, 1H, Thr CH), 4.60 (d, 4H, CH_2Ph), 5.00 (s, 2H, Z), 7.00−7.35 (m, 13H, CH═CH, Ph and NH), 7.85 (b, 1H, NH), 8.10 (d, 1H, NH), 8.60 (b, 1H, NH), 10.75 (b, 2H, COOH). HRMS (FAB, M+1) Calcd. for $C_{43}H_{53}N_6O_{12}$: 845.3721; Observed *m/z* 845.3731. Anal. ($C_{43}H_{52}N_6O_{12}$·$2H_2O$) C, H, N.

***N*²-(*N*-Benzyloxycarbonylleucylglutamylthreonyl)-*N*¹-carboxymethyl-*N*¹-*trans*-(3-ethoxycarbonylacryloyl)hydrazine (Cbz-Leu-Glu-Thr-AAsp-CH═CH−COOEt, 21h).** ¹H NMR (DMSO-d_6): 0.85 (t, 6H, Leu CH_3), 1.05 (d, 3H, Thr CH_3), 1.25 (t, 3H, OCH_2CH_3), 1.4 (m, 2H, Leu CH_2), 1.6 (m, 1H, CH Leu), 1.75 (m, 1H, Glu CH_2), 1.9 (m, 1H, Glu CH_2), 2.25 (m, 2H, Glu CH_2), 3.9−4.1 (m, 3H, NCH_2COOH and α-H), 4.1−4.3 (m, 3H, OCH_2CH_3 and *CH*-OH), 4.3−4.4 (m, 2H, α-H), 5.02 (m, 2H, Cbz), 6.6−6.65 (d, 1H, CH═CH), 7.20−7.40 (m, 6H, Ph and CH═CH), 7.50 (d, 1H, NH), 7.78 (m, 1H, NH), 8.05 (m, 1H, NH). HRMS (FAB, M+1) Calcd. for $C_{31}H_{44}N_5O_{13}$: 694.29356; Observed *m/z* 694.29963. Anal. ($C_{31}H_{43}N_5O_{13}$·H_2O) C, H, N.

***N*¹-*trans*-(3-Benzyloxycarbonylacryloyl)-*N*²-(*N*-benzyloxycarbonylleucylglutamylthreonyl)-*N*¹-carboxymethylhydrazine (Cbz-Leu-Glu-Thr-AAsp-CH═CH−$COOCH_2$Ph, 21i).** ¹H NMR (DMSO-d_6): 0.84 (t, 6H, Leu), 1.02 (d, 3H, Thr), 1.40 (m, 2H, Leu), 1.60 (m, 1H, Glu), 1.73 (m, 1H, Glu), 1.90 (m, 1H, Leu), 2.22 (m, 2H, Glu), 3.94 (m, 1H, α-H), 4.03 (m, 1H, α-H), 4.20 (m, 1H, α-H), 4.37 (m, 1H, Thr), 4.99 (s, 2H, Cbz), 5.19 (s, 2H, Bzl), 6.65 (d, 1H, db), 7.32−7.36 (m, 10H, Ph), 7.42 (d, 1H, db), 7.76 (d, 1H, NH), 8.03 (d, 1H, NH), 10.84 (s, 1H, *NH*-N). HRMS (ESI) Calcd. for $C_{36}H_{45}N_5O_{13}$: 755.3092; Observed *m/z*: 755.3150. Anal. ($C_{36}H_{45}N_5O_{13}$·0.27H_2O·0.28TFA) C, H, N.

***N*²-(*N*-Benzyloxycarbonylleucylglutamylthreonyl)-*N*¹-carboxylmethyl-*N*¹-*trans*-(3-phenylcarbamoylacryloyl)hydrazine (Cbz-Leu-Glu-Thr-AAsp-CH═CHCONHPh, 21k).** ¹H NMR (DMSO-d_6): 0.85 (t, 6H, Leu CH_3), 1.06 (m, 3H, Thr CH_3), 1.49 (m, 2H, Leu CH_2), 1.61 (m, 1H, Leu CH), 1.80 and 1.95 (d of m, 2H, Glu CH_2), 2.26 (m, 2H, Glu CH_2), 3.32 (s, 2H, AAsp CH_2), 4.03 (m, 2H, α-H), 4.25 (m, 1H, α-H), 4.40 (m, 1H, Thr CH), 5.00 (s, 2H, Z), 7.00−7.10 (m, 4H, CH═CH and Ph), 7.30 (m, 7H, Ph and NH), 7.64 (d, 2H, Ph), 7.85 (m, 1H, NH), 8.05 (b, 1H, NH), 8.20 (m, 1H, NH), 8.75 (b, 1H, NH), 10.45 (s, 2H, COOH). HRMS (FAB,

M+1) Calcd. for $C_{35}H_{45}N_6O_{12}$: 741.3095; Observed *m/z* 741.3064. Anal. ($C_{35}H_{44}N_6O_{12}\cdot 2H_2O$) C, H, N.

***N*^{1}-*trans*-(3-Benzylcarbamoylacryloyl)-*N*^{2}-(*N*-benzyloxycarbonylleucylglutamylthreonyl)-*N*^{1}-carboxylmethylhydrazine (Cbz-Leu-Glu-Thr-AAsp-CH=CHCONHCH$_2$Ph, 21l).** ^{1}H NMR (DMSO-d_6): 0.85 (t, 6H, Leu CH_3), 1.06 (m, 3H, Thr CH_3), 1.49 (m, 2H, Leu CH_2), 1.61 (m, 1H, Leu CH), 1.80 and 1.90 (d of m, 2H, Glu CH_2), 2.26 (m, 2H, Glu CH_2), 3.32 (s, 2H, AAsp CH_2), 4.03 (m, 2H, α-H), 4.25 (m, 1H, α-H), 4.45 (m, 3H, Thr CH and CH_2-Ph), 5.00 (s, 2H, Z), 7.00 (d, 1H, CH=CH), 7.20−7.40 (m, 13H, CH=CH, Ph and NH), 7.80 (b, 1H, NH), 8.05 (d, 1H, NH), 8.90 (d, 1H, NH), 10.65 (b, 2H, COOH). HRMS (FAB, M+1) Calcd. for $C_{36}H_{47}N_6O_{12}$: 755.3252; Observed *m/z* 755.3184. Anal. ($C_{36}H_{46}N_6O_{12}\cdot 2H_2O$) C, H, N.

***N*^{2}-(*N*-Benzyloxycarbonylleucylglutamylthreonyl)-*N*^{1}-carboxylmethyl-*N*^{1}-*trans*-(3-(4-fluorobenzyl)carbamoylacryloyl)hydrazine (Cbz-Leu-Glu-Thr-AAsp-CH=CHCONHCH$_2$-4-F-Ph, 21m).** ^{1}H NMR (DMSO-d_6): 0.85 (t, 6H, Leu CH_3), 1.04 (m, 3H, Thr CH_3), 1.60 (m, 2H, Leu CH_2), 1.75 (m, 1H, Leu CH), 1.90 (m, 2H, Glu CH_2), 2.24 (m, 2H, Glu CH_2), 3.32 (s, 2H, AAsp CH_2), 4.03 (m, 2H, α-H), 4.25 (m, 1H, α-H), 4.40 (m, 3H, Thr CH and CH_2Ph), 5.00 (s, 2H, Z), 6.93 (d, 1H, CH=CH), 7.10−7.40 (m, 10H, CH=CH and Ph), 7.85 (b, 1H, NH), 8.05 (d, 1H, NH), 8.70 (b, 1H, NH), 8.94 (m, 2H, NH), 10.60 (b, 2H, COOH). HRMS (FAB, M+1) Calcd. for $C_{36}H_{46}N_6O_{12}F$: 773.3153; Observed *m/z* 773.3061. Anal. ($C_{36}H_{45}N_6O_{12}F\cdot 2H_2O$) C, H, N.

***N*^{2}-(*N*-Benzyloxycarbonylleucylglutamylthreonyl)-*N*^{1}-carboxylmethyl-*N*^{1}-*trans*-(3-phenylethylcarbamoylacryloyl)hydrazine (Cbz-Leu-Glu-Thr-AAsp-CH=CH−CONHCH$_2$CH$_2$Ph, 21n).** ^{1}H NMR (DMSO-d_6): 0.85 (t, 6H, Leu CH_3), 1.06 (m, 3H, Thr CH_3), 1.45 (m, 2H, Leu CH_2), 1.60 (m, 1H, Leu CH), 1.75 and 1.88 (d of m, 2H, Glu CH_2), 2.25 (m, 2H, Glu CH_2), 2.75 (t, 2H, CH_2Ph), 3.30−3.35 (m, 4H, CH_2N and AAsp CH_2), 4.00 (m, 2H, α-H), 4.20 (m, 1H, α-H), 4.38 (m, 1H, Thr CH), 5.00 (s, 2H, Z), 6.90−7.15 (d of d, 2H, CH=CH), 7.20−7.40 (m, 12H, Ph and NH), 7.86 (m, 1H, NH), 8.06 (d, 1H, NH), 8.50 (b, 1H, NH), 10.60 (b, 2H, COOH). HRMS (FAB, M+1) Calcd. for $C_{37}H_{49}N_6O_{12}$: 769.3408; Observed *m/z* 769.3201. Anal. ($C_{37}H_{48}N_6O_{12}\cdot 2H_2O$) C, H, N.

***N*^{1}-*trans*-(3-Benzylmethylcarbamoylacryloyl)-*N*^{2}-(*N*-benzyloxycarbonylleucylglutamylthreonyl)-*N*^{1}-carboxylmethylhydrazine (Cbz-Leu-Glu-Thr-AAsp-CH=CH−CON(CH$_3$)CH$_2$Ph, 21o).** ^{1}H NMR (DMSO-d_6): 0.83 (t, 6H, Leu CH_3), 1.06 (m, 3H, Thr CH_3), 1.49 (m, 2H, Leu CH_2), 1.65 (m, 1H, Leu CH), 1.80 and 1.92 (d of m, 2H, Glu CH_2), 2.24 (m, 2H, Glu CH_2), 2.88 and 2.99 (d, 2H, CH_3), 3.32 (s, 2H, AAsp CH_2), 4.02 (m, 2H, α-H), 4.20 (m, 1H, α-H), 4.40 (m, 1H, Thr CH), 4.55 (m, 2H, CH_2Ph), 5.00 (s, 2H, Z), 7.10−7.45 (m, 14H, CH=CH, Ph and NH), 7.80 (m, 1H, NH), 8.05 (m, 1H, NH),10.85 (b, 2H, COOH). HRMS (FAB, M+1) Calcd. for $C_{37}H_{49}N_6O_{12}$: 769.3408; Observed *m/z* 769.3320. Anal. ($C_{37}H_{48}N_6O_{12}\cdot 2H_2O$) C, H, N.

***N*^{2}-(*N*-Benzyloxycarbonylleucylglutamylthreonyl)-*N*^{1}-carboxylmethyl-*N*^{1}-*trans*-(3-methylphenylethylcarbamoylacryloyl)hydrazine (Cbz-Leu-Glu-Thr-AAsp-CH=CH−CON(CH$_3$)CH$_2$-CH$_2$Ph, 21p).** ^{1}H NMR (acetone-d_6): 0.94 (m, 6H, Leu CH_3), 1.20 (m, 3H, Thr CH_3), 1.65 (m, 2H, Leu CH_2), 1.75 (m, 1H, Leu CH), 2.00 (m, 2H, Glu CH_2), 2.46 (m, 2H, Glu CH_2), 2.88 (m, 4H, CH_2-Ph and AAsp CH_2), 2.98 and 3.11 (d, 3H, NCH_3), 3.68 (m, 2H, NCH_2), 4.30 (m, 2H, α-H), 4.50 (m, 2H, α-H and Thr CH), 5.09 (m, 2H, Z), 5.65 (b, 1H, NH), 6.75 (b, 1H, NH), 7.10−7.40 (m, 12H, CH=CH and Ph), 7.85 (b, 1H, NH), 7.95 (b, 1H, NH). HRMS (FAB, M+1) Calcd. for $C_{38}H_{51}N_6O_{12}$: 783.3565; Observed *m/z* 783.3493. Anal. ($C_{38}H_{50}N_6O_{12}\cdot 2H_2O$) C, H, N.

***N*^{2}-(*N*-Benzyloxycarbonylleucylglutamylthreonyl)-*N*^{1}-carboxylmethyl-*N*^{1}-*trans*-(3-dibenzylcarbamoylacryloyl)hydrazine (Cbz-Leu-Glu-Thr-AAsp-CH=CH−CON(CH$_2$Ph)$_2$, 21r).** ^{1}H NMR (DMSO-d_6): 0.85 (t, 6H, Leu CH_3), 1.06 (m, 3H, Thr CH_3), 1.45 (m, 2H, Leu CH_2), 1.60 (m, 1H, Leu CH), 1.80 and 1.90 (d of m, 2H, Glu CH_2), 2.25 (m, 2H, Glu CH_2), 3.32 (s, 2H, AAsp CH_2), 4.03 (m, 2H, α-H), 4.25 (m, 1H, α-H), 4.40 (m, 1H, Thr CH), 4.60 (d, 4H, CH_2Ph), 5.00 (s, 2H, Z), 7.10−7.35 (m, 12H, CH=CH and Ph), 7.40 (b, 1H, NH), 7.80 (b, 1H, NH), 8.07 (b, 1H, NH), 8.65 (m, 1H, NH), 10.75 (b, 2H, COOH). HRMS (FAB, M+1) Calcd. for $C_{43}H_{53}N_6O_{12}$, 845.3721; Observed *m/z* 845.3777. Anal. ($C_{43}H_{52}N_6O_{12}\cdot 2H_2O$) C, H, N.

***N*^{2}-(*N*-Benzyloxycarbonylleucylglutamylthreonyl)-*N*^{1}-carboxylmethyl-*N*^{1}-*trans*-(3-(methyl-1-naphthylmethyl)carbamoylacryloyl)hydrazine (Cbz-Leu-Glu-Thr-AAsp-CH=CH−CON(CH$_3$)-CH$_2$-1-Naphth, 21s).** ^{1}H NMR (acetone-d_6): 0.92 (m, 6H, Leu CH_3), 1.22 (m, 3H, Thr CH_3), 1.65 (m, 2H, Leu CH_2), 1.75 (m, 1H, Leu CH), 2.00 (m, 2H, Glu CH_2), 2.47 (m, 2H, Glu CH_2), 3.08 (d, 4H, AAsp CH_2 and NCH_3), 4.25 (m, 1H, α-H), 4.35 (m, 2H, α-H), 4.50 (m, 1H, Thr CH), 5.07 (m, 2H, Z), 5.15 (m, 2H, CH_2-naphth), 6.75 (b, 1H, NH), 7.20−7.35 (m, 6H, CH=CH and Ph), 7.40−7.60 (m, 7H, Ph and NH), 7.90 (m, 2H, naphth), 7.80 (b, 1H, NH), 8.10 (b, 1H, NH). HRMS (FAB, M+1) Calcd. for $C_{41}H_{51}N_6O_{12}$, 819.3565; Observed *m/z* 819.3521. Anal. ($C_{41}H_{50}N_6O_{12}\cdot 2H_2O$) C, H, N.

***N*^{2}-(*N*-Benzyloxycarbonylleucylglutamylthreonyl)-*N*^{1}-carboxylmethyl-*N*^{1}-*trans*-(3-(3,4-dihydro-2*H*-quinolin-1-yloxo)acryloyl)hydrazine (Cbz-Leu-Glu-Thr-AAsp-CH=CH−CO-tetrahydroquinoline, 21t).** ^{1}H NMR (acetone-d_6): 0.94 (m, 6H, Leu CH_3), 1.22 (m, 3H, Thr CH_3), 1.66 (m, 2H, Leu CH_2), 1.78 (m, 1H, Leu CH), 1.98 (m, 2H, quinoline CH_2), 2.00 (m, 2H, Glu CH_2), 2.46 (m, 2H, Glu CH_2), 2.80 (m, 4H, quinoline CH_2 and Asp CH_2), 3.81 (m, 2H, NCH_2), 4.28 (m, 1H, α-H), 4.38 (m, 1H, α-H), 4.50 (m, 2H, α-H and Thr CH), 5.09 (m, 2H, Z), 6.75 (b, 1H, NH), 7.10−7.40 (m, 10H, CH=CH and Ph), 7.48 (d, 1H, Ph), 7.60 (d, 1H, NH), 7.90 (d, 1H, NH), 9.00 (s, 1H, NH). HRMS (FAB) Calcd. for $C_{38}H_{49}N_6O_{12}$: 781.3408; Observed *m/z* 781.3367. Anal. ($C_{38}H_{48}N_6O_{12}\cdot 2H_2O$) C, H, N.

Enzyme Assays. Caspase-2, -3, -6, -7, -8, -9 and -10. Caspases-2, -3, -6, -7, -8, -9, and −10 were expressed in *E. coli* and purified in Guy Salvesen's laboratory at the Burnham Institute, La Jolla, CA, according to the methods previously described by Stennicke and Salvesen.[41] Inhibition rates were determined by the progress curve method described by Tian and Tsou.[42] This method is suitable for measuring irreversible inhibition rates with fast inhibitors, where the inhibitor, the substrate, and the enzyme are incubated together and the rate of substrate hydrolysis is measured continuously. The rate of substrate hydrolysis in the presence of the inhibitor was monitored for 20 min. The progress curve of inhibition, where the product formation approaches an asymptote is described in the equation

$$\ln([P_\infty] - [P]) = \ln[P_\infty] - A[I]t$$

where [P] and [P_∞] are the product concentrations at t and $t = \infty$, respectively, A is the apparent rate constant in the presence of the substrate. The apparent rate constants were determined from the slopes of plots of ln([P_∞] − [P]) versus time (t) in seconds as previously described, where A = slope/[I].

For competitive and irreversible inhibition, the apparent rate constant is converted to the second-order rate constant k_2 by taking into consideration the effect of the substrate concentration on the apparent rate constant. The second-order rate constant is described as in the equation:

$$k_2 = A \times (1 + [S]/K_M)$$

Assays using the fluorogenic substrates Ac-DEVD-AMC (λ_{ex} = 360 nm, λ_{em} = 465 nm), Z-VDVAD-AFC (λ_{ex} = 430 nm, λ_{em} = 535 nm), and Ac-LEHD-AFC were carried out on a Tecan Spectra Fluor microplate reader at 37 °C. The K_M values for Ac-DEVD-AMC with caspase-3 (K_M = 9.7 μM), caspase-6 (K_M = 236.35 μM), caspase-7 (K_M = 23.0 μM), caspase-8 (K_M = 6.79 μM), and caspase-10 (K_M = 20.2 μM) were determined in the laboratory of Guy Salvesen. The K_M value for Ac-LEHD-AFC with caspase-9 (K_M = 114 μM) was also determined in the laboratory of Guy Salvesen. The K_M value for Z-VDVAD-AFC with caspase-2 was found to be 80.5 μM. The k_2 values are 2.24-fold higher than the apparent rate for caspase-2 because of the 100 mM [S] and K_M = 80.5 μM. The k_2 values are 11.31-fold higher than the apparent

rate for caspase-3 because of the 100 mM [S] and $K_M = 9.7\ \mu M$. The k_2 values are 1.42-fold higher than the apparent rate for caspase-6 because of the 100 mM [S] and $K_M = 236.35\ \mu M$. The k_2 values are 5.35-fold higher than the apparent rate for caspase-7 because of the 100 mM [S] and $K_M = 23.0\ \mu M$. The k_2 values are 15.73-fold higher than the apparent rate for caspase-8 because of the 100 mM [S] and $K_M = 6.79\ \mu M$. The k_2 values are 2.32-fold higher than the apparent rate for caspase-9 because of the 150 mM [S] and $K_M = 114\ \mu M$. The k_2 values are 8.43-fold higher than the apparent rate for caspase-10 because of the 150 mM [S] and $K_M = 20.2\ \mu M$.

The concentration of the caspase-3 stock solution was 2 nM in the assay buffer. Assay buffer is a 1:1 mixture of caspase buffer (40 mM Pipes, 200 mM NaCl, 0.2% (w/v) CHAPS, sucrose 20% (w/v)) and 20 mM DTT solution in H_2O at pH 7.2. The concentration of the substrate stock solution was 2 mM in DMSO. The enzyme was preactivated for 10 min at 37 °C in the assay buffer. The standard 100 μL reaction was started by adding 40 μL of assay buffer, 5 μL of various amounts of inhibitor (stock solution concentrations varied from 5×10^{-3} M to 4.84×10^{-7} M in DMSO), and 5 μL of substrate in DMSO (100 μM final concentration) at 37 °C. 50 μL of 2 nM enzyme stock solution (final concentration: 1 nM) was added to the mixture after 1 min and reading started immediately for 20 min at 37 °C. Inhibition experiments were repeated in duplicate and standard deviations determined.

Caspase-2 kinetic assays were performed using Z-VDVAD-AFC as the substrate (2 mM stock solution in DMSO) and with the same conditions as caspase-3. The concentration of the caspase-2 stock solution was 86.7 nM in the assay buffer (final concentration in the well: 43.3 nM). The inhibitor stock solution concentrations varied from 5×10^{-3} M to 1×10^{-4} M in DMSO.

Caspase-6 kinetic assays were performed using the same conditions and the same substrate (Ac-DEVD-AMC, 2 mM stock solution in DMSO). The enzyme stock solution was 10 nM (final concentration in the well: 5 nM) in the assay buffer. The inhibitor stock solution concentrations varied from 5×10^{-3} M to 2.42×10^{-6} M in DMSO.

Caspase-7 kinetic assays were performed using the same conditions and the same substrate (Ac-DEVD-AMC, 2 mM stock solution in DMSO). The enzyme stock solution was 10 nM (final concentration in the well: 5 nM) in the assay buffer. The inhibitor stock solution concentrations varied from 5×10^{-3} M to 2.5×10^{-6} M in DMSO.

Caspase-8 kinetic assays were performed using the same conditions and the same substrate (Ac-DEVD-AMC, 2 mM stock solution in DMSO). The enzyme stock solution was 100 nM (final concentration in the well: 50 nM) in the assay buffer. The inhibitor stock solution concentrations varied from 5×10^{-3} M to 2.42×10^{-6} M in DMSO.

Caspase-9 kinetic assays were performed using Ac-LEHD-AFC as the substrate (3 mM stock solution in DMSO) and with the following conditions. The concentration of the caspase-9 stock solution was 150 nM in the assay buffer (final concentration in the well: 75 nM). Assay buffer is a 1:1 mixture of buffer (200 mM HEPES, 100 mM NaCl, 0.01% (w/v) CHAPS, sucrose 20% (w/v)) and 20 mM DTT solution in H_2O at pH 7.0. The assay buffer was supplemented with 0.7 M sodium citrate. The enzyme was preactivated for 10 min at 37 °C in the assay buffer. The inhibitor stock solution concentrations varied from 5×10^{-3} M to 2.5×10^{-5} M in DMSO.

Caspase-10 kinetic assays were performed using the same substrate as caspase-3 (Ac-DEVD-AMC, 3 mM stock solution in DMSO) and with the following conditions. The concentration of the caspase-10 stock solution was 50 nM in the assay buffer (final concentration in the well: 25 nM). Assay buffer is a 1:1 mixture of buffer (200 mM HEPES, 0.2% (w/v) CHAPS, PEG 20% (w/v)) and 20 mM DTT solution in H_2O at pH 7.0. The enzyme was preactivated for 10 min at 25 °C in the assay buffer. The inhibitor stock solution concentrations varied from 5×10^{-3} M to 2.5×10^{-5} M in DMSO.

The progress curve data of all the ester derivatives (**16h**, **17h**, **18g**, **18h**, **19h**, **20h**, **20i**, **21h**, **21i**) was observed for a period of 20 min. However, only the data points corresponding to the first 10 min of the incubation were used for the kinetic calculations, during which time the inhibitors were still stable and the progress curve data had already reached its plateau.

***S. mansoni* Legumain.** Conor R. Caffrey in James McKerrow's laboratory performed the *S. mansoni* legumain kinetic assays at the Sandler Center for Basic Research in Parasitic Diseases, University of California at San Francisco, San Francisco, CA. The zymogen form of schistosome legumain SmAE was expressed in *Pichia*. The lyophilized enzyme (50−100 mg) was reconstituted in 1.5 mL 0.5 M sodium acetate, pH 4.5 containing 4 mM DTT, and left to stand at 37 °C for 3−4 h to allow for auto-activation of the zymogen. In a black 96-well microtiter plate, 50 μL of activated enzyme was added to an equal volume of 0.1 M citrate-phosphate buffer pH 6.8 containing 4 mM DTT. The inhibitors, added as 1 μL aliquots (serial water dilutions of DMSO stock solutions, 2 to 0.00002 μM [final]), were preincubated with the protease at room temperature for 20 min. After incubation, 100 μL of the same buffer containing 20 μM substrate (Cbz-Ala-Ala-Asn-AMC) was added to the wells and the reaction monitored for 20 min. A plot of the RFU/min versus the inhibitor concentration [μM] permitted calculation of an IC_{50} value.

Pichia cell culture medium containing recombinant *S. mansoni* pro-legumain was incubated overnight at room temperature in 0.3 M sodium acetate, pH 4.5, 2 mM DTT, to allow autoactivation of the endogenous zymogen. Inhibitor (1 μL) at 6 concentrations (to yield 0 to 1 μM [final]) was spotted into a 96-well black microtiter plate. To this was added 180 μL 0.1 M citrate-phosphate buffer, pH 6.8, containing 2 mM DTT and 20 μM Cbz-AAN-AMC substrate. Activated legumain (20 μL) was added to the mix and the progress of inhibition followed every 2 s for 30 min at 25 °C (Molecular Devices Flex Station fluorometer in the injection mode; ex 355/em 460).

Clostripain. Clostripain was purchased from Sigma Chemical Co. (St. Louis, MO) as a solid which was dissolved in an activation solution of 8 mM DTT at a concentration of 5.962 μM and stored at −20 °C prior to use. The inhibition of clostripain began with the addition of 25 μL of stock inhibitor solution (concentration varies by inhibitor) in DMSO to a solution of 250 μL of 20 mM Tris/HCl, 10 mM $CaCl_2$, 0.005% Brij 35, 2 mM DTT buffer, at pH 7.6 (clostripain buffer) and 5 μL of the stock enzyme solution. Aliquots (25 μL) of this incubation mixture were taken at various time points and added to a solution containing 100 μL of the clostripain buffer and 5 μL of Z-Phe-Arg-AMC substrate solution (0.139 mM) in DMSO. The enzymatic activity was monitored by following the change in fluorescence at 465 nm. All data obtained was processed by pseudo-first-order kinetics.

Gingipain K. Gingipain K stock solution was obtained from Jan Potempa's lab (University of Georgia, Athens, GA) in a buffer containing 20 mM Bis-Tris, 150 mM NaCl, 5 mM $CaCl_2$, 0.02% NaN_3, at pH 8.0 at a concentration of 9 μM, which was stored at −20 °C prior to use. Before using the enzyme, an aliquot (1 μL) of the stock enzyme was diluted to a concentration of 4.61 nM in 1.951 mL of a solution of 0.2 M Tris/HCl, 0.1 M NaCl, 5 mM $CaCl_2$, 2 mM DTT at pH 8.0 (gingipain K buffer) and kept at 0 °C. This solution was used only for 1 day, as freezing the enzyme at this concentration destroyed all activity. The inhibition of gingipain K began with the addition of 25 μL of stock inhibitor solution (concentration varies by inhibitor) in DMSO to 244 μL of the diluted enzyme solution (4.61 nM) in gingipain K buffer warmed to room temperature. Aliquots (20 μL) of this were taken at various time points and added to a solution containing 100 μL of the gingipain K buffer and 5 μL of Suc-Ala-Phe-Lys-AMC·TFA as the substrate (0.910 mM stock) in DMSO. The enzymatic activity was monitored by following the change in fluorescence at 465 nm. The data for gingipain K was processed by pseudo-first-order kinetics.

Cathepsin B. Irreversible kinetic assays were performed by the incubation method with human liver cathepsin B. Enzymatic

activities of cathepsin B were measured in 0.1 M $KHPO_4$, 1.25 mM EDTA, 0.01% Brij, pH 6.0 buffer and at 23 °C using Cbz-Arg-Arg-AMC as the substrate. To a freshly prepared enzyme stock solution of cathepsin B (approximately 6.98×10^{-3} μg/μL) in enzyme buffer containing DTT (0.1 mM) was added an additional 300 μL of enzyme buffer and 30 μL of a stock inhibitor solution in DMSO. At various time intervals 50 μL aliquots were withdrawn from the incubation mixture and added to 200 μL enzyme buffer containing Cbz-Arg-Arg-AMC (500 μM). Substrate hydrolysis was monitored using a Tecan Spectra Fluor microplate reader (λ_{ex} = 360 nm, λ_{em} = 465 nm). Pseudo first-order rate constants (k_{obs}) were obtained from plots of ln v_t/v_0 versus time.

Papain. Irreversible kinetic assays were performed by the incubation method with papaya latex papain. An enzyme stock solution for the papain assays was freshly prepared from 330 μL of enzyme storage solution (1.19 mg/mL) diluted with 645 μL papain buffer (50 mM HEPES, and 2.5 mM EDTA at pH 7.5) and 25 μL of DTT (0.1 M). The incubation mixture was prepared from 300 μL buffer, 30 μL of inhibitor stock solution (DMSO), and 30 μL of enzyme stock solution. At various times aliquots (50 μL) were withdrawn and added to 200 μL of Cbz-Phe-Arg-pNA substrate in buffer (53.7 μM). The absorbance of released *p*-nitroaniline was monitored at 405 nm on a Molecular Devices Thermomax plate reader.

Calpain I. Irreversible kinetic assays were performed by the incubation method with calpain I from porcine erythrocytes. Enzymatic activities of calpain I were measured at 23 °C in 50 mM HEPES buffer (pH 7.5) containing 10 mM cysteine and 5 mM $CaCl_2$, using Suc-Leu-Tyr-AMC as the substrate. To 30 μL of an enzyme stock solution (1 mg/mL) of calpain I were added 300 μL of incubation buffer and 30 μL of a stock inhibitor solution in DMSO. At various time intervals 50 μL aliquots were withdrawn from the incubation mixture and added to 200 μL of enzyme buffer containing Suc-Leu-Tyr-AMC (1.6 mM). Substrate hydrolysis was monitored using a Tecan Spectra Fluor microplate reader (λ_{ex} = 360 nm, λ_{em} = 465 nm). Pseudo first-order rate constants (k_{obs}) were obtained from plots of ln v_t/v_0 versus time.

Determination of the Stability of the Inhibitors in Buffer and in the Presence of DTT. The stability of a representative group of inhibitors was studied by monitoring the UV spectrum of solutions at 250 nm, at 25 °C. The concentrations of the inhibitors were 2.5−4.0 mM and of DTT was 10 mM. The pH of the buffer solution was 7.2 and it contained about 50% (v/v) DTT. The half-lives ($t_{1/2}$) were obtained from first-order rate plots of ln(A_t/A_0) versus time (15 h) and the correlation coefficients were greater than 0.99.

An aliquot (50 μL) of 4 mM Cbz-Asp-Glu-Val-AAsp-CH═CH−COOEt was added to 450 μL of assay buffer, and the stability of the inhibitor was monitored spectrophotometrically at 250 nm for every 30 min for 4 h. A half-life of 10 min was obtained from the first-order rate plot from absorbance (250 nm) versus time (15 h).

An aliquot (50 μL) of 2.5 mM Cbz-Asp-Glu-Val-AAsp-CH═CH−CONHCH$_2$Ph was added to 450 μL of assay buffer, and the stability of the inhibitor was monitored spectrophotometrically at 250 nm for every 30 min for 4 h. A half-life of 58 min was obtained from the first-order rate plot from absorbance (250 nm) versus time (15 h).

An aliquot (50 μL) of 2.5 mM Cbz-Asp-Glu-Val-AAsp-CH═CH−CON(CH$_3$)CH$_2$Ph was added to 450 μL of assay buffer, and the stability of the inhibitor was monitored spectrophotometrically at 250 nm for every 30 min for 4 h. A half-life of 116 min was obtained from the first-order rate plot from absorbance (250 nm) versus time (15 h).

An aliquot (50 μL) of 2.5 mM Cbz-Val-AAsp-CH═CH−CH═CH−CH$_3$ was added to 450 μL of assay buffer, and the stability of the inhibitor was monitored spectrophotometrically at 250 nm for every 30 min for 4 h. The inhibitor was essentially stable over the course of the study.

Crystal Structures. Caspase Purification. Human recombinant caspase-3 and caspase-8 were produced in *E.coli* as inclusion bodies, refolded, and purified. Briefly, for caspase-3, the cloned genes for the large p17 subunit (Met-Ser^{29}-Asp^{175}) and the small p12 subunit (Met-Ala-Glu^{376}-Asp^{479}) were inserted in the NcoI/BamHI sites of pET11d plasmids (Novagen). For caspase-8, the cloned genes for the large p18 subunit (Met-Gly-Glu218-Asp374) and the small p12 subunit (Met-Ala-Glu376-Asp479) were inserted in the NcoI/BamHI sites of pET11d plasmids (Novagen). For separate expression of both subunits, *E. coli* BL21-CodonPlus (DE3)-RIL cells (Stratagene), containing one of the two plasmids, were grown to a density of A_{600} = 0.5 at 37 °C in a 0.5-L LB medium. Expression was induced by the addition of IPTG (1 mM), and the culture was shaken at 37 °C for 4 h post induction. Cells were harvested, washed in PBS buffer, and lysed using a French press. Due to overexpression, the protein was localized in the inclusion body portion of the cells. Refolding was achieved by rapid mixing of equimolar amounts of each subunit to a final concentration of about 100 μg of subunit/mL in the refolding buffer (100 mM HEPES, pH 7.5, 10% sucrose, 1% CHAPS, 100 mM NaCl and 10 mM DTT) and was incubated overnight at room temperature with continuous stirring. Misfolded and aggregated protein was removed by centrifugation (5000*g*, 30 min), and the supernatant was concentrated using an Amicon-stirred cell. To reduce the salt concentration and to facilitate binding to an anion exchange column (ResQ 1 mL, Amersham Biosciences), the protein solution was dialyzed against the anion exchange buffer (20 mM Tris pH 8.0, 30 mM NaCl and 10 mM DTT) prior to chromatography. The protein was eluted using a 300 mM NaCl gradient. The pure and active caspase-3 and caspase-8 were further purified by size exclusion chromatography on an analytical S200 column with buffer containing 20 mM Tris pH 8.0, 50 mM NaCl, and 10 mM DTT. Fractions containing pure and active caspase were pooled and concentrated by ultrafiltration (centricon, NMWL 10000 Da) to a final concentration of 10 mg/mL and the final yield was about 5−7 mg/L culture. Eventually, the purified caspases were subsequently inhibited with a 3-fold molar excess of the inhibitor in a buffer containing 20 mM Tris pH 8.0 and 10 mM DTT.

Crystallization and Data Collection. Cocrystals of the complex between recombinant human caspase and the Michael acceptor inhibitors were grown from 2 μL hanging drops formed by mixing equal volumes of protein (10 mg/mL in 20 mM Tris/HCl pH 8.0, 10 mM DTT) and reservoir solution. The reservoir solution consists of 15% (w/v) poly(ethylene glycol) 6000, 100 mM sodium citrate, pH 5.0 in case of caspase-3 and 1.4 M sodium citrate, 100 mM HEPES/NaOH pH 8.0 in case of caspase-8. Crystals (~100 × 100 × 50 μm) grew within 2−3 days. For data collection, crystals were frozen in a nitrogen stream after a short soak in reservoir solution containing 20% glycerol for caspase-3. The crystals of caspase-3 complexes belong to the space group *I*222 and the typical unit cell dimensions were, a = 67.2 Å, b = 83.3 Å, c = 96.0 Å. Diffraction data were collected at the rotating anode generator (Bruker-Nonius, FR591) at 100 °K. Images were integrated with MOSFLM[43] and scaled with SCALA[44] from the CCP4 suite of programs.

Diffraction data for caspase-8:inhibitor complex was collected at the Swiss Light Source synchrotron (Paul Scherrer Institute, Villigen, Switzerland). The X-ray data was collected without utilizing any cryo protectant. The crystals of caspase-8 complex belongs to *P*3′21 space group and the unit cell dimensions are a = 67.2 Å, b = 83.3 Å, c = 96.0 Å. The data reduction were done with program XDS[45] and scaled with XSCALE.[46]

Structure Solution and Refinement. The structure was solved by the difference Fourier technique. Structure refinement and automated water addition were performed using the program CNS[47] and the model building was done with the program "O". Iterative cycles of refinement and model building was performed. Manual adjustments were done with program "O". The final crystallographic *R* and free *R* factors for caspase-3 complexes are in the range of 16−19% and 19−22%, respectively. The final model for caspase-3 complexes consisted of residues 29−174 of α subunit and 176−277 of β subunit. For the caspase-8 complex the final *R* and free *R* factors are 16.8% and 20.1%, respectively. The final model shows residues 223−371 of the α subunit and residues 390−479 of the β subunit, 326 water molecules and 1 DTT molecule.

Coordinates. The atomic coordinates for caspase−inhibitor complexes have been deposited with the Protein Data Bank (accession codes: 2C1E, 2C2K, 2C2M, 2C2O, and 2C2Z).

Acknowledgment. The work was supported by a grant from the National Institute of General Medical Sciences (GM61964). K.J. acknowledges a fellowship from the Center for the Study of Women, Science, and Technology (WST) at Georgia Tech, and J. A. acknowledges a fellowship from the Molecular Design Institute under prime contract from the Office of Naval Research. We thank Conor R. Caffrey and James McKerrow at the Sandler Center for Basic Research in Parasitic Diseases, University of California at San Francisco, San Francisco, CA, for the *S. mansoni* legumain kinetic assays. We also thank Jan Potempa and James Travis of the University of Georgia, Athens, GA for the gingipain K. We gratefully acknowledge the Swiss Light Source, Paul Scherrer Institute, Villigen, Switzerland, for providing synchrotron beam time and T. Tomizaki, A. Wagner, and C. Schulze-Briese for their excellent support during data collection. J. Tschopp from the University of Lausanne is acknowledged for providing the caspase-3 cDNA. The financial support from the Swiss National Science Foundation and the Baugartenstiftung (Zurich, Switzerland) is gratefully acknowledged.

Supporting Information Available: Analytical data (C, H, N analyses) for target componds. This material is available free of charge via the Internet at http://pubs.acs.org.

References

(1) Barrett, A. J.; Rawlings, N. D. Evolutionary Lines of Cysteine Peptidases. *Biol. Chem.* **2001**, *382*, 727−733.
(2) Barrett, A. J.; Rawlings, N. D.; O'Brien, E. A. The MEROPS Database as a Protease Information System. *J. Struct. Biol.* **2001**, *134*, 95−102.
(3) Denault, J. B.; Salvesen, G. S. Caspases: Keys in the Ignition of Cell Death. *Chem. Rev.* **2002**, *102*, 4489−4500.
(4) Yuan, J.; Yankner, B. A. Apoptosis in the Nervous System. *Nature* **2000**, *407*, 802−809.
(5) Talanian, R. V.; Brady, K. D.; Cryns, V. L. Caspases as Targets for Antiinflammatory and Anti-Apoptotic Drug Discovery. *J. Med. Chem.* **2000**, *43*, 3351−3371.
(6) Los, M.; Burek, C. J.; Stroh, C.; Benedyk, K.; Hug, H.; Mackiewicz, A. Anticancer Drugs of Tomorrow: Apoptotic Pathways as Targets for Drug Design. *Drug Discovery Today* **2003**, *8*, 67−77.
(7) Salgado, J.; Garcia-Saez, A. J.; Malet, G.; Mingarro, I.; Perez-Paya, E. Peptides in Apoptosis Research. *J. Pept. Sci.* **2002**, *8*, 543−560.
(8) Friedlander, R. M. Apoptosis and Caspases in Neurodegenerative Diseases. *N. Engl. J. Med.* **2003**, *348*, 1365−1375.
(9) Powers, J. C.; Asgian, J. L.; Ekici, O. D.; James, K. E. Irreversible Inhibitors of Serine, Cysteine, and Threonine Proteases. *Chem. Rev.* **2002**, *102*, 4639−4750.
(10) Nicholson, D. W. Caspase Structure, Proteolytic Substrates, and Function During Apoptotic Cell Death. *Cell Death Differ.* **1999**, *6*, 1028−1042.
(11) Rozman-Pungercar, J.; Kopitar-Jerala, N.; Bogyo, M.; Turk, D.; Vasiljeva, O.; Stefe, I.; Vandenabeele, P.; Bromme, D.; Puizdar, V.; Fonovic, M.; Trstenjak-Prebanda, M.; Dolenc, I.; Turk, V.; Turk, B. Inhibition of Papain-Like Cysteine Proteases and Legumain by Caspase-Specific Inhibitors: When Reaction Mechanism Is More Important Than Specificity. *Cell Death Differ.* **2003**, *10*, 881−888.
(12) Leist, M.; Jaattela, M. Triggering of Apoptosis by Cathepsins. *Cell Death Differ.* **2001**, *8*, 324−326.
(13) Turk, B.; Stoka, V.; Rozman-Pungercar, J.; Cirman, T.; Droga-Mazovec, G.; Oreic, K.; Turk, V. Apoptotic Pathways: Involvement of Lysosomal Proteases. *Biol. Chem.* **2002**, *383*, 1035−1044.
(14) Barrett, A. J.; Kembhavi, A. A.; Brown, M. A.; Kirschke, H.; Knight, C. G.; Tama, M.; Hanada, K. L-*Trans*-Epoxysuccinyl-Leucylamido-(4-Guanidino)Butane (E-64) and Its Analogues as Inhibitors of Cysteine Proteinases Including Cathepsin B, H, and L. *Biochem. J.* **1982**, *201*, 189−198.
(15) Hanzlik, R. P.; Thompson, S. A. Vinylogous Amino Acid Esters: A New Class of Inactivators for Thiol Proteases. *J. Med. Chem.* **1984**, *27*, 711−712.
(16) Thompson, S. A.; Andrews, P. R.; Hanzlik, R. P. Carboxyl-Modified Amino Acids and Peptides as Protease Inhibitors. *J. Med. Chem.* **1986**, *29*, 104−111.
(17) Palmer, J. T.; Rasnick, D.; Klaus, J. L. Irreversible Cysteine Protease Inhibitors Containing Vinyl Groups Conjugated to Electron Withdrawing Groups. US Patent 6,287,840, 2001.
(18) Matthews, D. A.; Dragovich, P. S.; Webber, S. E.; Fuhrman, S. A.; Patick, A. K.; Zalman, L. S.; Hendrickson, T. F.; Love, R. A.; Prins, T. J.; Marakovits, J. T.; Zhou, R.; Tikhe, J.; Ford, C. E.; Meador, J. W.; Ferre, R. A.; Brown, E. L.; Binford, S. L.; Brothers, M. A.; DeLisle, D. M.; Worland, S. T. Structure-Assisted Design of Mechanism-Based Irreversible Inhibitors of Human Rhinovirus 3C Protease with Potent Antiviral Activity against Multiple Rhinovirus Serotypes. *Proc. Natl. Acad. Sci. U.S.A.* **1999**, *96*, 11000−11007.
(19) Patick, A. K.; Binford, S. L.; Brothers, M. A.; Jackson, R. L.; Ford, C. E.; Diem, M. D.; Maldonado, F.; Dragovich, P. S.; Zhou, R.; Prins, T. J.; Fuhrman, S. A.; Meador, J. W.; Zalman, L. S.; Matthews, D. A.; Worland, S. T. *In Vitro* Antiviral Activity of AG7088, a Potent Inhibitor of Human Rhinovirus 3C Protease. *Antimicrob. Agents Chemother.* **1999**, *43*, 2444−2450.
(20) Zhang, K. E.; Hee, B.; Lee, C. A.; Liang, B.; Potts, B. C. Liquid Chromatography−Mass Spectrometry and Liquid Chromatography-NMR Characterization of in Vitro Metabolites of a Potent and Irreversible Peptidomimetic Inhibitor of Rhinovirus 3C Protease. *Drug Metab. Dispos.* **2001**, *29*, 729−734.
(21) Dragovich, P. S.; Prins, T. J.; Zhou, R.; Brown, E. L.; Maldonado, F. C.; Fuhrman, S. A.; Zalman, L. S.; Tuntland, T.; Lee, C. A.; Patick, A. K.; Matthews, D. A.; Hendrickson, T. F.; Kosa, M. B.; Liu, B.; Batugo, M. R.; Gleeson, J. P.; Sakata, S. K.; Chen, L.; Guzman, M. C.; Meador, J. W., 3rd; Ferre, R. A.; Worland, S. T. Structure-Based Design, Synthesis, and Biological Evaluation of Irreversible Human Rhinovirus 3C Protease Inhibitors. 6. Structure−Activity Studies of Orally Bioavailable, 2-Pyridone-Containing Peptidomimetics. *J. Med. Chem.* **2002**, *45*, 1607−1623.
(22) Sirois, S.; Wei, D. Q.; Du, Q.; Chou, K. C. Virtual Screening for SARS−CoV Protease Based on KZ7088 Pharmacophore Points. *J. Chem. Inf. Comput. Sci.* **2004**, *44*, 1111−1122.
(23) Ekici, O. D.; Gotz, M. G.; James, K. E.; Li, Z. Z.; Rukamp, B. J.; Asgian, J. L.; Caffrey, C. R.; Hansell, E.; Dvorak, J.; McKerrow, J. H.; Potempa, J.; Travis, J.; Mikolajczyk, J.; Salvesen, G. S.; Powers, J. C. Aza-Peptide Michael Acceptors: A New Class of Inhibitors Specific for Caspases and Other Clan CD Cysteine Proteases. *J. Med. Chem.* **2004**, *47*, 1889−1892.
(24) Choong, I. C.; Lew, W.; Lee, D.; Pham, P.; Burdett, M. T.; Lam, J. W.; Wiesmann, C.; Luong, T. N.; Fahr, B.; DeLano, W. L.; McDowell, R. S.; Allen, D. A.; Erlanson, D. A.; Gordon, E. M.; O'Brien, T. Identification of Potent and Selective Small-Molecule Inhibitors of Caspase-3 through the Use of Extended Tethering and Structure-Based Drug Design. *J. Med. Chem.* **2002**, *45*, 5005−5022.
(25) O'Brien, T., Lee, D. Prospects for Caspase Inhibitors. *Mini Rev. Med. Chem.* **2004**, *4*, 153−165.
(26) Becker, J. W.; Rotonda, J.; Soisson, S. M.; Aspiotis, R.; Bayly, C.; Francoeur, S.; Gallant, M.; Garcia-Calvo, M.; Giroux, A.; Grimm, E.; Han, Y.; McKay, D.; Nicholson, D. W.; Peterson, E.; Renaud, J.; Roy, S.; Thornberry, N.; Zamboni, R. Reducing the Peptidyl Features of Caspase-3 Inhibitors: A Structural Analysis. *J. Med. Chem.* **2004**, *47*, 2466−2474.
(27) Stennicke, H. R.; Renatus, M.; Meldal, M.; Salvesen, G. S. Internally Quenched Fluorescent Peptide Substrates Disclose the Subsite Preferences of Human Caspases 1, 3, 6, 7 and 8. *Biochem. J.* **2000**, *350*, 563−568.
(28) Thornberry, N. A. Caspases: Key Mediators of Apoptosis. *Chem. Biol.* **1998**, *5*, R97−R103.
(29) Thornberry, N. A.; Rano, T. A.; Peterson, E. P.; Rasper, D. M.; Timkey, T.; Garcia-Calvo, M.; Houtzager, V. M.; Nordstrom, P. A.; Roy, S.; Vaillancourt, J. P.; Chapman, K. T.; Nicholson, D. W. A Combinatorial Approach Defines Specificities of Members of the Caspase Family and Granzyme B. Functional Relationships Established for Key Mediators of Apoptosis. *J. Biol. Chem.* **1997**, *272*, 17907−17911.
(30) Talanian, R. V.; Quinlan, C.; Trautz, S.; Hackett, M. C.; Mankovitich, J. A.; Banach, D.; Ghayur, T.; Brady, K. D.; Wong, W. W. Substrate Specificities of Caspase Family Proteases. *J. Biol. Chem.* **1997**, *272*, 9677−9682.
(31) Blanchard, H.; Donepudi, M.; Tschopp, M.; Kodandapani, L.; Wu, J. C.; Grutter, M. G. Caspase-8 Specificity Probed at Subsite S(4): Crystal Structure of the Caspase-8-Z-Devd-CHO Complex. *J. Mol. Biol.* **2000**, *302*, 9−16.
(32) Wei, Y.; Fox, T.; Chambers, S. P.; Sintchak, J.; Coll, J. T.; Golec, J. M.; Swenson, L.; Wilson, K. P.; Charifson, P. S. The Structures of Caspases-1, -3, −7 and −8 Reveal the Basis for Substrate and Inhibitor Selectivity. *Chem. Biol.* **2000**, *7*, 423−432.

(33) Yang, W.; Guastella, J.; Huang, J. C.; Wang, Y.; Zhang, L.; Xue, D.; Tran, M.; Woodward, R.; Kasibhatla, S.; Tseng, B.; Drewe, J.; Cai, S. X. MX1013, a Dipeptide Caspase Inhibitor with Potent in Vivo Antiapoptotic Activity. *Br. J. Pharmacol.* **2003**, *140*, 402−412.
(34) Freidig, A. P.; Verhaar, H. J. M.; Hermens, J. L. M. Comparing the Potency of Chemicals with Multiple Modes of Action in Aquatic Toxicology: Acute Toxicity Due to Narcosis Versus Reactive Toxicity of Acrylic Compounds. *Environ. Sci. Technol.* **1999**, *33*, 3038−3043.
(35) Rotonda, J.; Nicholson, D. W.; Fazil, K. M.; Gallant, M.; Gareau, Y.; Labelle, M.; Peterson, E. P.; Rasper, D. M.; Ruel, R.; Vaillancourt, J. P.; Thornberry, N. A.; Becker, J. W. The Three-Dimensional Structure of Apopain/CPP32, a Key Mediator of Apoptosis. *Nature Struct. Biol.* **1996**, *3*, 619−625.
(36) Watt, W.; Koeplinger, K. A.; Mildner, A. M.; Heinrikson, R. L.; Tomasselli, A. G.; Watenpaugh, K. D. The Atomic-Resolution Structure of Human Caspase-8, a Key Activator of Apoptosis. *Structure Fold. Des.* **1999**, *7*, 1135−1143.
(37) Mittl, P. R.; Marco, S. D.; Krebs, J. F.; Bai, X.; Karanewsky, D. S.; Priestle, J. P.; Tomaselli, K. J.; Grütter, M. G. Structure of Recombinant Human CPP32 in Complex with the Tetrapeptide Acetyl-Asp-Val-Ala-Asp Fluoromethyl Ketone. *J. Biol. Chem.* **1997**, *272*, 6539−6547.
(38) Blanchard, H.; Kodandapani, L.; Mittl, P. R.; Marco, S. D.; Krebs, J. F.; Wu, J. C.; Tomaselli, K. J.; Grutter, M. G. The Three-Dimensional Structure of Caspase-8: An Initiator Enzyme in Apoptosis. *Structure Fold. Des.* **1999**, *7*, 1125−1133.
(39) Xu, G.; Cirilli, M.; Huang, Y.; Rich, R. L.; Myszka, D. G.; Wu, H. Covalent Inhibition Revealed by the Crystal Structure of the Caspase-8/P35 Complex. *Nature* **2001**, *410*, 494−497.
(40) Batchelor, M. J.; Mellor, J. M. The Use of Dichloromaleic and Bromomaleic Anhydrides in the Synthesis of Lactones by the Intramolecular Diels−Alder Reaction. *J. Chem. Soc., Perkin Trans. 1* **1989**, 985−995.
(41) Stennicke, H. R.; Salvesen, G. S. Caspases: Preparation and Characterization. *Methods* **1999**, *17*, 313−319.
(42) Tian, W. X.; Tsou, C. L. Determination of the Rate Constant of Enzyme Modification by Measuring the Substrate Reaction in the Presence of the Modifier. *Biochemistry* **1982**, *21*, 1028−1032.
(43) Leslie, A. G. W. Mosflm User Guide Version 6.2.3. Joint CCP4 and ESF-EAMCB Newsletter on Protein Crystallography, No. 26, 1992.
(44) Anonymous The CCP4 Suite: Programs for Protein Crystallography Collaborative Computational Project, Number 4. *Acta Crystallogr. D Biol. Crystallogr.* **1994**, *50*, 760−763.
(45) Kabsch, W. Automatic Indexing of Rotation Diffraction Patterns. *J. Appl. Crystallogr.* **1988**, *21*, 67−72.
(46) Kabsch, W. Evaluation of Single-Crystal X-ray Diffraction Data from a Position-Sensitive Detector. *J. Appl. Crystallogr.* **1988**, *21*, 916−924.
(47) Brunger, A. T.; Adams, P. D.; Clore, G. M.; DeLano, W. L.; Gros, P.; Grosse-Kunstleve, R. W.; Jiang, J. S.; Kuszewski, J.; Nilges, M.; Pannu, N. S.; Read, R. J.; Rice, L. M.; Simonson, T.; Warren, G. L. Crystallography & NMR System: A New Software Suite for Macromolecular Structure Determination. *Acta Crystallogr. D Biol. Crystallogr.* **1998**, *54*, 905−921.
(48) Garcia-Calvo, M.; Peterson, E. P.; Leiting, B.; Ruel, R.; Nicholson, D. W.; Thornberry, N. A. Inhibition of Human Caspases by Peptide-Based and Macromolecular Inhibitors. *J. Biol. Chem.* **1998**, *273*, 32608−32613.

JM0601405